

A Contribution to the Fight Against Malaria: Novel Synthesis and
Characertization of 3-Alkylarylether-4(1*H*)-quinolones with Antimalarial
Properties

A Thesis
Presented to
The Division of Mathematics and Natural Sciences
Reed College

In Partial Fulfillment
of the Requirements for the Degree
Bachelor of Arts

Lisa Frueh

May 2015

Approved for the Division
(Chemistry)

Aaron Nilsen

Arthur Glasfeld

Acknowledgements

The senior thesis presented here may involve only one year of academic work, but getting to this point has required the support of countless people including those who are mentioned below.

First, I'd like to thank Aaron Nilsen, who taught me everything I know about doing organic chemistry in the lab, and keeps me excited about what I'm doing. Aaron allowed me to make this project completely my own, and I couldn't have asked for a more supportive and knowledgeable adviser. Thank you to Arthur Glasfeld for teaching me everything I know about biochemistry and graciously backing my ambitions for this project. Further, thank you to the entire Reed chemistry department for teaching me, torturing me, and nurturing me.

This project could not have happened without the generous support of Michael Riscoe and the knowledgeable people in his lab, including Isaac Forquer, Martin Smilkstein, and Yuexin Li. Big ups to Kayla Sheridan for helping me out in the lab, and for calming me down when things got hairy.

I want to thank Maggie Geselbracht for encouraging me to become a chemistry major and for being a role model for me as a woman in a STEM field. Maggie's enthusiasm for teaching brought a human side to what I had first perceived as an emotionless world of academia. Learning from Maggie was an experience I will never forget, and her influence drove me toward, and kept me in, the natural sciences.

I'd like to thank the numerous friends who have made my last four years at Reed doable, and have kept me sane this year as I transition from Reed Life to Real Life. In no particular order, here we go:

Kat. Thanks for being my partner in cheap wine and living room dancing. I wouldn't operate the way I do without you.

Theo. Thank you for helping me grow into my own. Thanks for making this year,

and these last four years, the safest and most loving that they could be.



Monty. The ultimate homie, the constant support sytem.

The Scholz crew. For encouraging me to keep going.

Ivo. For always making me laugh and keeping it real.

Gaby, Arthur, and Joel. For making my house a home, for listening to me. For putting up with the smell of steamed cabbage.

Lucy. For fifteen years of love and honesty.

Ali. For your honest advice, for letting me lean on you, for keeping up with me.

Nik. For hearing me out all the time and for always pushing the envelope.

Drew. For always having a smile on your face, and being a fantastic ski buddy.

Wyatt. For being a fantastic desk partner and always keeping your aesthetic consistent.

Jack/Marisa/Pat for making Reed okay again, for throwing a kickass party.

My family. Last but certainly not least, thank you for putting up with me, and for supporting my academic and personal endeavours, no questions asked.

Thanks to everyone that's been there for me, it's been a wild ride.

Table of Contents

Chapter 1: Introduction	1
1.1 A Brief History	3
1.2 Recent Developments	9
1.3 The Cytochrome <i>bc</i> ₁ Complex	12
1.4 Selectivity and Resistance	16
1.5 Activity and Solubility: 3-alkylarylether-4(1 <i>H</i>)-quinolones	18
1.6 Pro-Drugs	20
Chapter 2: Results and Discussion I: Synthetic Methodology	23
2.1 Previous ELQ Synthesis	24
2.2 Development of a Synthetic Route	25
2.2.1 Selection of Quinolone Protecting Group	25
2.2.2 Experimental Hurdles: Toward a Synthesis of 3-Alkylarylether- 4(1 <i>H</i>)-quinolones	26
2.2.3 Synthetic Scheme	30
Chapter 3: Results and Discussion II: Biological Testing	35
3.1 Biological Results	35
3.1.1 <i>In vitro</i> Activity	35
3.1.2 Inhibition of Human Cytochrome <i>bc</i> ₁	38
3.2 Molecular Modeling	40
Chapter 4: Conclusion	45
Chapter 5: Experimental Methods	47
5.1 Molecular Modeling	47

5.2	Biology	47
5.2.1	Parasite Culture	47
5.2.2	EC ₅₀ Tests	48
5.2.3	Inhibition of Human Cytochrome <i>bc</i> ₁	49
5.3	Chemistry	49
5.3.1	General Materials and Methods	49
5.3.2	Quinolone Core Functionalization	52
5.3.3	Alkylarylether Side Chains	54
5.3.4	Target Compounds	58
	Appendix A: NMR Data	61
	References	81

List of Tables

1.1	Historical overview of discovery, understanding, and treatment of malaria.	7
1.2	Drug target selectivity in 3-diarylether-4(1 <i>H</i>)quinolones.	18
1.3	Summary of SAR studies on 3-alkyl-4(1 <i>H</i>)quinolones.	19

List of Figures

1.1	Map of malaria risk and total deaths in 2013 by country.	1
1.2	<i>Plasmodium</i> life cycle.	2
1.3	Methylene blue and 8-aminoquinolines	5
1.4	Quinine and 4-aminoquinolines	6
1.5	Endochin and “endochin-like quinolones” (ELQ).	10
1.6	The mitochondrial electron transport chain.	13
1.7	The cytochrome <i>bc</i> ₁ complex.	13
1.8	The protonmotive Q-cycle	14
1.9	Ubiquinone (coenzyme Q ₁₀), atovaquone and endochin.	15
1.10	Drug accumulation in plasma after oral administration of ethyl carbonate pro-drug ELQ-334 and parent compound ELQ-316.	22
2.1	Generalized scheme of previous 3-diarylether-4(1 <i>H</i>)-quinolone synthesis.	24
2.2	Ethyl ether protecting groups are not compatible with 3-alkylarylether-4(1 <i>H</i>)-quinolones.	25
2.3	Problems with anhydrous Suzuki-Miyaura cross-coupling conditions.	26
2.4	Catalytic cycle of the palladium(II)-catalyzed Suzuki-Miyaura cross-coupling reaction.	27
2.5	Methods employed for hydrolysis of boronic esters to their corresponding boronic acids.	29
2.6	Alternative aryl boronic acid synthesis.	29
2.7	Quinolone core functionalization and <i>O</i> -ethyl carbonate protection.	30
2.8	Synthesis of 3-alkylarylether-4(1 <i>H</i>)-quinolones ELQ-346, ELQ-348, and ELQ-349.	32
2.9	Attempted synthesis of 3-alkylarylether-4(1 <i>H</i>)-quinolone 23b	33
2.10	Synthesis of 3-alkylarylether-4(1 <i>H</i>)-quinolone ELQ-347.	33

3.1	Inhibition of <i>P. falciparum</i> strains by chloroquine, atovaquone, and ELQ-300 controls.	36
3.2	Inhibition of <i>P. falciparum</i> D1 strain by ELQ-346,347,348 and ELQ-349.	37
3.3	Kinetic trace of human cytochrome <i>bc</i> ₁ inhibition by target compounds ELQ-346, ELQ-347, ELQ-348, and ELQ-349.	39
3.4	3-alkylarylether-4(1 <i>H</i>)-quinolones docked into a <i>P. falciparum</i> Q _i site protein model.	40
3.5	Docked conformers of compounds ELQ-349, A , B , and C in the Q _i site of <i>P. falciparum</i>	41
3.6	ELQ-300 analogs docked into a Q _i site protein model.	42
3.7	ELQ-300 analog B docked into a Q _i site protein model.	43
3.8	Effect of 6- and 7- position substituents on Q _i -site binding conformation.	44
A.1	¹ H NMR spectrum of compound (2) in DMSO- <i>d</i> ₆	62
A.2	¹ H NMR spectrum of compound (3) in DMSO- <i>d</i> ₆	63
A.3	¹ H NMR spectrum of compound (9) in DMSO- <i>d</i> ₆	64
A.4	¹ H NMR spectrum of compound (25) in DMSO- <i>d</i> ₆	65
A.5	¹ H NMR spectrum of compound (26) in DMSO- <i>d</i> ₆	66
A.6	¹ H NMR spectrum of compound (19c) in CDCl ₃	67
A.7	¹ H NMR spectrum of compound (20a) in CDCl ₃	68
A.8	¹ H NMR spectrum of compound (20b) in CDCl ₃	69
A.9	¹ H NMR spectrum of compound (20c) in CDCl ₃	70
A.10	¹ H NMR spectrum of compound (21a) in CDCl ₃	71
A.11	¹ H NMR spectrum of compound (21b) in CDCl ₃	72
A.12	¹ H NMR spectrum of compound (21c) in CDCl ₃	73
A.13	¹ H NMR spectrum of compound (22a) in DMSO- <i>d</i> ₆	74
A.14	¹ H NMR spectrum of compound (22b) in DMSO- <i>d</i> ₆	75
A.15	¹ H NMR spectrum of compound (22c) in DMSO- <i>d</i> ₆	76
A.16	¹ H NMR spectrum of compound (23a) in CDCl ₃	77
A.17	¹ H NMR spectrum of compound (23c) in CDCl ₃	78
A.18	¹ H NMR spectrum of compound (27a) in DMSO- <i>d</i> ₆	79
A.19	¹ H NMR spectrum of compound (28a) in DMSO- <i>d</i> ₆	80

Abstract

Even with contemporary advancements in the field of tropical disease medicine, malaria continues to threaten the lives of millions of people globally today. Currently, malaria parasites have developed resistance to almost all available antimalarial drugs. Here, new work has been done toward the development of antimalarial quinolone compounds based on the structure of endochin. The novel synthesis presented here provides a route to 3-alkylarylether substituted quinolones, and four different 3-alkylarylether-4(1*H*) quinolone derivatives were successfully synthesized. All four target compounds showed some level of anti-plasmodial activity *in vitro*, and some structure-activity relationships were elucidated from these *in vitro* studies as well as through computational molecular docking studies.

Dedication

This thesis is dedicated to Levi Duclos, the most honest and curious person I've ever known.

Levi, I miss you dearly.

Chapter 1

Introduction

The global malaria epidemic today threatens the lives of nearly half of the world's population. In 2013, malaria killed between 473,000 and 789,000 people globally; 90% of deaths were in sub-saharan Africa, and 77% of victims were under five years of age. In short, a child dies of malaria every 60 seconds. There are currently 104 countries in which malaria is considered an epidemic, with 3.4 billion people at risk of infection.¹ These global statistics are visualized in Figure 1.1.

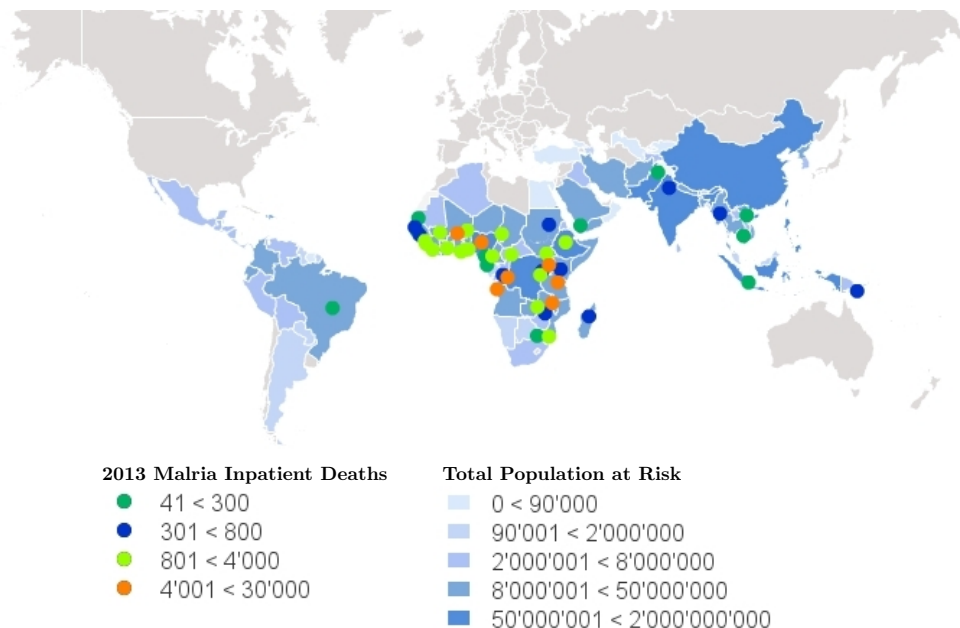


Figure 1.1: Global map of malaria based on data from the World Health Organization's Malaria Report 2013. Map created using the Global Malaria Mapper web application Medicines for Malaria Venture and the World Malaria Programme.²

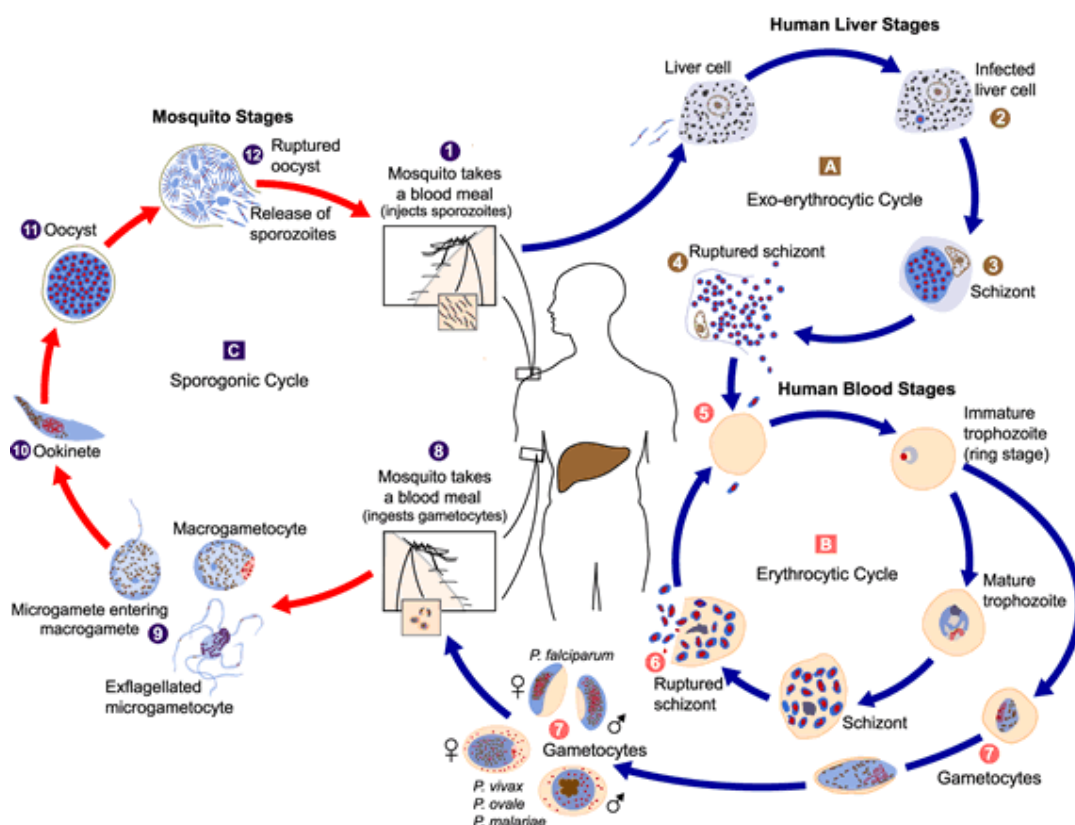


Figure 1.2: Life cycle of the malaria parasite in both human host and malaria vector, from the Center of Disease Control's web page on malaria.³

Malaria is a mammalian infection by parasitic protozoa of the genus *Plasmodium* (subgenus *Plasmodium*). Three species are common to humans, *P. falciparum*, *P. vivax*, and *P. ovale*;⁴ of these species, *P. falciparum* is responsible for the most severe forms of the disease.⁵ The malaria parasite has several phases in its life cycle, two phases in a mammalian host and three phases in mosquitoes of the *Anopheles* family (Fig. 1.2).⁶

The host stage of the malaria life cycle begins when mammalian blood is infected with parasite sporozoites through *Anopheles* saliva. Sporozoites migrate to the liver, beginning the exo-erythrocytic (liver) phase. Here, sporozoites develop into schizonts over a period of 5 to 15 days, each containing 10-30,000 merozoites. In *P. ovale* and *P. vivax*, the sporozoites become hypnozoites, which are dormant and responsible for malaria relapse. The merozoites then enter the blood stream,

beginning the erythrocytic cycle (blood phase). In red blood cells, merozoites transform into trophozoites and then into blood schizonts. Eventually the blood schizont ruptures, releasing new merozoites into the blood stream and thus propagating the erythrocytic cycle. In the blood phase, some merozoites develop into their sexual form (gametocytes) and are ingested by the mosquito during a blood meal.

Once in the mosquito's stomach, male and female gametocytes combine to form a zygote. Over the next 12-48 hours, the zygote elongates into an ookinete that penetrates the wall of the mosquito stomach, becoming an oocyst. The oocyst enlarges, forming upwards of 10,000 sporozoites. Upon oocyst rupture, sporozoites migrate to the salivary glands of the mosquito, where they are transferred to another mammalian host at the mosquito's next blood meal, completing the vector-host cycle.^{5,6}

Over the last two centuries our understanding of malaria has grown and a diversity of effective anti-malaria chemotherapeutics have been developed. However, with a rise in global resistance of the *Plasmodium* parasite to nearly all commercially available drugs, the need for new readily available chemical therapies with low propensity for resistance is as pressing as ever.

1.1 A Brief History

The wide variety of *Plasmodium* species with high host specificity is indicative of the antiquity of the malarial infection, as various species of the parasite have had ample evolutionary time to fit their specific hosts.⁵ Despite its antiquity, a full understanding of the cause and mechanism of malaria infection and transmission did not come to fruition until the late 19th and early 20th centuries. Seventeenth century Europeans noted that Peruvian natives used the bark of a certain 'fever tree' to treat common fevers. Linnaeus later named the tree 'Cinchona', and the active anti-fever compound quinine (Fig. 1.4) was isolated from the bark in France by Pelletier and Caventou in 1820.⁵

In 1847, Dr. Heinrich Meckel von Hemsbach described a "schwarzer farbstoff" (black dye) in the liver of a dead malaria victim. Though unbeknownst to him at the time, this was the first direct observation of the malaria parasite. Later in 1880, French physician Charles Louis Laveran observed malaria parasites through

a microscope, proving that the microscopic organisms were the cause of malarial infection. British doctor Ronald Ross' work on avian malaria in 1898 suggested that the infection was transmitted by mosquitos,⁷ and Italian zoologist Giovanni Battista Grassi later discovered that only certain types of *Anopheles* mosquitoes can transfer human malaria.⁸

With the mechanism of malaria infection and transmission reasonably well understood, interest turned to possible malaria treatments. At this time, quinine proved relatively effective in combating infection and large-scale Cinchona farming provided the bark extract for most of the world up until World War II. Nevertheless, there was a pre-World War II effort toward synthetic antimalaria drugs at Bayer in Elberfeld, Germany. This was born out of an 1891 observation by German scientist Paul Ehrlich, who noted that malaria parasites readily took up synthetic dye methylene blue (Fig. 1.3). He hypothesized that the dye could be used as a drug to poison the parasites and eventually used methylene blue to cure two patients of malaria. While the synthetic compound was not nearly as effective as quinine for malaria treatment, Ehrlich's observations led the textile dye company Bayer to begin research into synthetic medicinal chemistry.⁹

Modifications to methylene blue led Bayer scientist Werner Schulemann and his colleagues Fritz Schönhöfer and August Wingler to note a connection between introduction of basic dialkylamino side chains and increased antimalarial efficacy. The result of these early studies, deemed "Paludenblau" (Fig. 1.3) allowed the relationship between drug efficacy, compound type, and structure to become apparent.^{4,8}

The Elberfeld group then turned their attention to introducing basic side chains to quinoline analogs of quinine.⁴ These studies produced anti-malaria compounds apochrine and plasmoquine in 1924 (Fig. 1.3).⁸ Attaching a basic dialkylamino side chain to a tricyclic core led to the synthesis of mepacrine (Fig. 1.4) which proven effective against *P. falciparum* in 1932. Hans Andersag of Bayer discovered 4-aminoquinoline resochin in 1934, but deemed it too toxic for therapeutic use, leading him to synthesize its 3-methyl analog, sontochin, two years later (Fig. 1.4).⁸ Andersag also synthesized endochin (Fig. 1.5), a promising antimalarial lead that would eventually fail in mammalian tests.¹⁰

In the early 20th century, synthetic antimalarial development was isolated to the researchers at Bayer. However, international research interest grew when

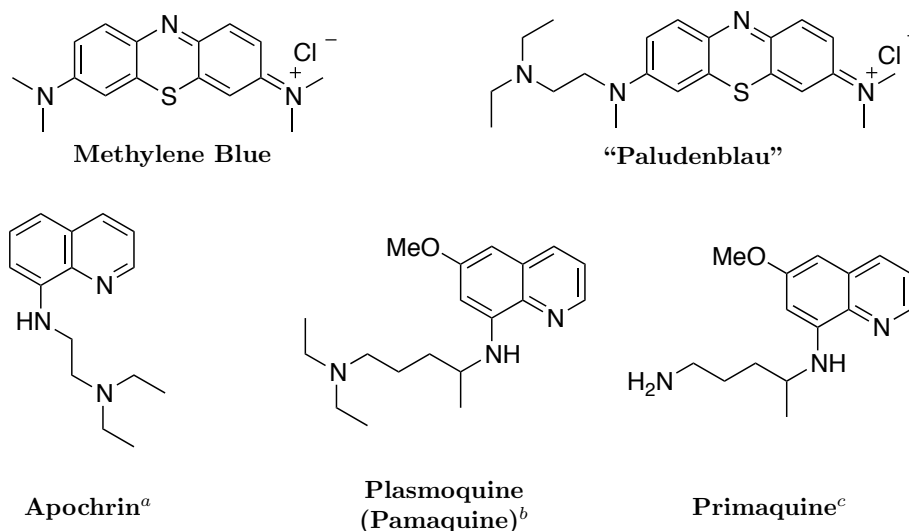


Figure 1.3: Methylene blue and analog “Paludenblau”, and 8-aminoquinolines.

^{a,b}Schulemann, Schönhöfer, and Wingler (Bayer, 1924)

^cElderfield (Columbia University, 1944)

World War II cut off the Indonesian supply of quinine. The shortage motivated the Office of Emergency Management created by President Franklin D. Roosevelt in 1941 to coordinate an extensive chemotherapeutic research program under the Office of Scientific Research and Development (OSRD).¹¹ British and American studies of Bayer’s mepacrine led to introduction of the drug for routine anti-malarial use in malaria-endemic war zones. Extensive evaluation of the German 4-aminoquinolines such as resochnin led to clinical development and eventual American marketing of resochnin under the new name chloroquine.⁴ Primaquine, closely related to Bayer’s plasmoquine (Fig. 1.3) was synthesized in 1944 by Dr. Robert C. Elderfield at Columbia University.^{5,12} Primaquine remains the only available drug effective against hypnozoites (preventing malaria relapse in *P. vivax*), though poor pharmacokinetics and a toxicity to patients with glucose-6-phosphate dehydrogenase deficiency limits the use of it as a drug.¹³ Further, resistance to primaquine has been observed.¹⁴

Though by this point many drugs had proven effective against malaria in the laboratory, the epidemic continued to have devastating effects in the developing world. The newly formed World Health Organization turned its focus to mosquito vector control in the form of sprayable insecticides. Discovery of the insecticidal properties of DDT (dichlorodiphenyltrichloroethane) in 1939 allowed a relatively

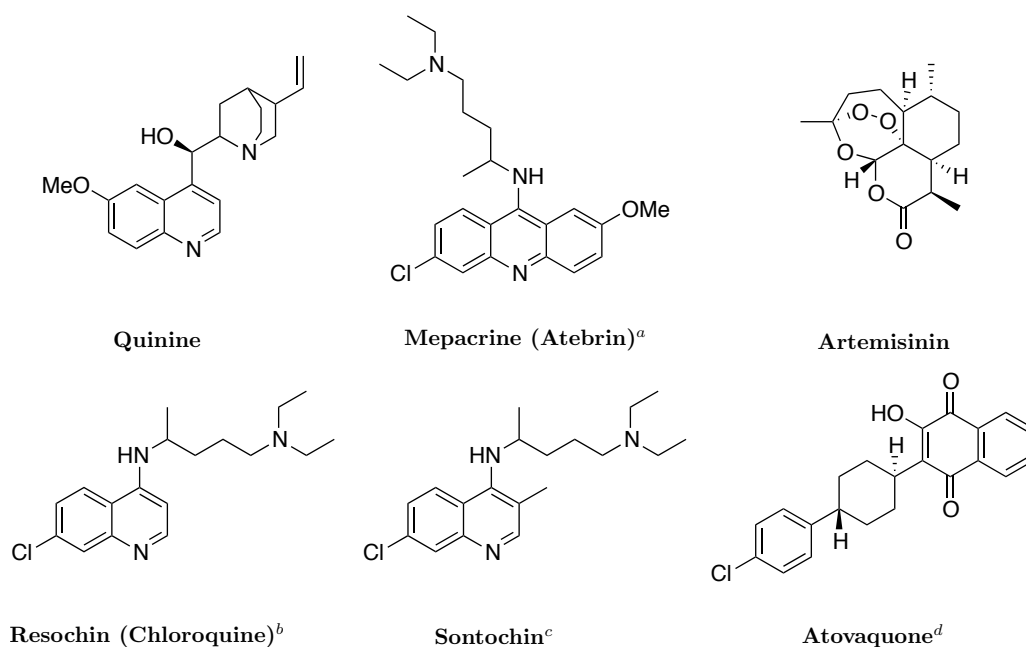


Figure 1.4: Quinine, synthetic 4-aminoquinolines, artemisinin and atovaquone.

^aSchönhöfer (Bayer, 1932)

^bAndersag (Bayer, 1934)

^cAndersag (Bayer, 1936)

^dHudson (Wellcome, 1991)

inexpensive method for widespread vector eradication in the tropical world, and the main strategy of the Global Malaria Eradication Campaign (1955-1969) involved indoor residual spraying (IRS) of houses with DDT.^{4,5} The campaign did not achieve global malaria eradication, but it did greatly reduce the burden of malaria in many countries where the parasite is endemic. While DDT was extremely effective initially at mosquito vector control, the insects quickly developed resistance against the poison.¹⁵

The discovery of the negative environmental impacts of DDT led to replacement of DDT with organophosphates, carbamates, and synthetic pyrethroids for indoor residual spraying, resulting in multiple-insecticide resistant mosquitoes. Many alternative options to widespread insecticide spraying, such as insect growth regulators, natural plant products, and bacterial insecticides, show promise but are not yet feasible for use on a large scale.^{16,17} Today, the World Health Organization recommends the use of insecticide treated bed nets, as well as short-term IRS of insecticides in areas where it is deemed necessary.¹⁸

In 1972, Chinese scientists extracted artemisinin (Fig. 1.4) from *Artemisia annua* (qinghao), a Chinese herb that had traditionally been used to treat malaria and

other fevers. By the late 1980s, artemisinin derivatives were being used in China as antimalarials, and Western pharmaceuticals later began to develop and market their own artemisinin (sesquiterpene lactone endoperoxides) derivatives.⁵ Due to their short half-lives, artemisinins are now used in combination with other drugs in accordance with WHO recommendation. Since artemisinins are so fast-acting, they can clear out the majority of the parasites quickly, at which point the longer half-life partner drug kicks in and remains effective even after the artemisinin is metabolized. Recently, resistance to artemisinins has also been reported in Southeast Asia.^{19,20}

In 1992, naphthoquinone atovaquone (branded as Mepron, Fig. 1.4) was published as an antimalarial by Hudson *et al.* at Wellcome.⁵ Though effective, parasites rapidly developed a resistance to atovaquone monotherapy. Today it is used with folate agonist proguanil under the name Malarone[®], though resistance to the atovaquone/proguanil combination have also been observed.²¹ Malarone[®] is still commonly used for malaria prophylaxis, though it is too expensive for widespread use and production.²²

The current malaria eradication campaign in sub-Saharan Africa focuses mostly on the use of insecticide-treated bed nets, indoor spraying of residual insecticides, and artemisinin combination therapies (ACT).²⁰ Current popular antimalarial prophylactics include Malarone[®], chloroquine, doxycycline, mefloquine, and primaquine.³ Unfortunately, global resistance of malaria parasites to most available drugs as well as difficulty controlling mosquito populations means that malaria remains an epidemic today. The brief history described above is organized into a timeline in Table 1.1 below.

Table 1.1: Historical overview of discovery, understanding, and treatment of malaria.^{4,5,7,8}

1600s	Jesuit missionary reports of the 'fever tree bark' that Peruvian natives use to treat fever. The bark is exported to Europe by the mid-century.
1820	Pelletier and Caventou isolate Quinine and cinchonine from Cinchona bark in France.
1847	Dr. Heinrich Meckel notes the presence of some black substance in the liver of a dead malaria victim.
1854-72	Large-scale cultivation of the Cinchona tree in Indonesia and later in India.

- 1856 William Henry Perkins sets out to synthesize quinine and fails, instead synthesizing 'mauve', the first synthetic textile dye, beginning the German synthetic dye industry.
- 1878 Patrick Manson, a Scottish physician, demonstrates that mosquitos transmit human filaria.
- 1880 Alphonse Laveran of France first describes the presence of foreign parasitic bodies in the blood of feverish patients in Algeria.
- 1886-90 *P. vivax* and *P. malariae* are described by Camillo Golgi in Italy, and later *P. falciparum* by Celli and Marchiafava.
- 1891 German scientist Paul Ehrlich uses methylene blue to stain malaria parasites. He hypothesizes that since the dye was absorbed into the parasites, methylene blue might poison the parasite.
- 1894 Manson suggests that malaria may be carried by mosquito vectors.
- 1898 Ronald Ross, a British medical doctor, documents the cycle of bird malaria.
- 1898 Italian scientists Giovanni Battista Grassi, Amico Bignami, and Giuseppe Bastianelli describe the life cycle of human malaria parasites in *Anopheles* mosquitoes.
- 1899 Ross initiates mosquito larva control in Sierra Leone, and successful large-scale control of mosquitoes in Cuba begins.
- 1900 Manson confirms that mosquitoes are malaria vectors using human volunteers.
- 1901-14 Successful malaria vector control carried out in Malaya, Egypt, Panama Canal area.
- 1907 Rabe *et al.* establish the structure of quinine.
- 1914-18 Quinine shortage during World War I.
- 1924 Schulemann, Schönhöfer and Wiegler (Bayer of Germany) develop pamaquine (plasmoquine) and other N-substituted aminoquinolines.
- 1930 Mietzsch and Kikuth (Germany) develop mepacrine (atabrine).
- 1934 Hans Andersag (Bayer, Germany) develops chloroquine (resochin).
- 1935-39 Large-scale spraying of pyrethrum insecticide aids vector control in South Africa, India, and the Netherlands.

- 1936-45** Discovery of the insecticidal properties of DDT (originally synthesized in 1874), followed by successful eradication of invading vectors in Brazil and Egypt using DDT.
- 1944** Cur, Davey, and Rose (England) develop folate agonist proguanil (Paludrine).
- 1942-46** New synthetic insecticides developed.
- 1944** Elderfield (USA) develops primaquine.
- 1952** Primaquine approved for use by the FDA.
- 1955-57** World Health Assembly declares plans for malaria eradication, followed by the World Health Organization's definition of malaria eradication in 1957. Most plans rely on DDT for successful vector control.
- 1961-65** Brazil and Southeast Asia report chloroquine-resistant *P. falciparum*.
- 1972** Artemisinin is extracted from sweet wormwood in China.
- 1976-83** Highly effective 8-amino quinoline antimalarials developed.
- 1979-86** Chloroquine-resistant *P. falciparum* confirmed in East Africa, and later in West Africa.
- 1991** Hudson (Wellcome) synthesizes atovaquone.
- 1992** Atovaquone is approved for use in the United States, resistance is observed soon after.
- 1998** Roll Back Malaria Partnership (between WHO, UNICEF, UNDP and the World Bank) is launched.
- 1999** The Medicines for Malaria Venture (MMV), a not-for-profit public-private partnership, is started in Switzerland.
- 2000** atovaquone/proguanil (Malarone[®]) combination approved for use in the United States.
- 2000s** Resistance to artemisinin derivatives reported.

1.2 Recent Developments

The Medicines for Malaria Venture (MMV) has set the following goals for the development of anti-malaria drugs: drugs should (1) kill gametocytes as well hypnozoites and other liver stages, (2) have limited cross-resistance with currently

available drugs, (3) have a low propensity for resistance development, and (4) be metabolically stable with a long half-life.¹³

One class of liver-stage active compounds are quinolones (Fig. 1.5). While quinolines (Fig. 1.5) such as chloroquine, plasmoquine, and primaquine (Fig. 1.3, 1.4) have been used extensively for malaria treatment, antimalarial quinolones were not studied fully until the last decade or so.

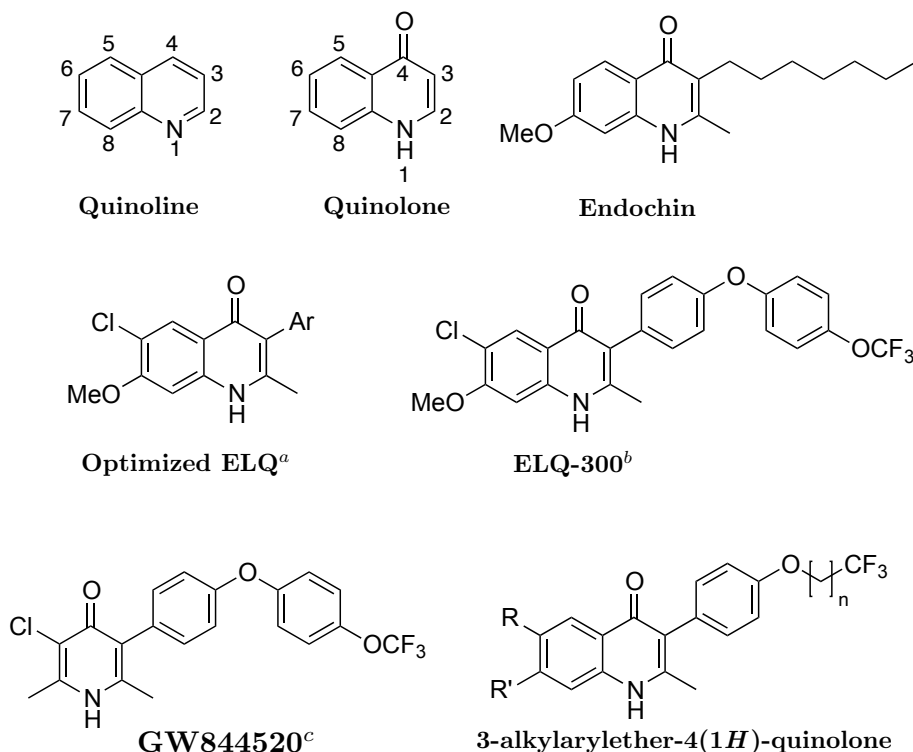


Figure 1.5: Endochin and endochin-like quinolones (ELQs).

^aBased on studies by Cross *et al.* (2010) and Winter *et al.* (2011).

^bNilsen *et al.* (2014)

^cYeates *et al.* (2008)

Hans Andersag of Bayer Pharmaceuticals is credited for the synthesis of chloroquine in the 1930's, which remains a widely used malaria prophylactic. Andersag also developed endochin (Fig. 1.5),^{8,10} which was proven effective against avian malaria in a canary model by Salzer *et al.* of Bayer in 1948. Later work by Wiselogle (1946) Kikuth and Mudrow-Reichenow (1947), and Steck (1972) indicated endochin's efficacy against malaria in the liver, blood, and transmission phases of bird models.¹⁰ In 1973, Adria C. Casey reported on the synthesis of various 4(1H)-quinolones, though disappointing activity was observed in mouse models.²³

Endochin failed in other mammalian models, and was abandoned as a potential drug.¹⁰ It was later shown that endochin is metabolized by mammalian microsomal enzymes (cytochrome P450), explaining its poor clinical efficacy.²⁴

In 2008, Riscoe, Winter *et al.* published the synthesis and antimalarial properties of a variety of 4(1*H*)-quinolones.²⁴ The “endochin-like quinolones” (ELQs) described were substituted at the 3 position (see quinolone numbering scheme in Fig. 1.5) with alkyl or alkoxy side chains. They concluded that antimalarial activity increased with longer side-chains at the 3-position, and termination of the side chain with a trifluoromethyl group decreased atovaquone cross-resistance compared to non-fluorinated derivatives of the same chain length. They hypothesized that termination of the side chain with a trifluoromethyl group would reduce its susceptibility to mammalian microsomal P450-mediated oxidation *in vivo*—which was the fate of endochin in mammals—relative to non-fluorinated derivatives.

In 2010, Cross *et al.* published structure-activity and structure-property relationships (SAR and SPR) of a variety of 4(1*H*)-quinolones.²⁵ By optimizing these analogs for antimalarial activity, they concluded that endochin-like quinolones with the best antimalarial activity are: unsubstituted on the nitrogen and oxygen, unsubstituted at positions 5 and 8, 6-chloro and 7-methoxy substituted, and 3-substituted with either an alkyl, alkenyl, or aryl group. Riscoe *et al.* added that alkyl groups at the 3-position are readily metabolized by mammalian cytochrome P450, while aryl groups are not.¹⁰ Further, aryl group substitution at the 3-position increases solubility of the compound significantly compared to alkyl and alkyenyl moieties.²⁵

Adequate aqueous solubility has proven difficult to achieve with quinolones due to extensive Z plane $\pi - \pi$ stacking networks and hydrogen bonding in the X-Y plane of the quinolone core, which was confirmed using X-ray crystallography.²⁶ Placing an aryl group at the 3-position adjacent to the 2-methyl group forces the aryl group out of the plane of the quinolone core, disrupting π stacking and thus increasing aqueous solubility.²⁶ From these SAR studies, a general optimized antimalarial quinolone substitution scheme is shown in Fig. 1.5.

Most recently, Nilsen and colleagues investigated 3-diarylether moieties of 4(1*H*)-quinolones.^{22,26} These diaryl ether ELQs were based on leads from a study by Yeates *et al.* in 2008 that found promising antimalarial activity in diphenylether pyridones such as GW844520 (Fig. 1.5).²⁷ Nilsen and colleagues synthesized 3-

diarylether-4(1*H*)-quinolone ELQ-300 (Fig. 1.5), which shows low nanomolar *in vitro* EC₅₀ values as well as metabolic stability *in vivo* with a low non-recrudescence dose. While ELQ-300 has proven effective against malaria, problems with aqueous solubility have caused setbacks in its clinical development. Drugs must have an established therapeutic index (the ratio of therapeutic dose to toxic dose), and ELQ-300's insolubility has made it difficult to assess a toxic dose because at high concentrations the drug precipitates out of blood or gastric solution before showing toxic effects.²²

1.3 The Cytochrome *bc*₁ Complex

The mechanism of antimalarial activity for both endochin and atovaquone is attributed to their inhibition of a critical piece of the parasite's metabolism. The electron transport chain (Fig. 1.6) is located in the inner membrane of the mitochondria and is responsible for moving electrons from glycolysis and the citric acid cycle through a number of protein complexes via redox reactions. This electron transport in turn pumps protons from the matrix to the intermembrane space, creating a proton gradient across the inner membrane that drives the synthesis of ATP by powering the ATP synthase enzyme (complex V).

The specific target for endochin and atovaquone is complex III (also called the cytochrome *bc*₁ complex or coenzyme Q : cytochrome *c*-oxidoreductase) of the electron transport chain. Inhibition of complex III is lethal for the parasite.²⁸

The major respiratory subunit of the complex is cytochrome *b*, which spans the inner membrane of the mitochondria. Cytochrome *b* provides the quinol oxidation site (Q_o), quinone reduction site (Q_i), and two b-type hemes (b_L and b_H) for the transmembrane transfer of electrons. A color-coded representation of the complex is shown in Fig. 1.7. Electrons are moved through complex III through a series of one-electron oxidation and reductions of Coenzyme Q (CoQ₁₀, ubiquinone, Fig. 1.9)²⁹ and then transferred from complex III to complex IV via cytochrome *c*.

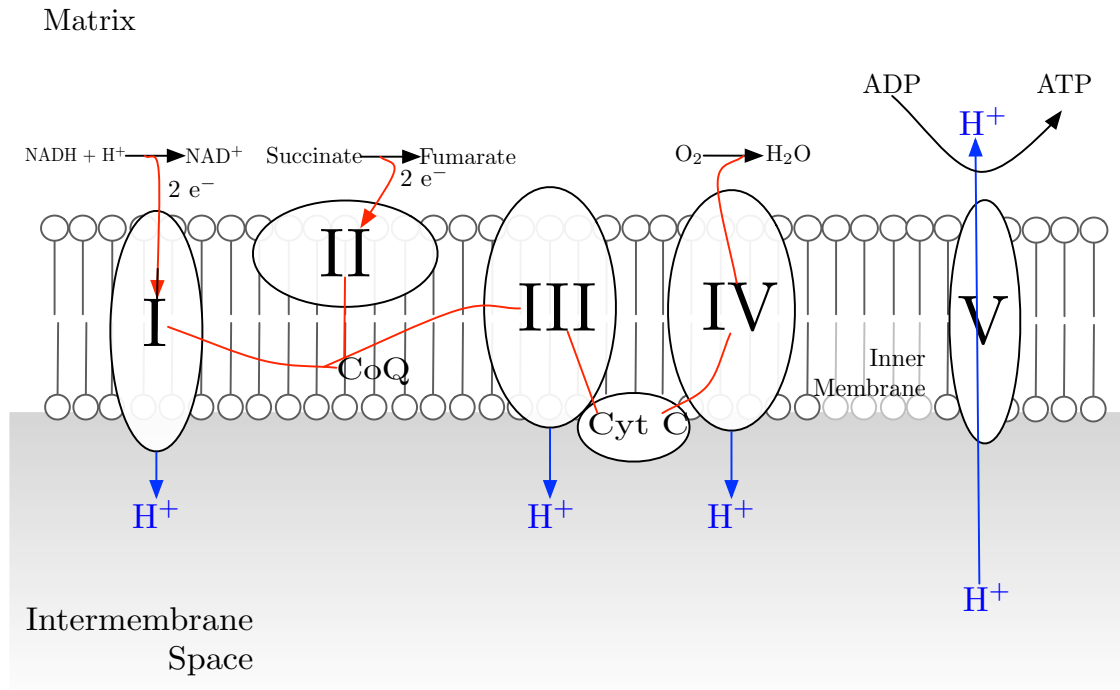


Figure 1.6: The mitochondrial electron transport chain. Area of net high concentration of H^+ shaded. Proton movements shown in blue arrows, electron movements in red arrows.

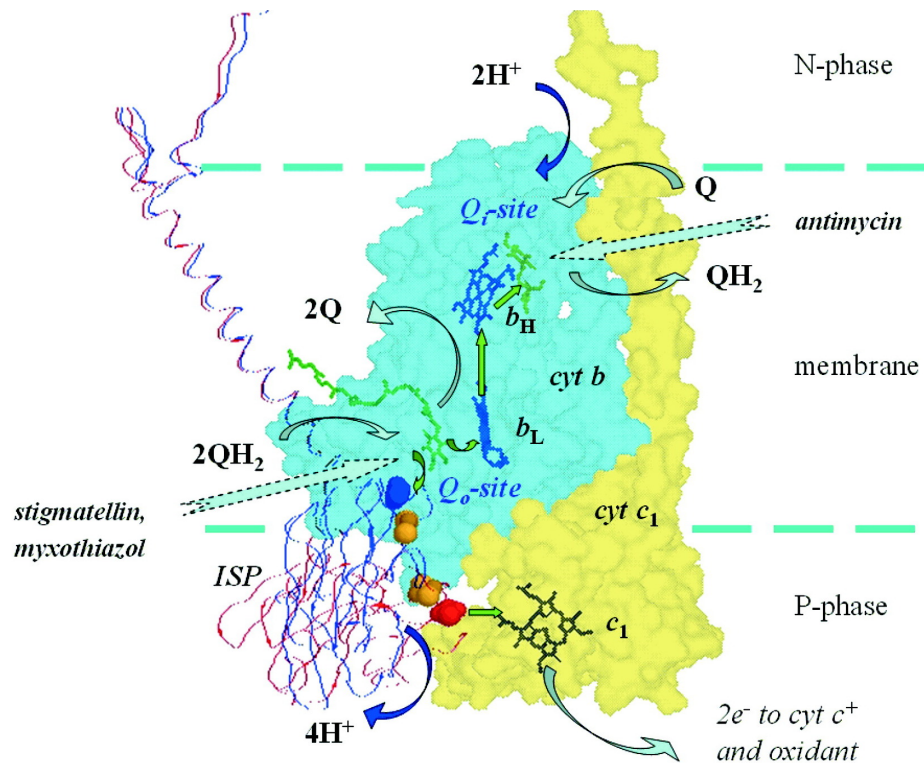


Figure 1.7: The cytochrome bc_1 complex. Cytochrome b is shown in cyan, with cytochrome c_1 in yellow. The Rieske iron sulfur protein (ISP) is shown in red and blue ribbons. Inhibitors indicate their binding sites with an arrow. From Crofts, 2004.³⁰

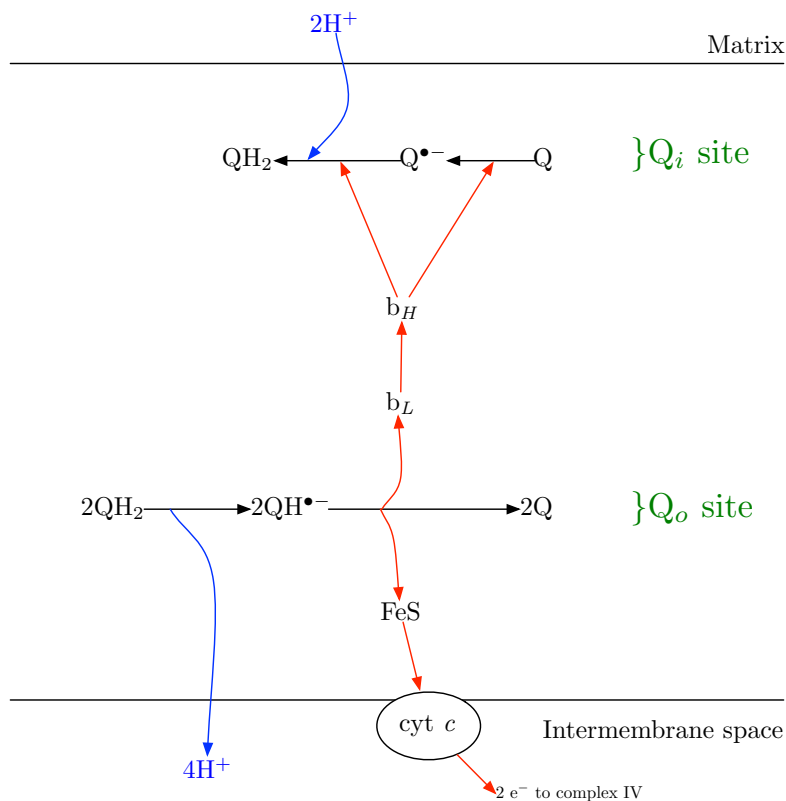
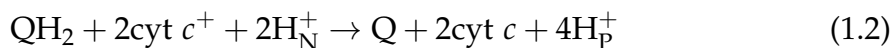


Figure 1.8: A schematic of the protonmotive Q-cycle in the cytochrome bc_1 complex. Movement of electrons are shown with red arrows, and proton movement with blue arrows.

The bc_1 complex moves electrons in a mechanism described by Mitchell's Q-cycle hypothesis.^{30,31} A schematic of electron movement through the complex is illustrated in Figure 1.8. The cycle begins with a bifurcated reaction at the Q_o site, where two electrons from ubiquinol (QH_2) are transferred to two different acceptors. The first electron acceptor is the $[2Fe-2S]$ cluster of the Rieske iron sulfur protein, which in turn passes the electron to cytochrome c , a mobile electron carrier that will carry the electron to complex IV. The second electron is accepted by the lower-potential heme group of cytochrome b , denoted in Fig. 1.8 as b_L . In oxidizing the ubiquinol to ubiquinone (Q) at the Q_o site, two protons are liberated to the intermembrane space. The reaction at the Q_o site happens twice for every one turnover of the entire complex, thus producing two oxidized ubiquinones and providing a net of two electrons each to $cyt\ c$ and b_L .

Next, the reduced heme b_L passes its electron to a higher potential heme of cytochrome b , denoted in Fig. 1.8 as b_H . Since a total of two electrons are available at b_L from the oxidation of two ubiquinol molecules at the Q_o site, b_H has two

electrons to provide at the Q_i site. These two electrons reduce an ubiquinone to ubiquinol, requiring two protons from the matrix.



The mechanism is summarized in Eq. 1.1, which can be reduced further to Eq. 1.2. The subscripts N and P indicate the location of the corresponding proton in either the matrix (N) or the intermembrane space (P). The Q-cycle effectively “moves” two protons across the mitochondrial inner membrane, while providing two electrons to complex IV and liberating one net oxidized ubiquinone for every one turnover of the complex. For *Plasmodium* parasites, complex III provides oxidized ubiquinone that is used by dihydroorotate dehydrogenase (DHODH) in pyrimidine biosynthesis. Blocking complex III, and thus the source of oxidized ubiquinone, is effective in killing parasites.²⁸

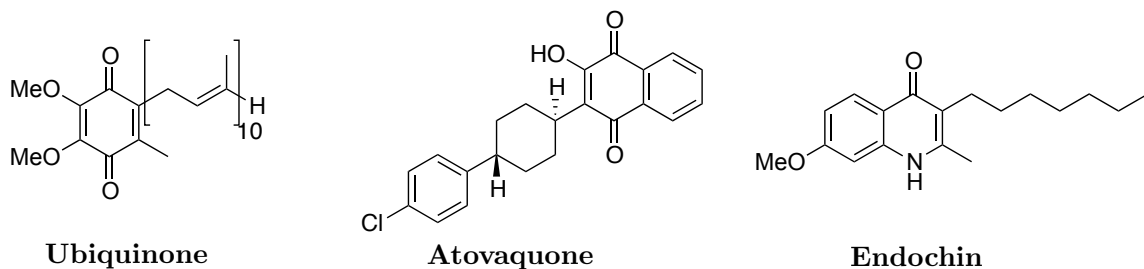


Figure 1.9: Structural similarities between ubiquinone (Coenzyme Q_{10}), atovaquone, and endochin.

Atovaquone and endochin both inhibit the cytochrome bc_1 complex due to their structural similarity with the native complex III substrate, ubiquinone (Fig. 1.9).^{24,32} Natural inhibitors of the bc_1 complex have been extensively studied, such as antimycin (Q_i inhibitor), myxothiazol and stigmatellin (Q_o inhibitors). Though these natural antibiotics are usually toxic to mammals and thus not feasible for therapeutic use, they have been used to understand at which site other complex III inhibitors bind.²⁹ Atovaquone collapses the mitochondrial membrane potential in *Plasmodium* by competitively inhibiting at the Q_o site, which was confirmed by a recent crystal structure by Birth *et al.*³³

Winter *et al.* showed that endochin and ELQs inhibit the cytochrome bc_1 complex by noting that they block oxygen consumption in parasitized blood cells similarly to the way that atovaquone does.²⁴ Referring back to Fig. 1.6, we see that blocking electron transport in complex III disallows oxygen reduction at complex IV. Thus the ability of ELQs to block oxygen consumption suggests inhibition at complex III.²⁴

1.4 Selectivity and Resistance

In the above section, the antimalarial mechanisms of atovaquone and endochin were traced to their affinity for complex III of the *Plasmodium* mitochondrial electron transport chain. However, since all animals have mitochondria, good anti-malaria drugs must also be selective for the *Plasmodium* cytochrome bc_1 complex over the (human) host's.

To explain drug selectivity on a chemical level we must begin by understanding how genetic information instructs the chemical interactions between target and drug. The “central dogma” of molecular biology explains the flow of genetic information from DNA to protein. DNA is transcribed to mRNA, and mRNA is translated into proteins.

Drugs that are selective for the *Plasmodium* mitochondrial complex III over human's must interact better with the parasite's target binding site than the analogous site in the human complex III. Since the *Plasmodium* species of interest and *H. sapiens* have different genomes, they will therefore express different proteins in the target site which will interact in unique ways with chemical inhibitors. Atovaquone, for instance, has a selectivity index (IC_{50} Human / IC_{50} *Plasmodium*) of 230. ELQ-300 shows a remarkable selectivity index of over 20,000.^{22,26}

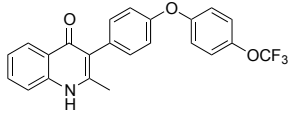
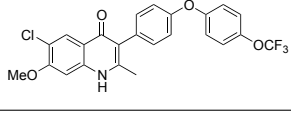
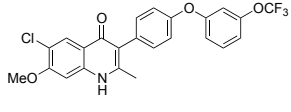
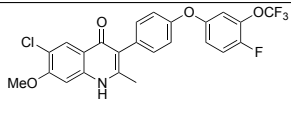
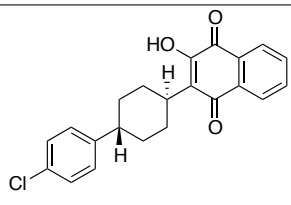
Beyond the selectivity between host and vector mitochondria, inhibition at complex III provides two binding site options for an inhibitor. Thus a second level of selectivity between the Q_o site and the Q_i site can be elucidated for known complex III inhibitors. It is in this second level of selectivity that the mechanism of drug resistance is found. *Plasmodium* resistance to available antimalarial drugs can be explained by genetic mutations that alter the binding site of these drugs. Random point mutations in DNA are constantly occurring, and for parasites under drug pressure, those parasites who express mutations that prevent the drug

from binding survive.³⁴ For instance, atovaquone resistance has been attributed to mutations in the region of the mitochondrial genome that encodes cytochrome *b*, studied mostly in yeast as a model organism. Most atovaquone-resistant parasites show the same pattern of mutations expressed in the Q_o site, such as the Y268S mutation. This mutation from tyrosine to serine in the presence of atovaquone suggests that tyrosine's phenyl group provides a necessary hydrophobic interaction for atovaquone that may be unnecessary for binding of the native substrate ubiquinone.^{29,35}

Knowing that atovaquone binds in the Q_o site and that mutations in the Q_o site are responsible for atovaquone resistance, the level of atovaquone cross-resistance indicate whether cytochrome *bc*₁-inhibitors are binding preferentially at the Q_i or Q_o sites. Comparing the EC₅₀ values between *P. falciparum* isolate strain Tm90-C2B (atovaquone-resistant) and *P. falciparum* isolate strain D6 (atovaquone-sensitive), one can compare an atovaquone cross-resistance index across new drugs. A cross-resistance index higher than 1 indicates that the compound inhibits preferentially at the Q_o-site, as it loses efficacy in strains with Q_o mutations. Table 1.2 suggests that quinolones substituted at the 6-position with a chlorine and at the 7-position with a methoxy group (such as ELQ-300) bind preferentially at the Q_i site, while those unsubstituted at the 6 and 7 positions (such as ELQ-271) show less Q_i-site selectivity.

The data summarized in Table 1.2 also tell us that inhibition at the Q_i-site is very conformationally sensitive. By moving the trifluoromethoxy from its *para* position in ELQ-300 to a *meta* position in ELQ-307, activity increases almost tenfold. While ELQ-307 was a promising lead due to its excellent *in vitro* activity, it was inactive *in vivo* due to the metabolically unstable *para*-hydrogen on the second ring of the 3-diarylether substitution. To remedy this, ELQ-352 (fluorine-substituted at the *para* position) was synthesized and also showed low nanomolar EC₅₀ values *in vitro*. While metabolically stable compared to ELQ-307, ELQ-352 showed poor *in vivo* activity. To summarize, the structure-activity relationships shown in Table 1.2 indicate that 3-diarylether quinolones are highly effective against malaria, Q_i selectivity can be driven by introducing bulky substituents at the 6 and 7 positions, and binding at the Q_i site is conformationally sensitive.

Table 1.2: Drug target selectivity in 3-diarylether-4(1H)quinolones. Data from Nilsen, *et al.*²⁶

Compound	Structure	cLogP ^a	EC ₅₀ D ₆ (nM) ^b	EC ₅₀ Dd2 (nM)	EC ₅₀ TM90- C2B (nM)	ATQ Cross- Resistance Index ^c
ELQ-271		5.22	4.1	5.9	7.5	1.89
ELQ-300		5.66	2.2	2.5	1.4	0.65
ELQ-307		5.66	0.3	0.3	<0.03	<0.1
ELQ-352		5.81	0.4	0.5	0.3	0.75
Atovaquone		3.68	0.10	0.10	7,700	77,000

^aCalculated log of the partition coefficient in octanol-water.

^bEC₅₀ is defined as the concentration of drug *in vitro* at which 50% of parasite growth is inhibited after 72 hours.

^cRatio of EC₅₀s of Q₀-mutated TM90-C2B strain to unmutated D6.

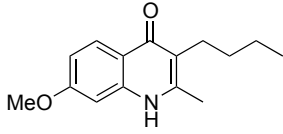
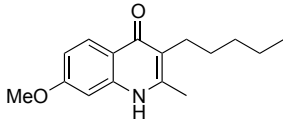
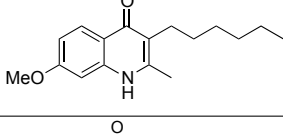
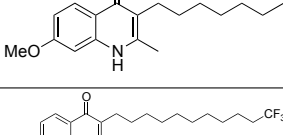
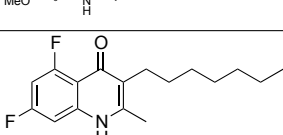
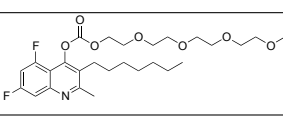
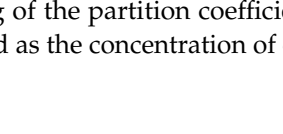
1.5 Activity and Solubility:

3-alkylarylether-4(1H)-quinolones

While 3-diarylether quinolones show good antimalarial activity and improved solubility, let us return briefly to the 3-alkyl quinolones, which have shown remarkable antimalarial activity.

Table 1.3 illustrates that in structurally similar 3-alkyl-4(1H)quinolones, lengthier alkyl chains lead to better antimalarial activities. Comparing ELQ-115, 114, 108, endochin, and ELQ-103, we see that by just varying the length of the alkyl chain at the 3-position from four carbons (ELQ-115) to eleven carbons (ELQ-103),

Table 1.3: Summary of SAR studies on 3-alkyl-4(1H)quinolones.^{10,24}

Compound	Structure	cLogP ^a	EC ₅₀ D ₆ (nM) ^b	EC ₅₀ Dd2 (nM)	EC ₅₀ TM90-C2B (nM)
ELQ-115		2.10	29.1	29.3	91.8
ELQ-114		2.52	8.1	11.9	52.0
ELQ-108		2.93	6.0	5.5	21.4
Endochin		3.35	3.8	3.1	11
ELQ-103		5.31	1.2	1.4	4.7
ELQ-121		3.79	0.15	0.15	80.9
ELQ-125		5.68	0.4	0.4	146.1

^aCalculated log of the partition coefficient in octanol-water.

^bEC₅₀ is defined as the concentration of drug *in vitro* at which 50% of parasite growth is inhibited after 72 hours.

antimalarial activity increases almost thirty-fold. This, however, comes at the cost of solubility – longer, “greasier” side chains have lower water solubility, which is necessary for feasible drug development. ELQ-121 is included in Table 1.3 because it has the same 3-alkyl chain length as endochin, but varying the substituents at the 6 and 8 positions of the quinolone core increases *in vitro* activity by a factor of 25. It should be noted, however, that the 3-alkyl ELQs are not viable for use *in vivo*, as most meet the same metabolic fate as endochin in mammalian systems.

The *O*-carbonate version of ELQ-121, called ELQ-125, was the first ELQ to show *in vivo* efficacy against malaria by the Riscoe group. This is likely attributed to ELQ-125's improved solubility, allowing higher concentrations of the drug to be

absorbed by the animal model even if the 3-alkyl group causes some amount of the drug to be metabolized. Many of the 3-diarylether-4(1*H*)-quinolones (Table 1.2) show comparable activity to the 3-alkyl moieties, and most also show *in vivo* activity. As mentioned above, substitution at the 3-position with an aryl group also greatly increases the solubility of ELQs relative to unsubstituted counterparts.^a

Combining the findings summarized in Tables 1.2 and 1.3, the following conclusions can be drawn regarding antimalarial 4(1*H*)-quinolones:

1. Long alkyl chains at the 3-position show the highest antimalarial activity,
2. Aryl groups at the 3-position markedly improve solubility compared to 3-alkyl quinolones,
3. Substitution with 6-chloro and 7-methoxy substituents decreases atovaquone cross-resistance (increases Q_i -site direction) relative to unsubstituted counterparts.

It is the goal of this thesis to synthesize 3-alkylarylether-4(1*H*)-quinolones (Fig. 1.5). These 3-alkylarylether quinolones strive to capture the high antimalarial activity of 3-alkyl quinolones as well as the increased solubility of 3-aryl moieties. Further, previous quinolone synthetic methods have failed to produce 3-alkylaryl ether quinolones, the reasons for which will be explained below. Thus this particular quinolone variety has antimalarial potential and poses a synthetic challenge.

1.6 Pro-Drugs

Above, I attributed the *in vivo* activity of ELQ-125 to its improved solubility relative to ELQ-121. However, there is more to be said about the *O*-carbonate derivatives of 4(1*H*)-quinolones. Namely, carbonates are readily cleaved by esterases in biological systems, thus ELQ-125 can be called a “pro-drug” of ELQ-121. Pro-drugs are derivatives of drugs that undergo some chemical transformation *in vivo* to the pharmacologically active compound.

^aThis is not reflected in cLogP values, which are much higher for 3-diarylether quinolones than for 3-alkyl quinolones, indicating poor aqueous solubility for the 3-diarylether moieties. However, as discussed above, X-ray crystallography of quinolones illustrates π -stacking of the quinolone core that is disrupted by introducing steric bulk (such as an aryl group) at the 3-position. Thus observed solubility is vastly improved by 3-aryl quinolones compared to those without substitution at the 3-position.

Pro-drugs accumulate in higher concentrations in cells than their pharmacologically active parent compounds alone. Figure 1.10 shows plasma drug concentrations in mice of *O*-ethyl carbonate 3-diarylether-4(1*H*)-quinolone pro-drug ELQ-334 compared to its parent compound ELQ-316. These data indicate that even when the ethyl carbonate pro-drug is administered *in vivo*, very little of the pro-drug remains after a short amount of time; it is mostly converted to its parent compound after biological cleavage of the carbonate group. Further, the pharmacologically active ELQ-316 (administered at a molar equivalent dose compared to its pro-drug counterpart ELQ-334) never achieves the same plasma concentration as it does after administration in pro-drug form and biological transformation to the pharmacologically active parent compound. The maximum plasma concentration that is achieved when ELQ-316 is administered orally is six times less than the ELQ-316 concentration achieved when administered in pro-drug form (237 ng/mL of ELQ-316 from ELQ-316 administration and 4378 ng/mL of ELQ-316 from ELQ-334 administration).

Carbonate pro-drugs of endochin-like quinolones are thus more effective at delivering the active parent compound *in vivo* than administration of the parent compound alone. Generally, carbonate pro-drugs also show similar *in vitro* activity than their parent compounds. In this way, *in vivo* efficacy of a promising ELQ drug lead can be improved by using a carbonate pro-drug derivative of the ELQ of interest.

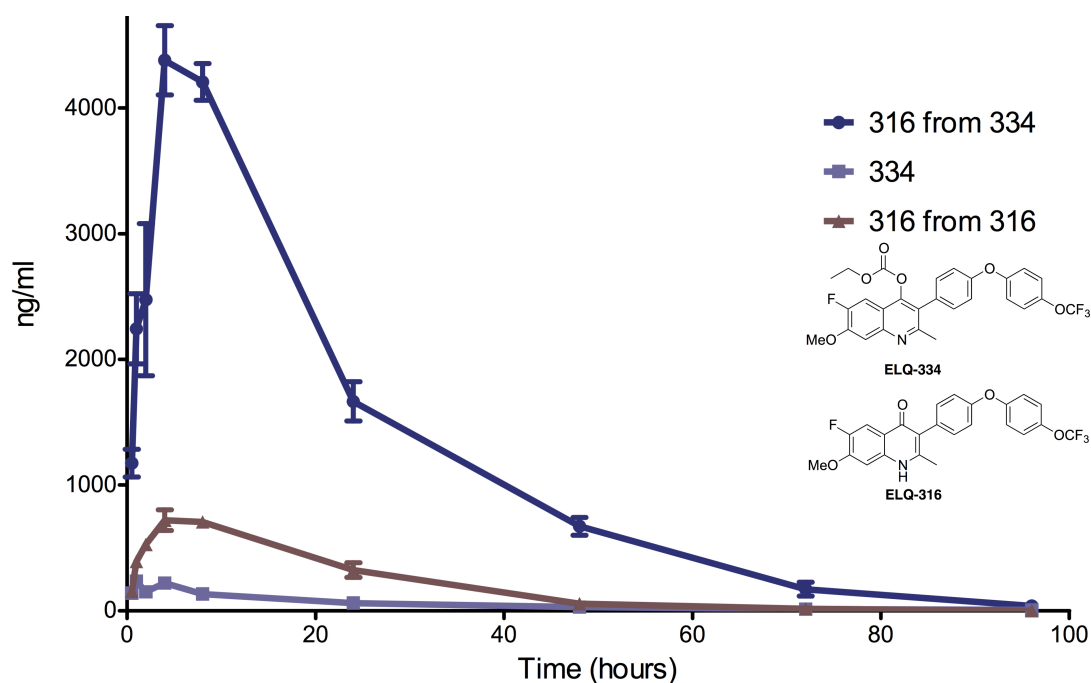


Figure 1.10: Plasma drug concentrations in ng/mL of ethyl carbonate pro-drug ELQ-334 and parent compound ELQ-316 in mice after one oral dose of 10 mg/kg of ELQ-316 or 11.57 mg/kg ELQ-334 as a function of time. The blue line indicates the amount of parent compound ELQ-316 found in plasma after one oral dose of 11.57 mg/kg of its ethyl carbonate pro-drug ELQ-334. The purple line shows plasma concentrations of ELQ-334 after one oral dose of 11.57 mg/kg of ELQ-334, and the red line shows plasma concentrations of ELQ-316 after one oral dose of ELQ-316. Courtesy of Stone Dogget, MD.³⁶

Chapter 2

Results and Discussion I: Synthetic Methodology

The synthesis of 3-alkylarylether-4(1*H*)-quinolones described here was developed based on the synthesis of 3-diarylether-4(1*H*)-quinolones reported by Nilsen, *et al.* in 2014.²⁶ From this precedent, the synthesis was modified as problems presented themselves experimentally.

2.1 Previous ELQ Synthesis

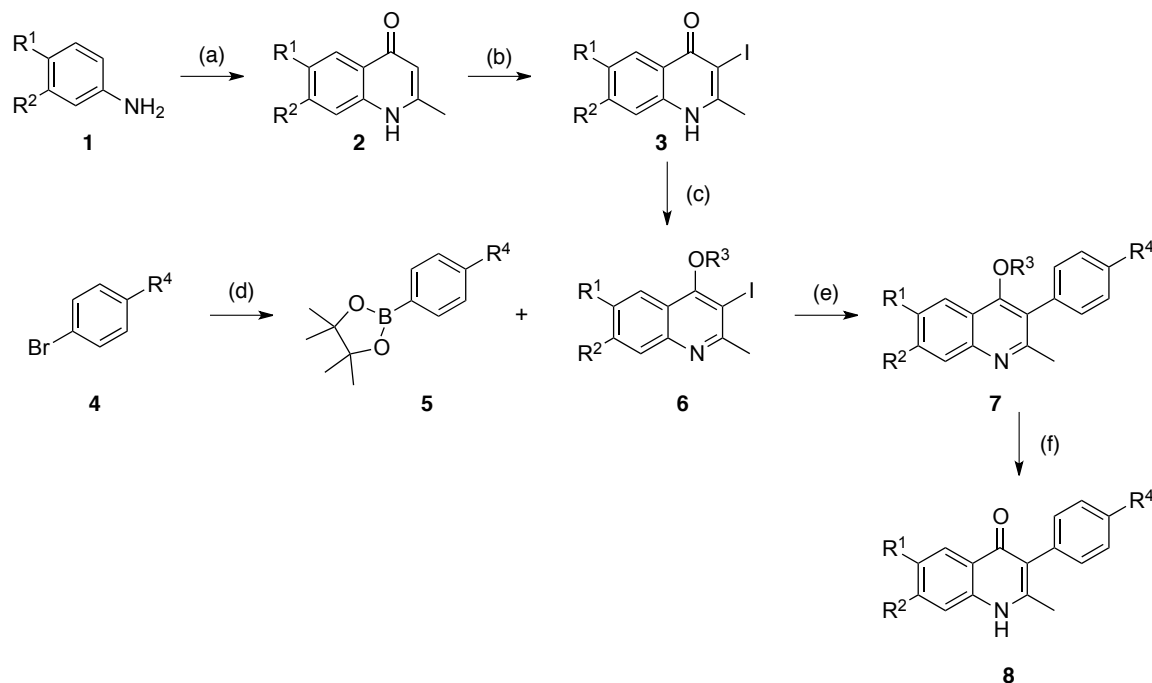


Figure 2.1: Generalized scheme of ELQ synthesis. R^4 = diaryl ethers.

(a) (1) Ethyl acetoacetate, *p*-TSH, benzene, reflux, (2) DOWTHERM A, 250°C; (b) Iodine, aq KI, *n*-butylamine, DMF; (c) Ethyl iodide, aq K_2CO_3 , DMF; (d) $Pd(dppf)_2Cl_2$, bis(pinacolato)diboron, KOAc, DMF, 80°C; (e) $Pd(PPh_3)_4$, aq K_2CO_3 , DMF, 85°C; (f) BBr_3 or 48% aq HBR, AcOH, 90°C.²⁶

Establishing a synthetic route toward 3-alkylarylether-4(1*H*)-quinolones requires an examination of the synthesis of ELQ-300 and the other diaryl ether quinolones described by Nilsen *et al.* in 2014.²⁶ The general synthesis scheme is shown in Figure 2.1 and is summarized here. First, the quinolone core is functionalized beginning with a Conrad-Limpach cyclization of aniline **1** with ethyl acetoacetate. Subsequent iodination at the 3 position of quinolone **2** with molecular iodine and *n*-butylamine yields **3**. Ethyl ether protection of quinolone **3** with ethyl iodide and aqueous potassium carbonate yields *O*-ethyl ether quinolone **6**. Aryl boronic ester **5** is synthesized from corresponding aryl bromide **4** in a palladium-catalyzed boronation with bis(pinacolato)diboron. This side chain **5** is then coupled to the protected, iodinated quinolone core **3** in a Suzuki-Miyaura cross-coupling step (c) yielding **7**. Finally, acidic deprotection of the alkyl ether protecting group yields final 3-aryl-4(1*H*)-quinolone **8**.

Using this general synthesis of 3-diarylether-4-(1*H*)-quinolones, I made modifi-

cations to the scheme to accommodate the particular reactivity of the novel 3-alkylaryl ether moiety targets of this thesis.

2.2 Development of a Synthetic Route

2.2.1 Selection of Quinolone Protecting Group

While ethyl ethers work as effective quinolone protecting groups for 3-diarylether-4(1*H*)-quinolones such as ELQ-300, they cannot be selectively cleaved in the presence of a 3-alkylaryl ether group. That is, the 3-alkylaryl ether is cleaved upon acidic deprotection of the ethyl ether protecting group (Fig. 2.2).^a The first challenge in developing a synthetic route toward 3-alkylaryl ether-4(1*H*)-quinolones was therefore the selection of a new protecting group.

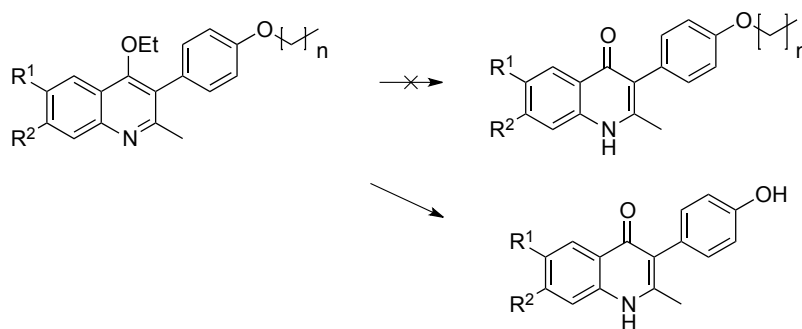


Figure 2.2: Ethyl ether protecting groups are not compatible with 3-alkylaryl ether-4(1*H*)-quinolones under normal deprotection conditions: 48% aq. HBr, AcOH, 90°. ²⁶

Due to difficulties owing most likely to steric hinderance in the quinolone core as well as the quinolone carbonyl's aromatic character, attempts to introduce highly selective protecting groups such as silyl ethers have failed. Therefore, a protecting group was chosen that lent itself to both facile introduction to the quinolone core as well as selective cleavage in the presence of the 3-alkylaryl ether group. The ethyl carbonate protecting group satisfies both these requirements, as it is easily introduced into the quinolone core with a strong base and ethyl chloroformate, and can be removed in relatively mild aqueous basic conditions to which the 3-alkylaryl ether group is inert. Further, as discussed in Section 1.6, ethyl carbonate

^aReed student Ariana Rimmel showed that 3-alkylarylethers are cleaved in acidic conditions in 2013.

“pro-drugs” of ELQs can increase *in vivo* activity of the final ELQ.

Thus the benefit of *O*-ethyl carbonate protected quinolones is two-fold: (a) the ethyl carbonate group is easily cleaved in basic conditions to yield the final quinolone product and (b) the protected intermediate should show a similar level of efficacy to the final product due to its pro-drug character.

2.2.2 Experimental Hurdles: Toward a Synthesis of 3-Alkylarylether-4(1*H*)-quinolones

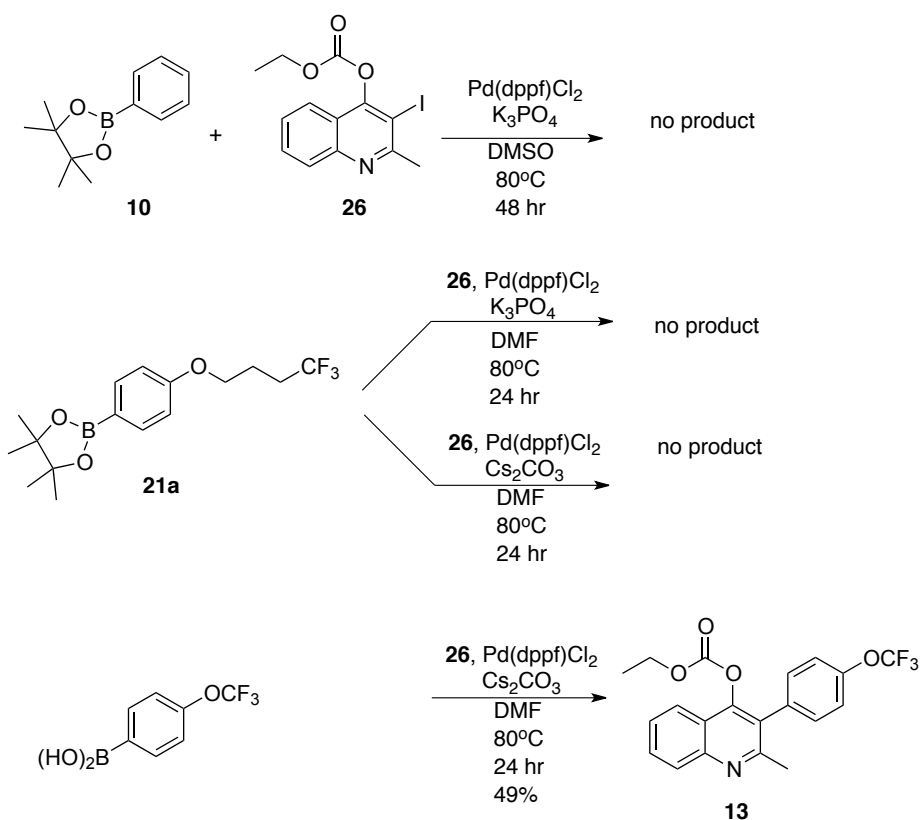


Figure 2.3: Problems with anhydrous Suzuki-Miyaura cross-coupling conditions. Two different sets of conditions were employed, using either K_3PO_4 ³⁷ or Cs_2CO_3 ³⁸ as a base.

The relative lability of the ethyl carbonate protecting group to basic hydrolysis is useful in the ways described above, but imposes constraints on the palladium-catalyzed Suzuki-Miyaura coupling necessary to substitute the quinolone core at the 3 position with an aryl group. Suzuki couplings usually involve a stoichiometric amount of aqueous base, which would hydrolytically cleave the ethyl carbonate

protecting group in this case. In the presence of this water-labile protecting group, new anhydrous Suzuki coupling conditions must be found.

In the 3-diarylether quinolone synthesis by Nilsen, *et al.* (summarized in Figure 2.1), the Suzuki cross-coupling was performed using the 3-iodonated quinolone and an aryl boronic pinacol ester. Boronic esters are easily synthesized and purified using a palladium-catalyzed coupling between the aryl bromide and bis(pinacolato)diboron. However, when I attempted a Suzuki cross-coupling in various anhydrous conditions between an iodinated quinolone core **26** and aryl boronic esters **10** and **21a**, little to no product was obtained (Fig. 2.3). Under the same anhydrous conditions, commercially available 4-trifluoromethoxy phenylboronic acid readily coupled with **9** to yield protected quinolone **13** in 49% yield.

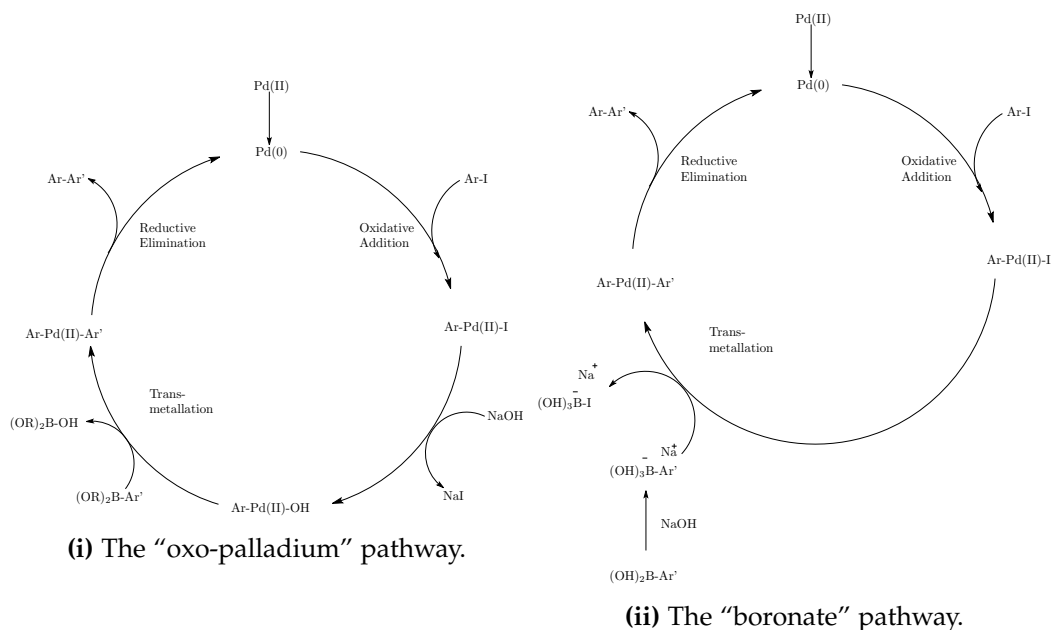


Figure 2.4: Catalytic cycle of the palladium(II)-catalyzed Suzuki-Miyaura cross-coupling reaction.³⁹

This reactivity pattern is unsurprising, as it has been shown that the active transmetalation species in the palladium-catalyzed Suzuki-Miyaura coupling is the boronic acid. That is, in normal aqueous conditions the organoborate (pinacol ester) species hydrolyzes to its corresponding boronic acid that goes on to react with the active palladium species.⁴⁰

A stoichiometric ratio of base interacts either with the reactive palladium or boron species during transmetalation. These two possible transmetalation pathways are called the "oxo-palladium" and "boronate" pathways, shown in

Figure 2.4i and Figure 2.4ii, respectively.

Based on this reactivity, boronic acids (instead of esters) should be used for the final Suzuki-Miyaura cross-coupling step. While boronic acids can be directly synthesized from their corresponding aryl bromides, this direct synthesis poses its own challenges that will be discussed below.⁴⁰ Therefore I decided to first synthesize and purify the boronic esters from their corresponding aryl bromides, then hydrolyze them before using the boronic acid in a Suzuki cross-coupling reaction.

Figure 2.5 illustrates the methods used to attempt hydrolysis of aryl boronic esters to their corresponding aryl boronic acids. Originally hydrolysis of pinacol ester **10** with a diethanolamine-protected boronic ester intermediate **14** gave phenyl boronic acid **15** in good yield, using Sun *et al.*'s method.⁴¹ When attempted with the more electron-rich boron species **21a**, no conversion was seen to the expected diethanolamine-protected boronate species and acidic workup failed to produce the desired aryl boronic acid. Using a method reported by Tzschucke, *et al.*,⁴² boronate **21a** was stirred at room temperature with 3.5 equivalents sodium periodate overnight, followed by acidic workup in 1 M hydrochloric acid. The new method produced alkylarylether boronic acid **22a** in good yield. Subsequent Suzuki cross-coupling between boronic acid **22a** with iodinated quinolone **9** in anhydrous conditions yielded ethyl carbonate protected quinolone **27a** in 12% yield.

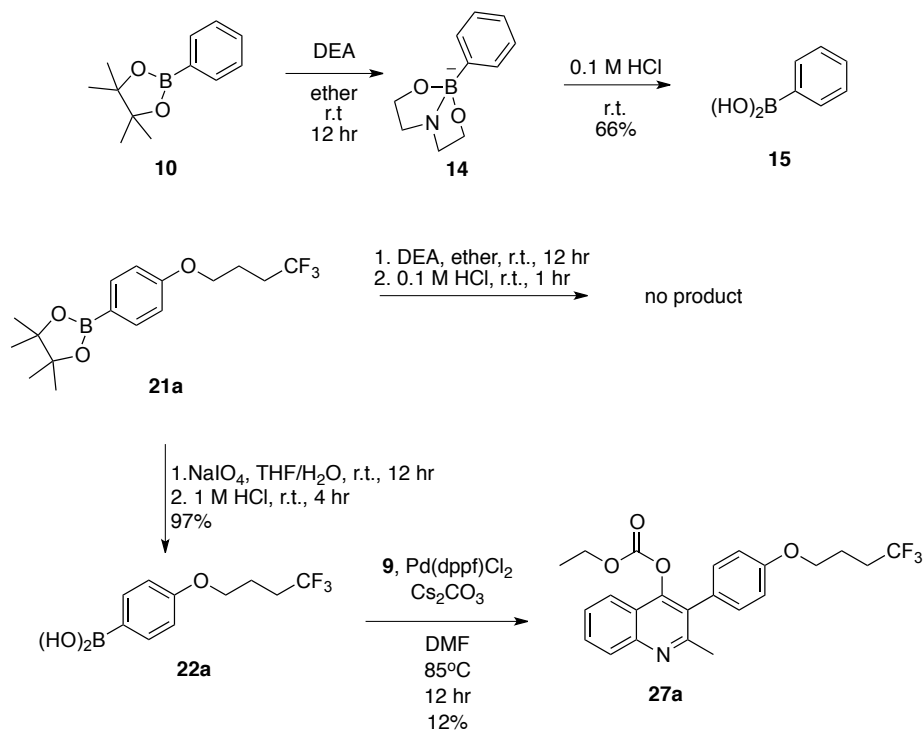


Figure 2.5: Methods employed for hydrolysis of boronic esters to their corresponding boronic acids. A diethanolamine / HCl deprotection method was employed⁴¹ as well as a sodium periodate / HCl method.⁴²

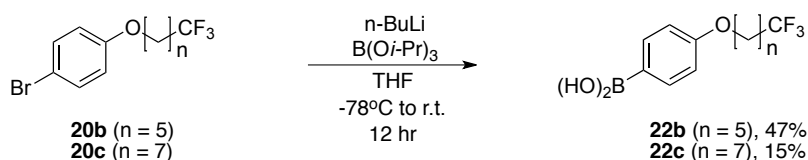


Figure 2.6: Alternative aryl boronic acid synthesis.

In practice, aryl boronic ester hydrolysis with sodium periodate and acidic workup was extremely low-yielding. In light of a limited supply of original trifluoromethyl alkane starting materials for chain lengths $n = 5$ and $n = 7$ toward the end of the synthesis, aryl boronic acids were prepared directly from their corresponding aryl bromides using *n*-butyl lithium and triisopropylborate followed by acidic workup (Fig. 2.6). The boronic acids could be purified using silica column chromatography with a methanol / dichloromethane solvent system. This slightly improved the overall yield from initial starting material to aryl boronic acid compared to the boronic ester intermediate method described above. However, this reaction may not be practical for scale up due to the dangers of using *n*-butyl

lithium, and while yields were relatively low already, they decrease even more significantly if the *n*-butyl lithium is not fresh.

2.2.3 Synthetic Scheme

With the boronic acid synthesis finished and anhydrous Suzuki-Miyaura coupling conditions optimized, a synthesis of 3-biarylether-4(1*H*)-quinolones was attempted. Figure 2.8 shows the synthesis of ELQ-346, ELQ-348, and ELQ-349 with alkyl chain length *n* = 3. Figure 2.9 shows the attempted, yet uncompleted synthesis of **23b** (with alkyl chain length *n* = 5). Finally, Figure 2.10 shows the synthesis of ELQ-347, with alkyl chain length *n* = 7.

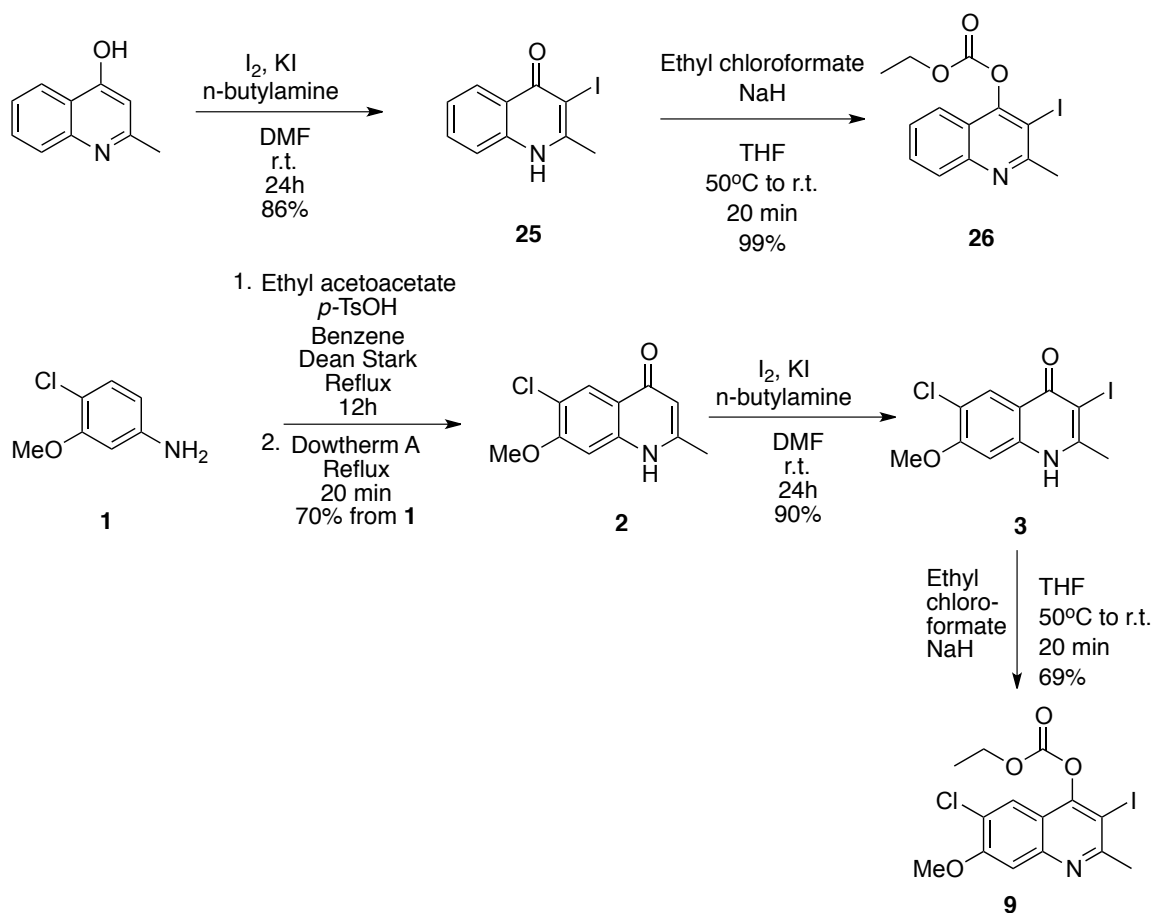


Figure 2.7: Quinolone core functionalization and *O*-ethyl carbonate protection.

Two functionalized quinolone cores were synthesized, the ELQ-300 core (6-chloro-7-methoxy-4(1*H*)-quinolone, **9**), and the ELQ-271 core (unsubstituted at 6

and 7 positions, **26**). ELQ-300 core synthesis (Fig. 2.7) followed previous ELQ syntheses in Conrad-Limpach cyclization of aniline **1** to yield quinolone **2**. The ELQ-271 core was commercially available. Quinolone cores were then iodinated to yield **3** and **25** in good yield. Protection of quinolones **3** and **25** with ethyl chloroformate in dry THF and sodium hydride yielded ethyl carbonate protected quinolones **9** and **26**.

Generally, 3-position alkylarylether boronic acid side chains were synthesized in a 4-step process from 1-bromoalkyl carboxylic acids **18** using SF₄ gas. This was done for most side chain lengths by Dr. Rolf Winter in his lab at Portland State University, though I participated in the synthesis of 1-bromo-8-trifluoromethyloctane **19c**. The subsequent fluorinated species **19** were combined with 4-bromophenol and base to yield 4-bromophenoxy species **20**. Following the optimization discussed above, aryl bromides were converted to aryl boronic acids **22** either through boronic ester intermediates **21** or directly.

With aryl boronic acids **22a**, **22b**, and **22c** in hand, anhydrous Suzuki-Miyaura couplings with either protected ELQ-300 core **9** or ELQ-271 core **26** were attempted. In the end, 3-alkylarylether-4(1*H*)-quinolone *O*-ethyl carbonate ELQ-300 analogs ELQ-348 and ELQ-347 (chain lengths $n = 3$, Fig. 2.8, and $n = 7$, Fig. 2.10) were successfully synthesized in low overall yield. Further, both the *O*-ethyl carbonate ELQ-348 and deprotected ELQ-349 (3-alkylarylether ELQ-271 analogs) were successfully synthesized for chain length $n = 3$ (Fig. 2.8). While all intermediates were successfully synthesized for chain length $n = 5$ (Fig. 2.9), the amount of product from the final Suzuki coupling step proved to be too little to provide more than a negligible amount of purified product.

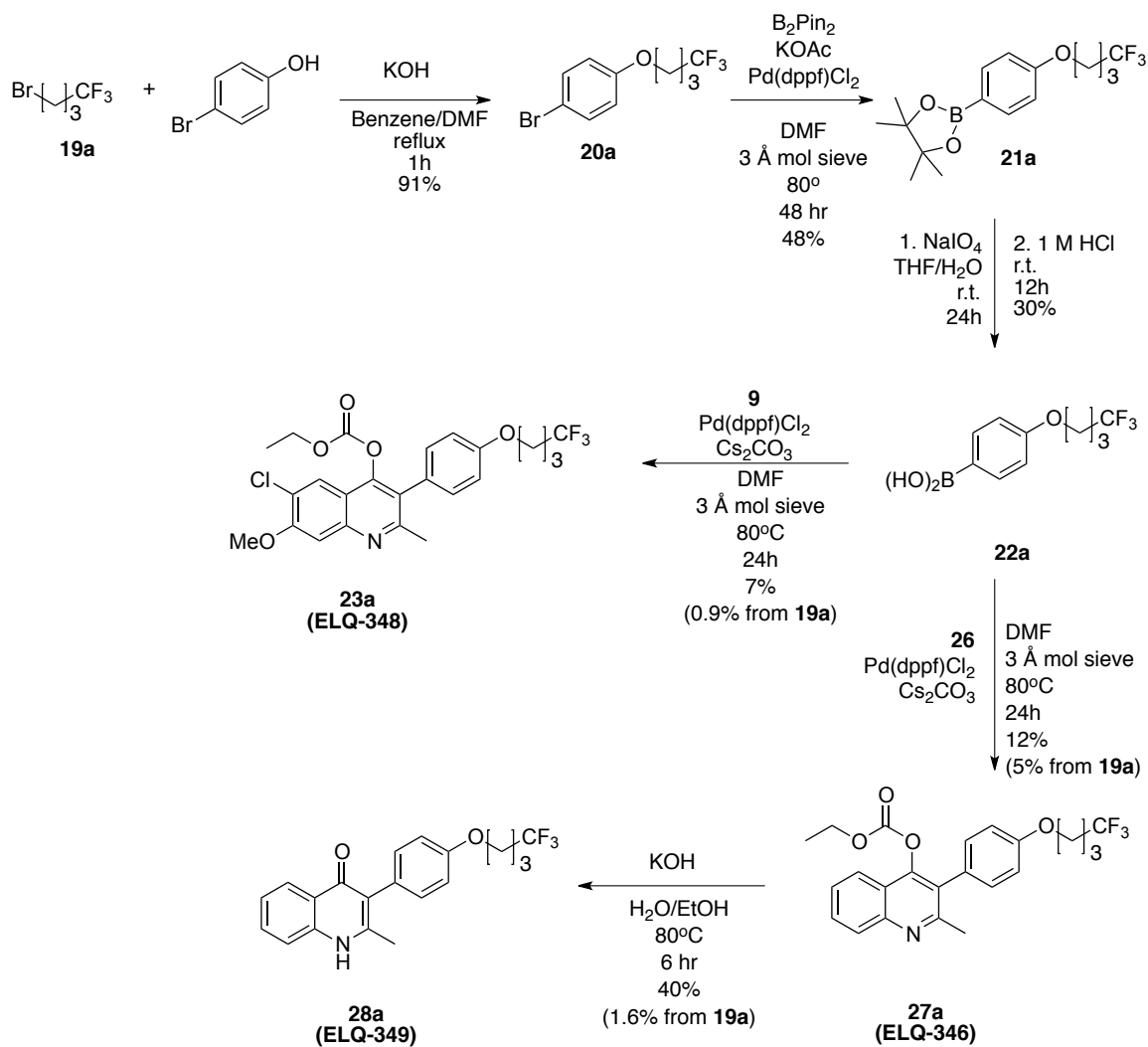
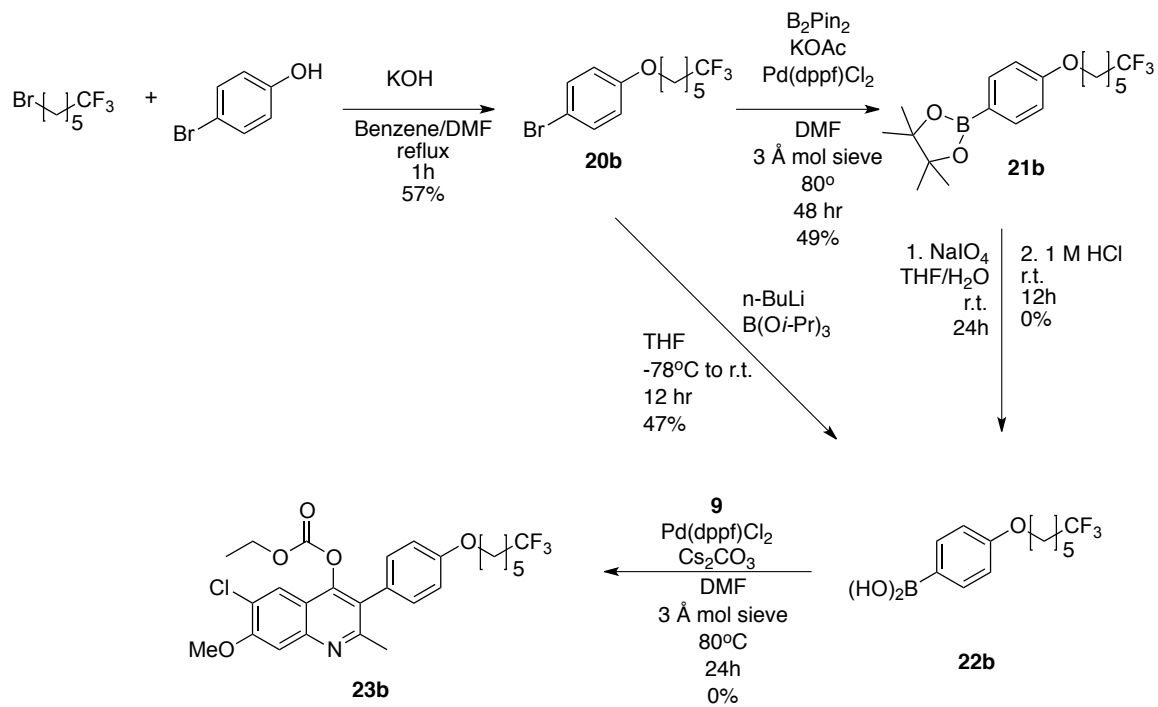
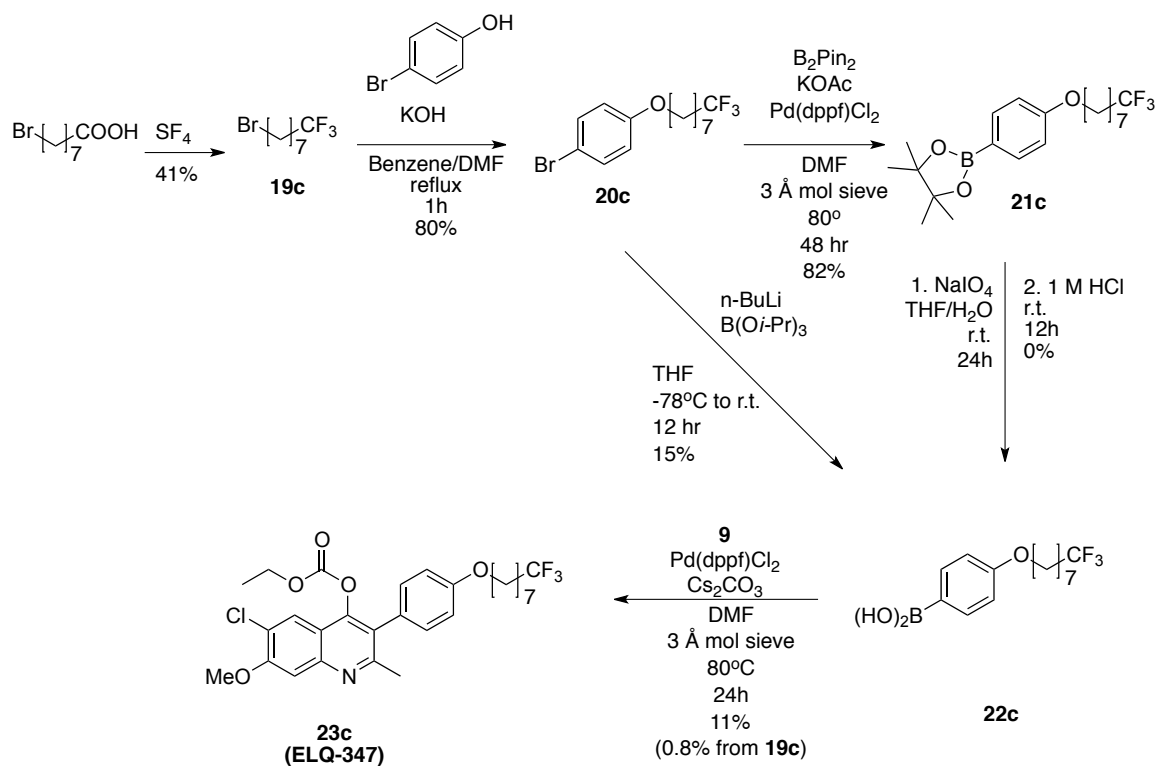


Figure 2.8: Synthesis of 3-alkylarylether-4(1H)-quinolones ELQ-346, ELQ-348, and ELQ-349.

Figure 2.9: Attempted synthesis of 3-alkylarylether-4(1H)-quinolone **23b**.Figure 2.10: Synthesis of 3-alkylarylether-4(1H)-quinolone **ELQ-347**.

Chapter 3

Results and Discussion II: Biological Testing

3.1 Biological Results

3.1.1 *In vitro* Activity

In vitro antiplasmodial activities of target compounds were determined using the SYBR Green I fluorescence-based method developed by Smilkstein *et al.* in 2004.⁴³ ELQ-346, 347, 348 and 349 were tested in various concentrations against TM90-C2B (atovaquone-resistant), and D1 (ELQ-300 resistant) strains of *P. falciparum* in human erythrocytes. Three days after drug administration, red blood cells were lysed and DNA dye SYBR Green I was added. Since *Plasmodium* parasites have DNA but red blood cells do not, measuring fluorescence provides a directly correlated quantification of parasite count. Antiplasmodial activity is quantified by the EC₅₀ value, or the drug dose at which 50% of parasite growth is inhibited relative to uninhibited growth under identical growth conditions.

First, I should note that the data presented cannot be numerically accurate, because the controls used (chloroquine, atovaquone, ELQ-300) did not display activity in line with previous results. Dose-response curves for atovaquone, chloroquine, and ELQ-300 (Fig. 3.1) verified the identity of the parasites (atovaquone was not active against the atovaquone-resistant C2B strain and ELQ-300 was inactive against the ELQ-300 resistant D1 strain). However, the calculated EC₅₀ values for control drug activity against these strains do not agree with literature values.

While the high EC_{50} calculated for atovaquone against C2B (calculated 6600 nM) is near the literature value of 7700 nM,²⁶ both atovaquone and chloroquine show near total growth inhibition at sub-nanomolar concentrations, which is uncharacteristic of their previously reported activity against C2B. Control inhibition of D1 confirms ELQ-300 resistance, but the calculated EC_{50} value is extremely low, at 1.13 nM. While calculated EC_{50} s of control compounds do not agree with literature values, the data presented in Figure 3.1 do indicate with certainty the identity of the *P. falciparum* strains used.

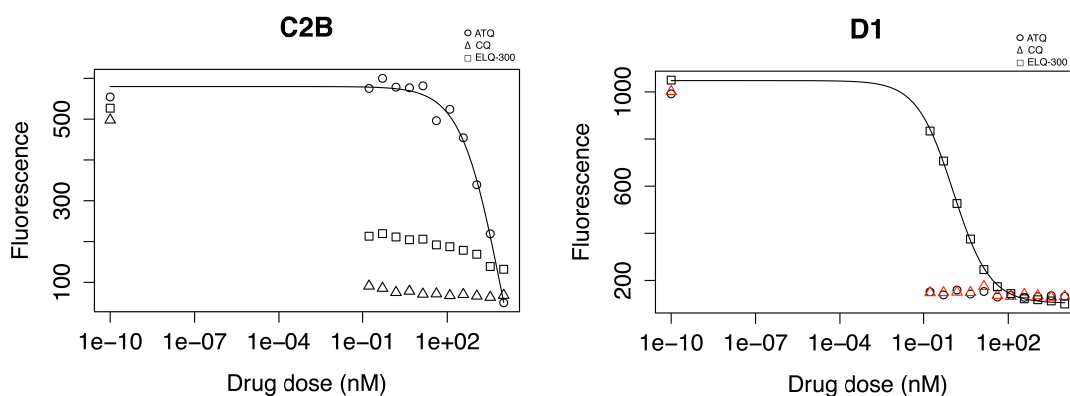


Figure 3.1: Inhibition of TM90-C2B (left) and D1 (right) strains of *P. falciparum* by chloroquine (triangles), atovaquone (circles), and ELQ-300 controls (squares). Parasite count quantified by fluorescence using SYBR Green I fluorescent DNA dye.

Because control EC_{50} s do not agree with literature values, EC_{50} tests for target compounds should be repeated to yield more accurate quantification of *in vitro* antimalarial activity of the target compounds. However even without accurate EC_{50} measurements for target compounds, conclusions can still be made about the relative activity across the target compounds and *P. falciparum* strains. Dose-response curves for all four target compounds against two *P. falciparum* strains are shown in Figure 3.2.

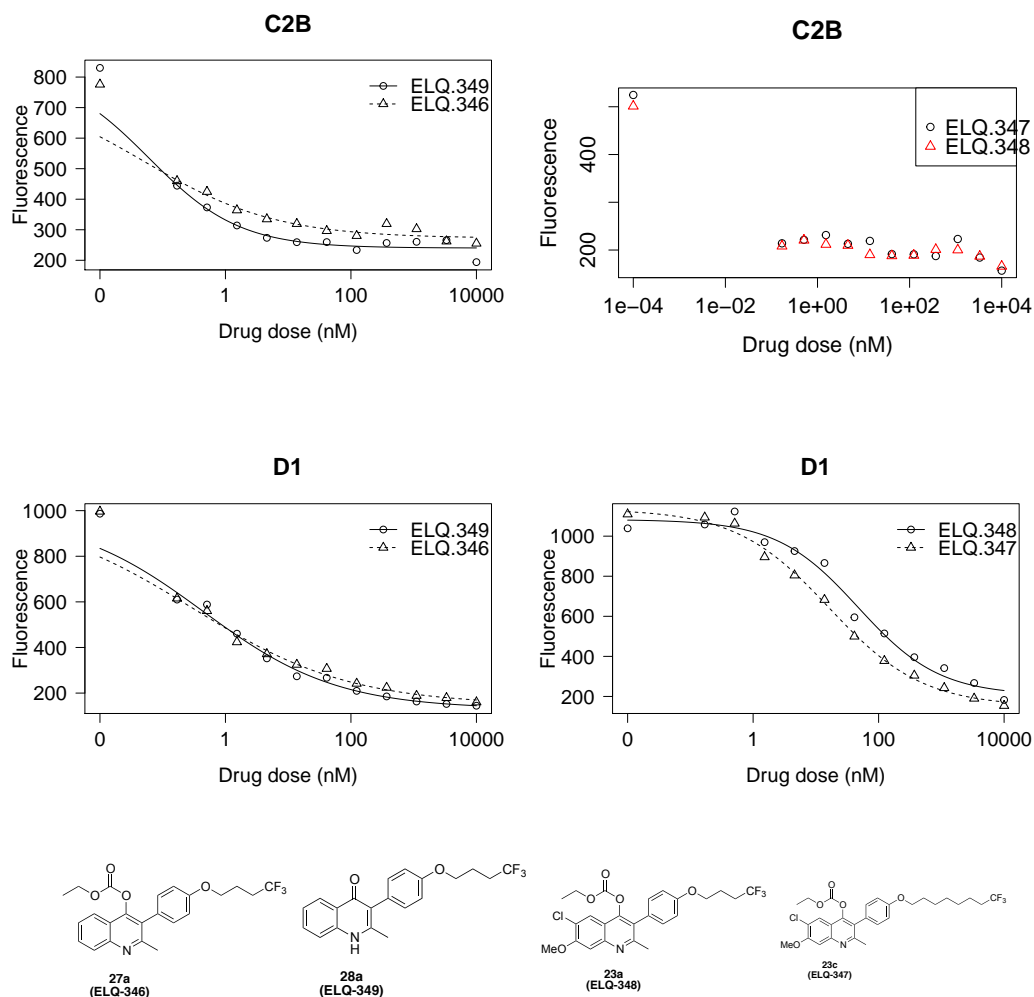


Figure 3.2: Inhibition of D1 strain of *P. falciparum* by ELQ-346,347,348 and ELQ-349. Parasite count quantified by fluorescence using SYBR Green I fluorescent DNA dye.

The relative activities of the target compounds against TM90-C2B and D1 *P. falciparum* isolates (Fig. 3.2) support three hypotheses that were posited above that I will reiterate here.

First, it was noted in Section 1.6 that an ELQ should show similar antimalarial activity to its ethyl carbonate pro-drug. In Figure 3.2, ELQ-349 and its ethyl carbonate pro-drug ELQ-346 demonstrate similar activity against C2B ($EC_{50} = 0.06$ and 0.05 nM, respectively) as well as against D1 ($EC_{50} = 0.44$ and 0.30 nM, respectively).

Second, previous SAR studies described in Section 1.5 led me to predict that longer alkyl chains at the 3-position should lead to better antiplasmodial activity.

Comparing ELQ-347, showing total inhibition of C2B at all tested concentrations, to ELQ-346 ($EC_{50} = 0.05$ nM against C2B), supports this hypothesis.

Finally, earlier studies highlighted in Section 1.4 suggest that substitution of the quinolone core with 6-chloro 7-methoxy substituents increases the Q_i -directing nature of a given antimalarial quinolone. Since *P. falciparum* D1 isolates are resistant to ELQ-300 due to a mutation in the Q_i -site of the parasite's cytochrome bc_1 complex, drugs that target the Q_i site will have their activity significantly dampened by this mutation.

This relationship is confirmed in the comparison of D1 inhibition by ELQ-346 (6/7-unsubstituted, $EC_{50} = 0.30$ nM) and ELQ-348 (6-chloro 7-methoxy, $EC_{50} = 47$ nM). Noting that ELQ-348 was *more* active than ELQ-346 against C2B, but over ten times *less* active than ELQ-346 against D1 demonstrates that in this case, bulky substituents at the 6 and 7 positions do indeed increase selectivity of the drug for the Q_i -site over Q_o .

3.1.2 Inhibition of Human Cytochrome bc_1

ELQ-346, 347, 348, and 349 were tested for inhibitory activity against human cytochrome bc_1 . UV/visible spectrophotometry (absorbance at 550 nm) was used to trace the reduction of cytochrome c in the presence of isolated human mitochondria, ubiquinol, and the drugs of interest over time.

Referring to the schematic of the cytochrome bc_1 mechanism in Section 1.3 (Fig. 1.8), successful turnover of the cytochrome bc_1 enzyme oxidizes cytochrome c . Thus in an uninhibited enzyme, cytochrome c will be oxidized and absorbance at 550 nm will increase over time. Alternatively, if enzyme activity is inhibited absorbance at 550 nm will increase at a slower rate (or not at all) over time. Thus by comparing the rates of absorbance over time relative to uninhibited enzyme rate of cytochrome c oxidatino, one can deduce the fractional velocity of enzyme activity after inhibition by drugs of interest.

Absorbance at 550 nm over time is shown in Figure 3.3 for each of the target compounds as well as uninhibited (black circles) and completely inhibited (antimycin, pink triangles) enzyme. Visually, ELQ-346, ELQ-347, and ELQ-348 have an almost identical slope to the uninhibited enzyme after enzyme addition (note the 20-30 second time frame in Figure 3.3). ELQ-349, has a significantly decreased slope relative to the uninhibited enzyme, suggesting that ELQ-349 is

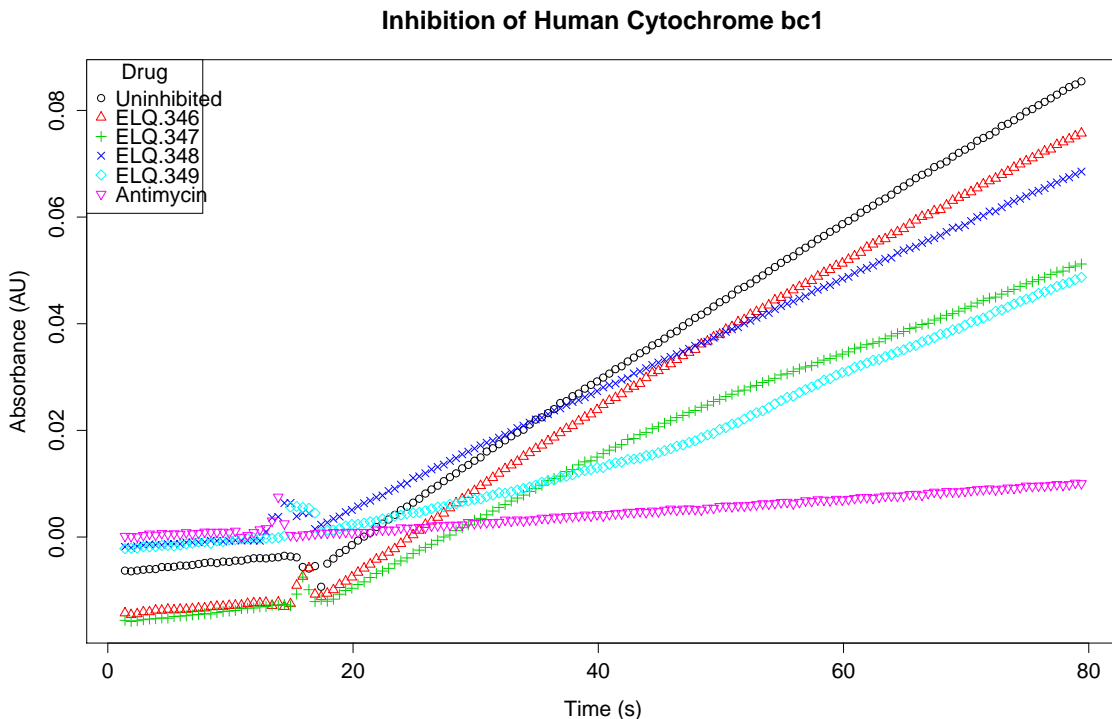


Figure 3.3: Kinetic trace of absorbance of human bc_1 inhibition by $10 \mu\text{M}$ of target compounds ELQ-346, ELQ-347, ELQ-348, and ELQ-349 against uninhibited and completely inhibited (antimycin) controls. Absorbance at 550 nm traces the oxidation of cytochrome c over time. Uninhibited enzyme shown in black circles, completely inhibited enzyme shown in pink triangles. From zero to about 15 seconds shows the background reaction of cytochrome c oxidation by ubiquinol, a jump in the data around 15 seconds comes from the addition of human mitochondria, and slopes after that are indicative of the bc_1 -catalyzed oxidation of cytochrome c .

indeed inhibiting human bc_1 activity.

For the ethyl carbonate quinolones ELQ-346, ELQ-347, and ELQ-348 administered at a high dose ($10 \mu\text{M}$), almost no inhibition of human cytochrome bc_1 activity was observed. After subtracting the slope of background ubiquinol oxidation of cytochrome c in the 0-15 second time frame and finding the fractional velocity of enzyme activity relative to the uninhibited enzyme, enzyme activity when subjected to ELQ-346, ELQ-347, and ELQ-348 had fractional velocities of 1.1, 0.69, and 0.83, respectively. Practically speaking, such little inhibition of enzyme activity at a relatively high dose of drug ($10 \mu\text{M}$) indicates very low affinity of the human enzyme for the three *O*-ethyl carbonate quinolones.

When ELQ-349 was administered at $10 \mu\text{M}$, the enzyme showed a fractional velocity of 0.44, indicating that the IC_{50} of ELQ-349 against human cytochrome

bc_1 is near, but less than, $10 \mu\text{M}$. Repetition of this experiment over various drug concentrations would yield a more accurate IC_{50} value for ELQ-349 inhibition of human cytochrome bc_1 .

It is promising that none of the target compounds presented here showed significant inhibition of human cytochrome bc_1 , even at high drug concentration, while all of them showed some level of antiplasmodial activity. This indicates that the target compounds are selective for the *Plasmodium* over the analogous site in the human host, which is essential for development of a drug with this target.

However, the three drugs that showed no inhibition of human cytochrome bc_1 at $10 \mu\text{M}$ are all ethyl carbonate pro-drugs, which as discussed above, should cleave into their bioactive quinolone counterparts *in vivo*. Thus to more accurately emulate the interaction between human complex III and these drugs *in vivo*, the pharmacologically active quinolones should be used. Since ELQ-347 and ELQ-348 were not synthesized in high enough yield to allow for the final ethyl carbonate deprotection, this poses a future synthetic project to garner a better understanding of their potential inhibitory activity against human cytochrome bc_1 .

3.2 Molecular Modeling

Based on a recent crystal structure by Capper *et al.*⁴⁴ showing that 4-(1H)-pyridones bind to the Q_i site in cytochrome bc_1 in a bovine model, computational modeling was performed to predict analogous ligand / active site interactions with 3-alkylarylether-4(1H)-quinolones. The crystallographic *B. taurus* bc_1 protein information was used as a template to create a homology model of *P. falciparum* cytochrome bc_1 based on the primary sequence of *P. falciparum* cytochrome *b*. The homology model was created using the PHYRE online homology modelling tool.⁴⁵

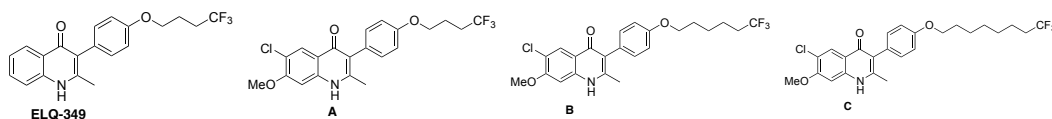


Figure 3.4: 3-alkylarylether-4(1H)-quinolones docked into a *P. falciparum* Q_i site protein model.

Using Glide (Schrödinger, LLC)⁴⁶ the binding of 3-alkylarylether-4(1H)-quinolones was predicted. The compounds docked are shown in Figure 3.4. For each of these compounds, the best five poses after energy minimization in the Q_i binding site are

shown in Figure 3.5. For each compound, there was little variation in quinolone core position across the five docked poses. Longer alkyl chain lengths in compounds **B** and **C** show less tail-end alkyl chain variation in position than the shorter chains of ELQ-349 and **A**.

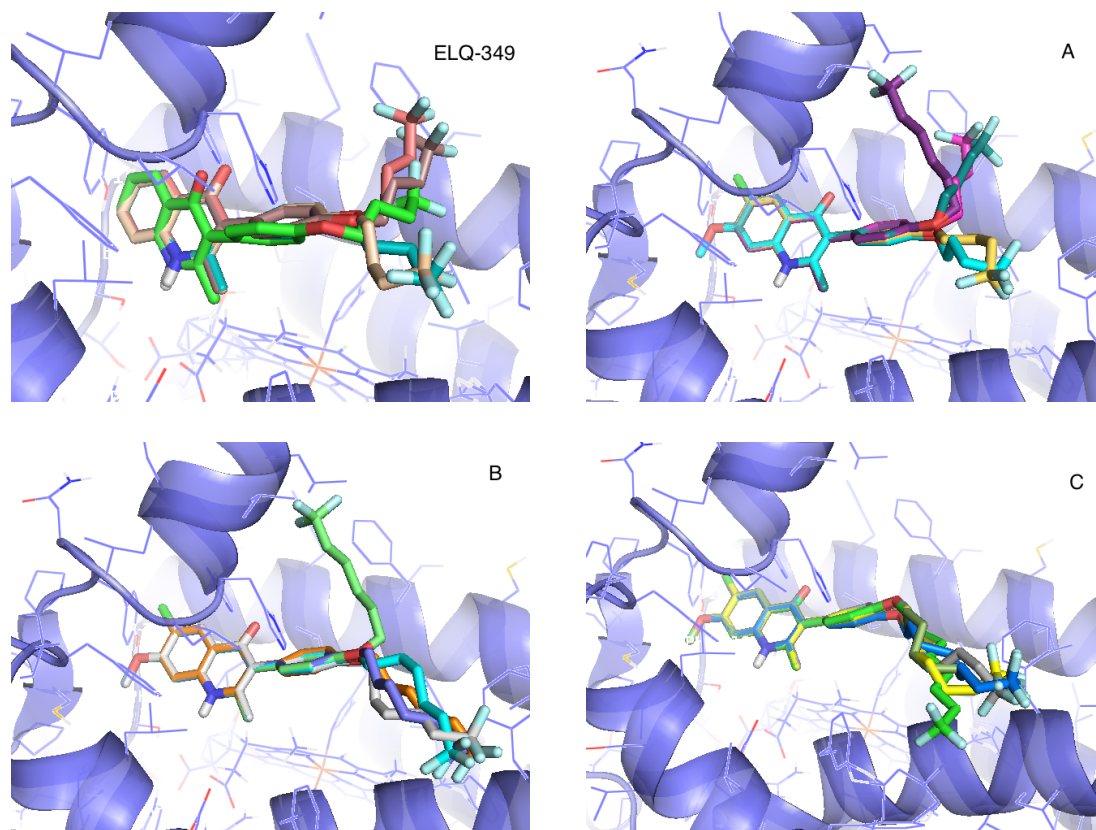


Figure 3.5: Five best-scoring poses for each ligand, ELQ-349, **A**, **B**, and **C** in the Q_i site of *P. falciparum*. Protein rendered as a cartoon in lavender with residues rendered as lines. Ligands rendered as sticks with oxygen in red, nitrogen in blue, chlorine in bright green, and fluorine in seafoam.

Using the best-scoring docking pose for each compound, the positions of **A**, **B**, and **C** docked in the Q_i site are overlaid in Figure 3.6, with **A** in fuschia, **B** in orange, and **C** in orange. Glide docking provided a “Gscore” for each docked ligand that described a combination of calculated coulombic and van der Waals interactions between ligand and receptor. A comparison of these scores suggests that **B** and **C** have the best ligand/receptor interaction (Gscore = - 7.04 and - 6.96 kcal/mol respectively) while **A** performed worse with a Gscore of - 6.63 kcal/mol. While docking scores numerically have little significance, relative comparison

between them suggests that longer alkyl chain 3-alkylarylether-4(1*H*)-quinolones should show tighter binding to the Q_i site of *P. falciparum* than those with shorter alkyl chain lengths.

This relative relationship was substantiated by *in vitro* antimalaria tests in Section 3.1.1 as ELQ-347 (chain length $n=7$) showed better antimalarial activity than ELQ-348 (chain length $n=3$). Docking visualization of **C** in Figure 3.7 suggests a favorable hydrophobic interaction between the end of the alkyl chain of **C** and Phe37. With a shorter alkyl chain length, **A** may not be able to capitalize on this interaction, hence the lower binding affinity for **A** than **C** for the Q_i site. Thus molecular modeling supports the hypothesis that increasing alkyl chain length substitution at the 3 position of an antimalarial will increase antimalarial activity, which was posited in Section 1.5.

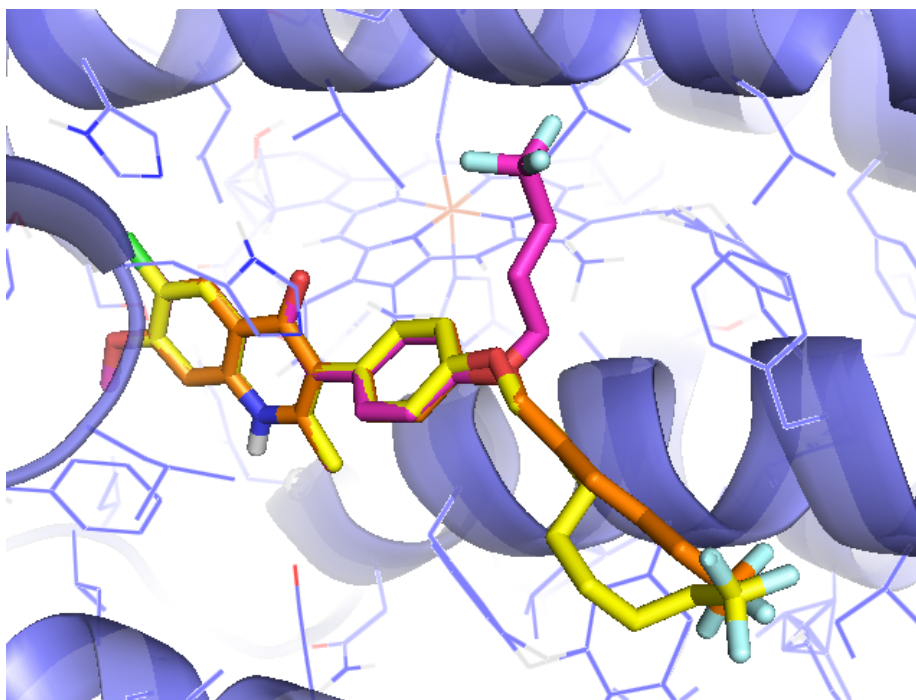


Figure 3.6: ELQ-300 core analogs docked into a Q_i site protein model. Protein rendered as a cartoon in lavender with residues rendered as sticks. Docked compounds are 6-chloro-7-methoxy-3-alkylarylether-4(1*H*)-quinolones **A** (fuschia), **B** (orange), and **C** (yellow). Nonpolar hydrogens are hidden, polar hydrogens in white. Other heteroatoms are colored as: oxygen, red; nitrogen, blue; fluorine, cyan; chlorine, bright green.

As described in Section 1.4 above, earlier SAR studies on ELQs led me to hypothesize that 6-chloro 7-methoxy quinolones should be more Q_i -directing than those unsubstituted at the 6 and 7 positions. This was confirmed in docking

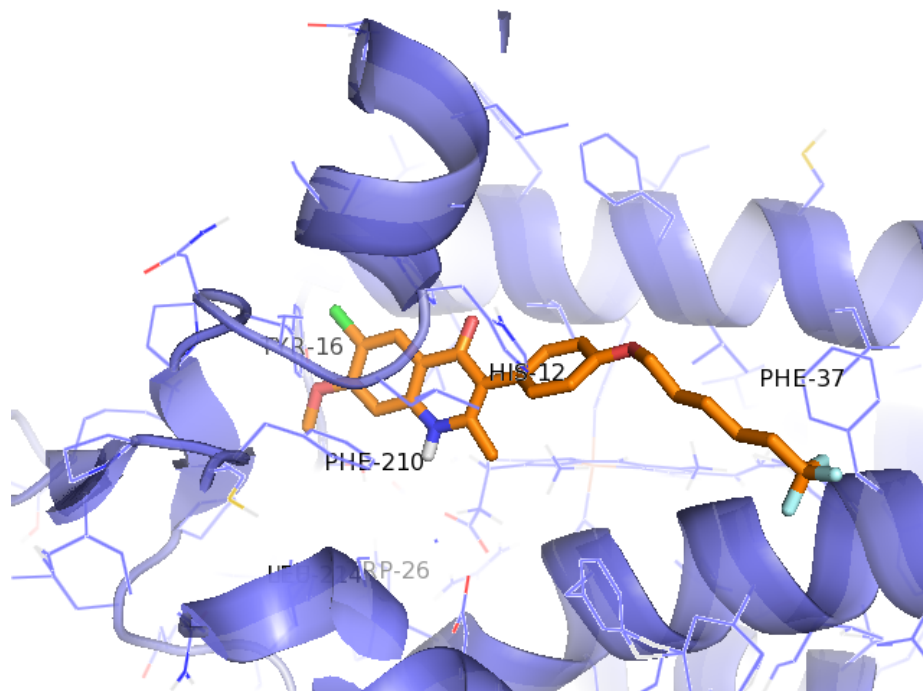


Figure 3.7: **B** docked into a Q_i site protein model. Protein rendered as a cartoon in lavender with residues rendered as sticks, with docked quinolone **B** in orange.

studies, as ELQ-271 core 3-alkylarylether quinolone ELQ-349 scored worse in docking experiments than ELQ-300 analog **A** of the same chain length. Figure 3.8 shows these two compounds docked in the Q_i site (Gscore ELQ-349 = - 6.35 kcal/mol, **A** = - 6.63 kcal/mol). ELQ-349 is shown in green while **A** is shown in pink. The quinolone cores sit in a hydrophobic pocket created by Phe210, Trp26, Ile22 and Tyr16. The greater affinity of 6-chloro 7-methoxy quinolones (or other bulky substituents at these positions) for the Q_i site compared to 6/7-unsubstituted quinolones can be attributed to better hydrophobic interactions with the hydrophobic pocket. This relationship was also seen in *in vitro* experiments in Section 3.1.1 as ELQ-348 (6-chloro 7-methoxy) showed more Q_i -directing character than ELQ-346/ELQ-349 (6/7 unsubstituted).

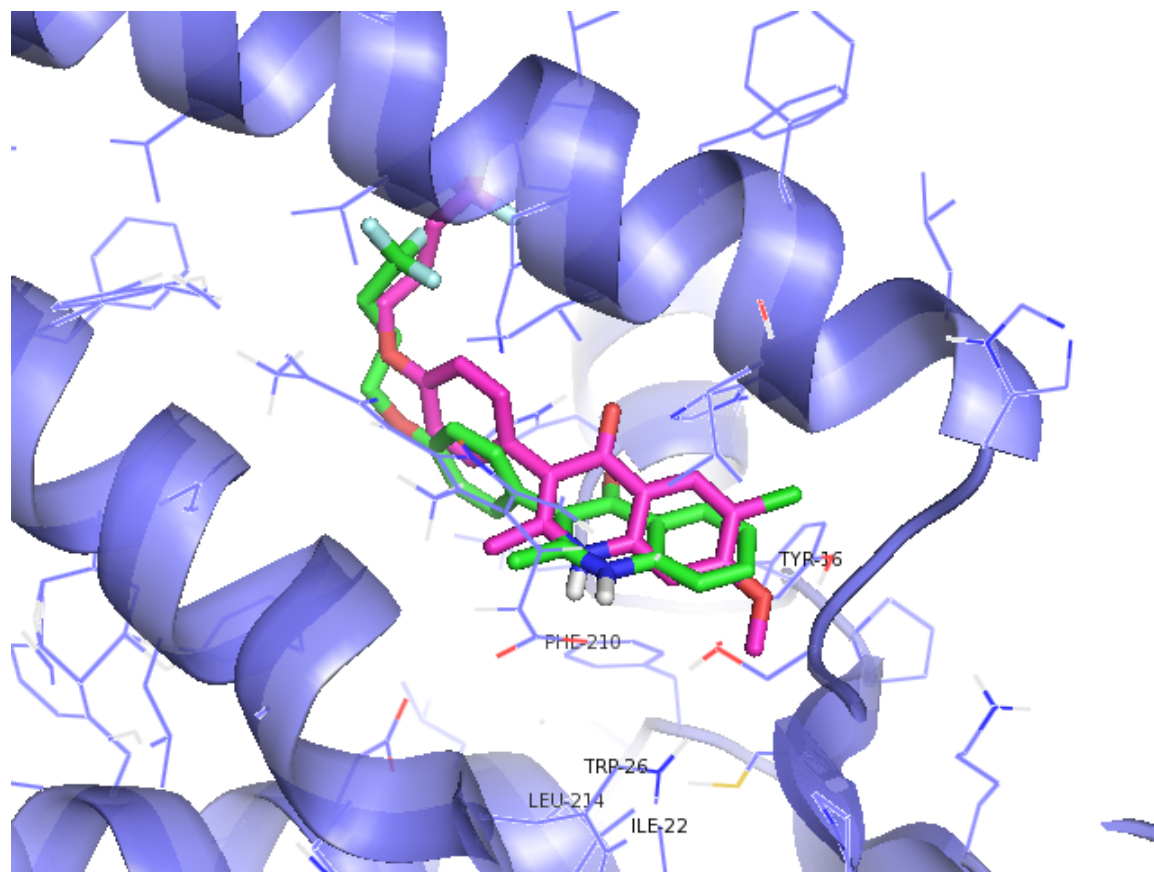


Figure 3.8: Effect of 6- and 7- position substituents on Q_i -site binding conformation. Protein rendered as a cartoon in lavender with residues rendered as sticks. Docked 3-alkylarylether-4(1H)-quinolones are shown in pink (ELQ-349) and green (A).

Chapter 4

Conclusion

The target compounds ELQ-346, ELQ-347, ELQ-348, and ELQ-349 were successfully synthesized in low overall yield (5%, 0.8%, 0.9%, 1.6% respectively). The optimization of anhydrous Suzuki-Miyaura coupling conditions allowed for a novel introduction of base-sensitive ethyl carbonate protecting group to quinolones. Further optimization is needed for the synthesis of alkylarylether boronic acids, as this step proved to be most difficult to obtain the purity necessary for a successful anhydrous Suzuki-Miyaura coupling.

In vitro activity of all four targets against *P. falciparum* isolates indicate promising antimalarial potential, though these experiments should be repeated to obtain more reliable EC₅₀ values for each drug. None of the target compounds showed significant inhibition of human cytochrome *bc*₁. Some previously reported structure-activity relationships were confirmed, namely that longer alkyl chains lead to better antimalarial activity, and that 6-chloro 7-methoxy substitution leads to greater Q_i-site direction and thus lower atovaquone cross-resistance. These relationships were further substantiated by computational docking studies.

Further optimization of 3-alkylarylether-4(1*H*)-quinolone synthesis as well as more accurate quantification of their activity would fine-tune the observations made here, and *in vivo* testing would elucidate their potential as antimalarials. From that point, if this class of ELQ remains a promising antimalarial lead, SAR studies could optimize their antimalarial activity.

The synthesis and characterization of 3-alkylarylether-4(1*H*)-quinolones presented here contributes to the fight against the global malaria epidemic, and future studies on this class of compounds will bolster this contribution.

Chapter 5

Experimental Methods

5.1 Molecular Modeling

The *Plasmodium falciparum* cytochrome *b* primary sequence (Q02768) was downloaded from UNIPROT.⁴⁷ Using the PHYRE online homology tool,⁴⁵ a homology model of *Plasmodium falciparum* cytochrome *bc*₁ was generated using a one to one threading tool with a confidence score of 100% and the available crystal structure for bovine cytochrome *bc*₁ as a template.⁴⁴

Docking was performed using Glide from Schrödinger, LLC and visualized using PyMOL.^{46,48}

5.2 Biology

5.2.1 Parasite Culture

Plasmodium falciparum parasite line Dd2 (multidrug resistant, MRA-156) was obtained from MR24, ATCC Collection, Manassass, Virginia. Atovaquone-resistant clinical isolate Tm90-C2B (containing Y268 to S268 mutation) was originally collected from patients in Thailand exhibiting atovaquone-resistant malaria. The Tm90-C2B isolate was obtained from the frozen parasite repository of the Walter Reed Army Institute of Research, Division of Experimental Therapeutics in Silver Spring, Maryland. The D1 strain (ELQ-300 resistant) was generated at Columbia University in the lab of David Fidock by starting with hypermutable Dd2 under increasing ELQ-300 drug pressure at sublethal but inhibitory concentrations until

ELQ-300 resistant parasites could be clonally isolated.

P. falciparum strains were cultured in human erythrocytes by standard methods.⁴⁹ Human erythrocytes were isolated from blood purchased from Lampire Biologicals (Pipersville, PA, USA) by centrifugation to remove white blood cells. The culture medium used was RPMI-1640 supplemented with 25 mg/L gentamicin sulfate, 45 mg/L Albumax II, 10 mM glucose, and 25 mM HEPES buffer. The parasites were grown in this culture medium with fresh human erythrocytes at a 2% hematocrit level and maintained at less than 10% parasitemia by transfer of infected cells to new erythrocytes in clean culture medium every 3 days.²⁴ Parasites were kept under low-oxygen conditions (5% O₂, 5% CO₂, 90% N₂) at 37°C in an environmental chamber.⁵⁰

5.2.2 EC₅₀ Tests

In vitro antimalarial activity of the compounds described was determined using the SYBR Green I fluorescence-based method described by Smilkstein in 2004.⁴³

Experiments were set up in 96-well plates with a total of 100 μ L total volume per well and a final 2% hematocrit, and 0.2% parasitemia in complete culture medium. Drug concentrations were prepared via 3-fold dilutions of drugs (from 10 mM stock solutions in DMSO), beginning at 10 μ M in complete RPMI medium. Experiments were performed in triplicate for each drug/*P. falciparum* isolate combination. After addition of drugs to the prepared wells, the plates were incubated for 72 hours at 37°C under low-oxygen conditions (5% O₂, 5% CO₂, 90% N₂) in an environmental chamber. After 72 hours, 100 μ L of fluorescent dye-detergent mixture (0.2 μ L SYBR Green I : 1 mL lysing buffer) was added per well and the plates were incubated for 1 hr at room temperature in the dark. After this second incubation period, the plates were read using a 96-well plate reader (Spectramax Gemini-EM, Molecular Diagnostics) with excitation wavelength set at 497 nm and emission at 520 nm. Fluorescence readings were analyzed by plotting against drug concentration, and EC₅₀ values were determined using a nonlinear (four parameter log-logistic function) curve fitting analysis in R.⁵¹ EC₅₀ values were given by the drug concentration at which a 50% decline of fluorescence was observed from drug-free wells.

5.2.3 Inhibition of Human Cytochrome *bc*₁

Isolation of HEK-293 Mitochondria: HEK-293 cells were obtained from Robert Johnson (PVAMC, cells cultured in DMEM with 10% FCS using standard methods). Cell monolayers were treated with trypsin and incubated at 37°C for 30 minutes, at which point they were pelleted (1500 rpm for 10 min) and washed twice with PBS. After resuspending the pellet in PBS with 1 mM PMSF, the cells were passed through a French press at 20000 psi. The lysed cells were centrifuged at 800 *g* for 10 minutes and the supernatant centrifuged at 20000 *g* for 20 minutes. The resulting supernatant was discarded and the pellet was resuspended in 1 mL 30% v/v glycerol/PBS and aliquoted for storage at -80°C.

Measurement of Human Cytochrome *bc*₁ Inhibition: Mitochondria were thawed and suspended in 2 mg/mL *n*-dodecyl β -D-maltoside. After 45 minute incubation at 0°C, the mixture was centrifuged for 5 minutes at 10000 *g*.

Enzymatic activity was measured using a UV/Visible (Agilent 8453 diode array) spectrophotometer measuring absorbance at 550 nm with single reference wavelength 542 nm over 80 seconds at 30°C. The reaction buffer (pH = 8.0) used was 50 mM Tricine, 100 mM KCl, 4 mM NaN₃, 50 μ M cytochrome *c*, 0.1 mg/mL *n*-dodecyl β -D-maltoside. Background cytochrome *c* reductase measurements were recorded after addition of decylubiquinol (prepared by reduction of decylubiquinone with sodium borohydride followed by neutralization with HCl) to the reaction buffer for 5-10 seconds. After this short time, 4 μ L mitochondria were added to the cuvette and the reaction was left to proceed for the remaining 80 seconds of data collection. Activity is calculated as the fractional activity of enzyme under inhibitory conditions relative to uninhibited enzyme under identical conditions.

5.3 Chemistry

5.3.1 General Materials and Methods

All solvents and reagents used in the following syntheses were purchased commercially and used without further purification. Reactions requiring inert atmospheres were carried out in flame-dried glassware under argon atmosphere. All NMR spectra were obtained using a Bruker 400 MHz instrument. NMR data

obtained were calibrated to the internal TMS standard (0.0 ppm) and are reported as: chemical shift (ppm), multiplicity (s, singlet; d, doublet; t, triplet; q, quartet; quint, quintet; m, multiplet; b, broad), coupling constant, and integration.

General Procedure A: Molecular iodine (17.32 mmol, 1 equiv) was dissolved in 18 mL saturated aqueous potassium iodide and added to 4(1*H*)-quinolone (17.32 mmol, 1 equiv) in 35 mL dimethylformamide. To this was added *n*-butylamine (173 mmol, 10 equiv) and the reaction mixture was left to stir for 12 hours. After 12 hours, the reaction was quenched with 0.1 M aqueous thiosulfate, concentrated *in vacuo*, resuspended in water and filtered. Rinsing with ether yielded the 3-iodo-4(1*H*)-quinolone product.

General Procedure B: 3-Iodo-4(1*H*)-quinolone (15.6 mmol, 1 equiv) was dissolved in 75 mL anhydrous tetrahydrofuran under inert atmosphere at 50°C. To this was added sodium hydride (31.2 mmol, 2 equiv) and the mixture was stirred for 15 minutes and allowed to cool to room temperature. Ethyl chloroformate (31.2 mmol, 2 equiv) was added dropwise and the reaction was left to stir for another 15 minutes at which point the mixture was quenched with 1 M HCl. The reaction mixture was taken up in water (15 mL) and dichloromethane (5 mL). The aqueous phase was extracted with dichloromethane (4 × 20 mL) and the organic layers were combined. The combined organic layers were washed with water and brine, dried with magnesium sulfate and concentrated *in vacuo* to yield the 3-iodo-4(1*H*)-quinolone O-ethyl carbonate product.

General Procedure C: 4-Bromophenol (5.13 mmol, 1 equiv.) and potassium hydroxide (5.6 mmol, 1.2 equiv) were dissolved in 8 mL benzene/DMF (1:1 volume:volume) at 70°C for 30 minutes. After 30 minutes, 1-bromo-4,4,4-trifluorobutane (5.6 mmol, 1.1 equiv) was added dropwise and the reaction was heated to reflux until complete by TLC (1 hour). After cooling to room temperature, the reaction mixture was taken up in water (10 mL) and diethyl ether (5 mL) and separated. The aqueous phase was extracted with diethyl ether (3 × 20 mL) and the organic layers were combined. The combined organic layers were washed with water and aqueous potassium carbonate, dried with magnesium sulfate, and concentrated *in vacuo* to give the 4-alkoxybromobenzene product.

General Procedure D: 4-Alkoxybromobenzene (13.6 mmol, 1 equiv), bis(pinacolato)diboron (15.0 mmol, 1.1 equiv), potassium acetate (40.8 mmol, 3 equiv), and 1,1'-bis(diphenylphosphino)ferrocene dichloropalladium (II) (0.68 mmol, 0.05 equiv) were combined in a flame-dried round bottom flask under inert atmosphere with activated 3 Å molecular sieves and 75 mL dimethylformamide. The reaction mixture was stirred at 80°C under inert atmosphere for 48 hours. After 48 hours, the flask was cooled to room temperature and taken up in water (50 mL) and ethyl acetate (15 mL) and separated. The aqueous phase was extracted with ethyl acetate (4 x 15 mL) and the organic layers were combined. Combined organic layers were washed with water and brine, dried over magnesium sulfate, and concentrated *in vacuo*. The crude mixture was purified using silica gel chromatography (ethyl acetate/hexanes) to yield the boronic ester product.

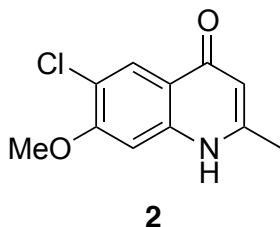
General Procedure E: To a solution of boronic ester (2.27 mmol, 1 equiv) in tetrahydrofuran/water (8 mL, 3:1 THF:water) was added sodium periodate (7.9 mmol, 3.5 equiv). The solution was stirred at room temperature for 18 hours, at which point 1 M HCl was added (5 mmol, 2 equiv) and stirred for 16 hours at room temperature. The reaction was neutralized with 1 M aqueous potassium hydroxide and taken up in water (10 mL) and dichloromethane (5 mL) and separated. The organic layers were combined, washed with water and brine, dried over magnesium sulfate and concentrated *en vacuo*. The crude product mixture was purified using silica gel chromatography (methanol/dichloromethane) to yield the boronic acid product.

General Procedure F: To a solution of 4-alkoxybromobenzene (0.23 mmol, 1 equiv) in 2 mL anhydrous tetrahydrofuran under inert atmosphere at -78°C, n-butyl lithium (0.46 mmol, 2 equiv) was added dropwise and the mixture was stirred at -78°C for 30 minutes. After 30 minutes, triisopropyl borate (0.46 mmol, 2 equiv) was added in one portion and the reaction was allowed to reach room temperature, stirring overnight. After 12 hours, 1 M HCl (1 mmol, 2 equiv) was added and the reaction stirred at room temperature for 6 hours. The mixture was taken up in water (5 mL) and dichloromethane (5 mL) and separated. The aqueous layer was extracted with dichloromethane (3 x 5 mL) and the combined

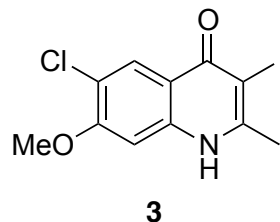
organic layers were washed with water and brine, dried over magnesium sulfate and concentrated *in vacuo*. Subsequent purification by silica gel chromatography (methanol/dichloromethane) yielded the boronic acid product.

General Procedure G: To a solution of boronic acid (3.02 mmol, 1 equiv) in 50 mL anhydrous dimethylformamide and activated 3 Å molecular sieves under inert atmosphere was added 3-iodo-4(1*H*)-quinolone *O*-ethyl carbonate (2.42 mmol, 0.8 equiv), cesium carbonate (2.72 mmol, 0.9 equiv), and 1,1-bis(diphenylphosphino)ferrocene dichloropalladium (II) (0.30 mmol, 0.1 equiv). The reaction mixture was stirred under inert atmosphere at 85°C for until complete by TLC (4 hours). The precipitate was filtered and the filtrate was taken up in water (20 mL) and ethyl acetate (5 mL). The aqueous layer was extracted with ethyl acetate (5 x 5 mL) and the organic layers combined. The combined organic layers were washed with water, brine, dried over magnesium sulfate, and concentrated *in vacuo*. Purification by silica column chromatography (ethyl acetate/hexanes) yielded the 3-alkylarylether-4(1*H*)-quinolone *O*-ethyl carbonate product.

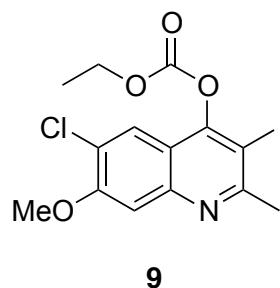
5.3.2 Quinolone Core Functionalization



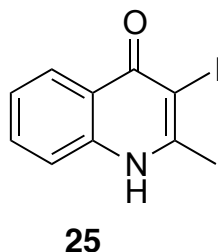
6-Chloro-7-methoxy-2-methylquinolin-4(1*H*)-one (2). Ethylacetoacetate (8.1 mL, 63.5 mmol) and 4-chloro-3-methoxyaniline (10.0 g, 63.5 mL) were stirred with *p*-TsOH (0.30 g, 1.59 mmol) in benzene under Dean-Stark conditions for 12 hours. After 12 hours, the solution was concentrated *in vacuo* and the resulting Schiff base was added dropwise to 150 mL of boiling DOWTHERM-A (250°C). After 20 minutes, the reaction was allowed to cool and the precipitate filtered out. Precipitate was triturated with ethyl acetate and filtered, yielding **2** as a tan fluffy crystal (9.91 g, 70%). ¹H NMR (400 MHz, DMSO-*d*₆) δ 11.57 (s, 1H), 7.95 (s, 1H), 7.03 (s, 1H), 5.87 (q, *J* = 0.8 Hz, 1H), 3.94 (s, 3H), 2.31 (s, 3H).



6-Chloro-3-iodo-7-methoxy-2-methylquinolin-4(1H)-one (3). The title compound was prepared from 4(1H)-quinolone **2** (17.32 mmol) according to general procedure A, yielding 3-iodo-4(1H)-quinolone **3** as a white powder (5.46 g, 90%). ^1H NMR (400 MHz, DMSO- d_6) δ 12.14 (bs, 1H), 8.00 (s, 1H), 7.06 (s, 1H), 3.97 (s, 3H), 2.61 (s, 3H).

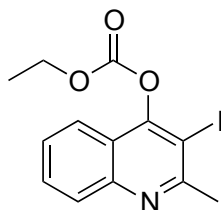


6-Chloro-3-iodo-7-methoxy-2-methylquinolin-4-yl ethyl carbonate (9). The title compound was prepared from 3-iodo-4(1H)-quinolone **3** (15.6 mmol) according to general procedure B, yielding 3-iodo-4(1H)-quinolone *O*-ethyl carbonate **9** as a pale yellow crystalline solid (5.04 g, 69%). ^1H NMR (400 MHz, DMSO- d_6) δ 8.03 (s, 1H), 7.59 (s, 1H), 4.38 (q, $J = 7.0$ Hz, 2H), 4.03 (s, 3H), 2.87 (s, 3H), 1.37 (t, $J = 7.2$ Hz, 3H).



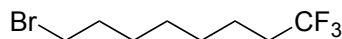
3-Iodo-2-methylquinolin-4(1H)-one (25). The title compound was prepared from commercially available 2-methyl-4-hydroxyquinoline (15.7 mmol) according

to general procedure A, yielding 3-iodo-4(1*H*)-quinolone **25** as a white powder (3.86 g, 86%). ¹H NMR (400 MHz, DMSO-*d*₆) δ 12.14 (bs, 1H), 8.08 (m, 1H), 7.68 (m, 1H), 7.55 (m, 1H), 7.36 (m, 1H), 2.64 (s, 3H).

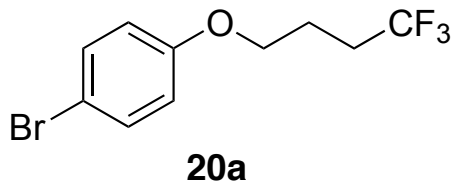
**26**

Ethyl (3-iodo-2-methylquinolin-4-yl) carbonate (26). The title compound was prepared from 3-iodo-4(1*H*)-quinolone **25** according to general procedure B, yielding 3-iodo-4(1*H*)-quinolone **25** *O*-ethyl carbonate **26** as a pale yellow crystalline solid (4.65 g, 99%). ¹H NMR (400 MHz, DMSO-*d*₆) δ 8.09 (m, 1H) 7.94 (m, 1H), 7.88 (m, 1H), 7.70 (m, 1H), 4.40 (q, *J* = 7.2 Hz, 2H), 2.94 (s, 3H), 1.38 (t, *J* = 7.2 Hz, 3H).

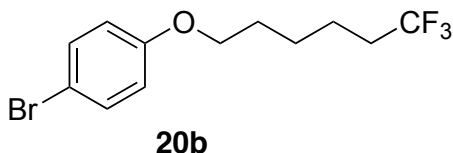
5.3.3 Alkylarylether Side Chains

**19c**

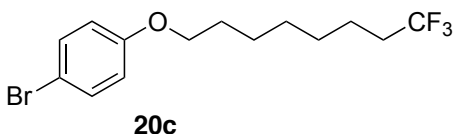
1-Bromo-8,8,8-trifluorooctane (19c). 8-Bromooctanoic acid (10.18 g, 45.7 mmol) was taken up in 10 mL dichloromethane and loaded into a bomb. The bomb was chilled and air removed via vacuum. SF₄ (2.5 L, 91.3 mmol) was condensed to liquid form at -78°C, and subsequently boiled into the bomb containing the octanoic acid. The bomb was sealed and left at room temperature for 72 hours. After 72 hours, the reaction was heated to 100°C for 15 minutes, cooled, and the bomb purged. After quenching with potassium carbonate and extraction with dichloromethane, purification by vacuum distillation yielded **19c** as a clear oil (4.61 g, 41%). ¹H NMR (400 MHz, CDCl₃) δ 3.41 (t, *J* = 6.8 Hz, 2H), 2.05 (m, 2H), 1.86 (quint, *J* = 6.8 Hz, 2H), 1.56 (m, 2H), 1.36-1.45 (m, 6H).



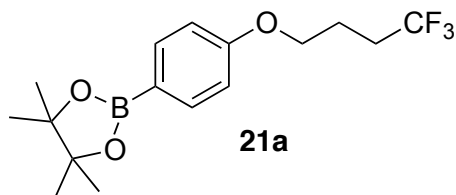
1-Bromo-4-(4,4,4-trifluorobutoxy)benzene (20a). The title compound was prepared from 1-bromo-4,4,4-trifluorobutane (5.6 mmol) according to general procedure C, yielding **20a** as a clear oil (1.32 g, 91%). $^1\text{H NMR}$ (400 MHz, CDCl_3) δ 7.37 (m, 2H), 6.77 (m, 2H), 3.97 (t, $J = 6.0$ Hz, 2H), 2.30 (m, 2H), 2.04 (m, 2H).



1-Bromo-4-((6,6,6-trifluorohexyl)oxy)benzene (20b). The title compound was prepared from 1-bromo-6,6,6-trifluorohexane (5.6 mmol) according to general procedure C, yielding **20b** as a clear oil (0.405 g, 90%). $^1\text{H NMR}$ (400 MHz, CDCl_3) δ 7.36 (m, 2H), 6.76 (m, 2H), 3.93 (t, $J = 6.3$ Hz, 2H), 2.11 (m, 2H), 1.80 (m, 2H), 1.50-1.63 (m, 4H).

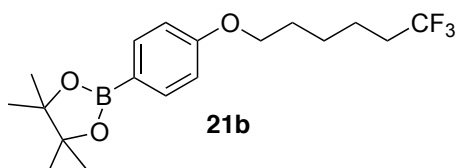


1-Bromo-4-((8,8,8-trifluorooctyl)oxy)benzene (20c). The title compound was prepared from 1-bromo-8,8,8-trifluorooctane (17 mmol) according to general procedure C, yielding **20c** as a clear oil (4.61 g, 80%). $^1\text{H NMR}$ (400 MHz, CDCl_3) δ 7.36 (m, 2H), 6.77 (m, 2H), 3.91 (t, $J = 6.5$ Hz, 2H), 2.06 (m, 2H), 1.77 (m, 2H), 1.30-1.40 (m, 8H).

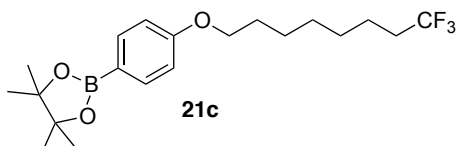


4,4,5,5-Tetramethyl-2-(4-(4,4,4-trifluorobutoxy)phenyl)-1,3,2-dioxaborolane (21a).

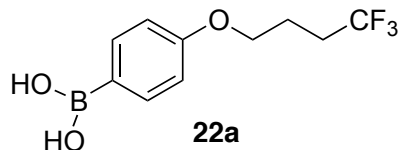
The title compound was prepared from aryl bromide **20a** (4.7 mmol) according to general procedure D, yielding aryl boronic ester **21a** as a clear oil (0.75 g, 48%). $^1\text{H NMR}$ (400 MHz, CDCl_3) δ 7.74 (m, 2H), 6.88 (m, 2H), 4.04 (t, $J = 5.9$ Hz, 2H), 2.28-2.35 (m, 2H), 2.03-2.09 (m, 2H), 1.33 (s, 12H).



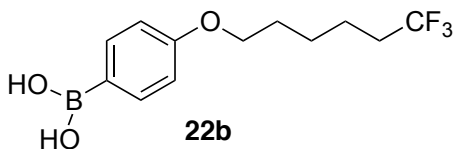
4,4,5,5-Tetramethyl-2-(4-((6,6,6-trifluorohexyl)oxy)phenyl)-1,3,2-dioxaborolane (21b). The title compound was prepared from aryl bromide **20b** (5.32 mmol) according to general procedure D, yielding aryl boronic ester **21b** as a clear oil (0.94 g, 49%). $^1\text{H NMR}$ (400 MHz, CDCl_3) δ 7.74 (m, 2H), 6.87 (m, 2H), 3.99 (t, $J = 6.3$ Hz, 2H), 2.11 (m, 2H), 1.80 (m, 2H), 1.50-1.63 (m, 4H), 1.33 (s, 12H).



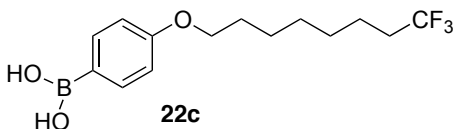
4,4,5,5-Tetramethyl-2-(4-((8,8,8-trifluorooctyl)oxy)phenyl)-1,3,2-dioxaborolane (21c). The title compound was prepared from aryl bromide **20b** (13.6 mmol) according to general procedure D, yielding aryl boronic ester **21c** as a clear oil (4.3 g, 82%). $^1\text{H NMR}$ (400 MHz, CDCl_3) δ 7.74 (m, 2H), 6.88 (m, 2H), 3.98 (t, $J = 6.5$ Hz, 2H), 2.05 (m, 2H), 1.78 (m, 2H), 2.57 (m, 8H), 1.33 (s, 12H).



(4-((4,4,4-Trifluorobutoxy)phenyl)boronic acid (22a). The title compound was prepared from aryl boronic ester **21a** (2.27 mmol) according to general procedure E, yielding aryl boronic acid **22a** as a white solid (0.170 g, 30%). ^1H NMR (400 MHz, DMSO- d_6) δ 7.85 (bs, 1H), 7.74 (m, 2H), 6.90 (m, 2H), 4.06 (t, $J = 6.2$ Hz, 2H), 2.41 (m, 2H), 1.93 (m, 2H).

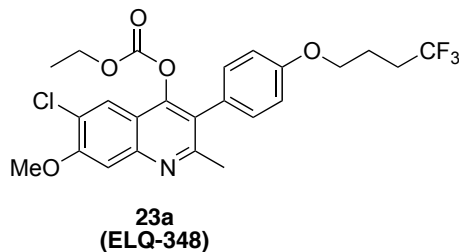


(4-((6,6,6-Trifluorohexyloxy)phenyl)boronic acid (22b). The title compound was prepared from aryl bromide **20b** (0.23 mmol) according to general procedure F, yielding aryl boronic acid **22b** as a white solid (30 mg, 47%). ^1H NMR (400 MHz, DMSO- d_6) δ 7.72 (m, 2H), 6.87 (m, 2H), 3.99 (t, $J = 6.5$ Hz, 2H), 2.23-2.31 (m, 2H), 1.75 (m, 2H), 1.48-1.59 (m, 4H).

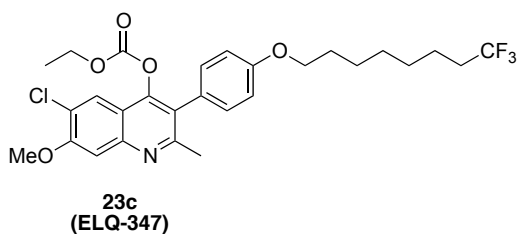


(4-((8,8,8-Trifluorooctyloxy)phenyl)boronic acid (22c). The title compound was prepared from aryl bromide **20c** (2.37 mmol) according to general procedure F, yielding aryl boronic acid **22c** as a white solid (0.11 g, 15%). ^1H NMR (400 MHz, DMSO- d_6) δ 7.72 (m, 2H), 6.87 (m, 2H), 3.96 (t, $J = 6.7$ Hz, 2H), 2.19-2.26 (m, 4H), 1.70 (m, 4H), 1.28-1.42 (m, 4H).

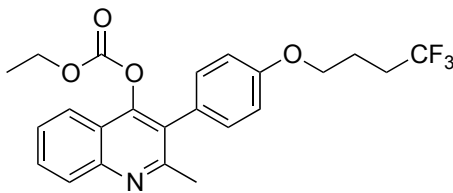
5.3.4 Target Compounds



6-Chloro-7-methoxy-2-methyl-3-(4-(4,4,4-trifluorobutoxy)phenyl)quinolin-4-yl ethyl carbonate (23a, ELQ-348). The title compound was prepared from boronic acid **22a** (0.68 mmol) and protected quinolone **9** according to general procedure G, yielding **23a** as a white solid (25 mg, 7%). ¹H NMR (400 MHz, CDCl₃) δ 7.88 (s, 1H), 7.48 (s, 1H), 7.22 (m, 2H), 6.97 (m, 2H), 4.12 (q, *J* = 7.1 Hz, 2H), 4.09 (t, *J* = 6.1 Hz, 2H), 4.05 (s, 3H), 2.51 (s, 3H), 2.35 (m, 2H), 2.10 (m, 2H), 1.17 (t, *J* = 7.1 Hz, 3H).

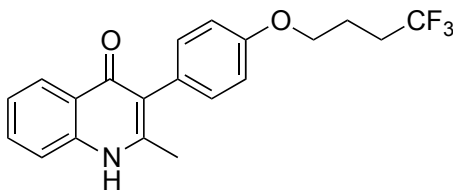


6-Chloro-7-methoxy-2-methyl-3-(4-((8,8,8-trifluorooctyl(oxy)))phenyl)quinolin-4-yl ethyl carbonate (23c, ELQ-347). The title compound was prepared from boronic acid **22c** (0.43 mmol) and protected quinolone **9** according to general procedure G, yielding **23c** as a white solid (26 mg, 11%). ¹H NMR (400 MHz, CDCl₃) δ 7.88 (s, 1H), 7.48 (s, 1H), 7.20 (m, 2H), 6.98 (m, 2H), 4.12 (q, *J* = 7.1 Hz, 2H), 4.05 (s, 3H), 4.01 (t, *J* = 6.5 Hz, 2H), 2.51 (s, 3H), 2.05-2.12 (m, 2H), 1.79-1.84 (m, 2H), 1.42 (m, 4H), 1.32-1.36 (m, 4H), 1.17 (t, *J* = 7.1 Hz, 3H).



27a
(ELQ-346)

Ethyl (2-methyl-3-(4-(4,4,4-trifluorobutoxy)phenyl)quinolin-4-yl) carbonate (27a, ELQ-346). The title compound was prepared from boronic acid **22a** (3.02 mmol) and protected quinolone **26** according to general procedure G, yielding **27a** as a white solid (0.160 g, 12%). ^1H NMR (400 MHz, $\text{DMSO-}d_6$) δ 8.06 (m, 1H), 7.86 (m, 1H), 7.81 (m, 1H), 7.64 (m, 1H), 7.25 (m, 2H), 7.09 (m, 2H), 4.11 (m, 4H), 2.46 (2, 3H), 2.45 (m, 2H), 1.99 (m, 2H), 1.10 (t, $J = 7.1$ Hz, 3H).



28a
(ELQ-349)

2-methyl-3-(4-(4,4,4-trifluorobutoxy)phenyl)quinolin-4(1H)-one (28a, ELQ-349). To 5 mL water was added potassium hydroxide (0.54 g, 9.6 mmol), which was stirred until dissolved at 80°C . *O*-ethyl carbonate quinoline **23a** (0.13 g, 0.30 mmol) was dissolved in 15 mL ethanol and added to the aqueous potassium hydroxide solution. The reaction mixture was stirred at 80°C until complete by TLC (6 hours) at which point the title compound was triturated with water and filtered, yielding **28a** as a white solid (0.043 g, 40%). ^1H NMR (400 MHz, $\text{DMSO-}d_6$) δ 11.59 (bs, 1H), 8.07 (m, 1H), 7.64 (m, 1H), 7.53 (m, 1H), 7.29 (m, 1H), 7.17 (m, 2H), 6.97 (m, 2H), 4.09 (t, $J = 6.3$ Hz, 2H), 2.41-2.48 (m, 2H), 2.24 (s, 3H), 2.94-2.02 (m, 2H).

Appendix A

NMR Data

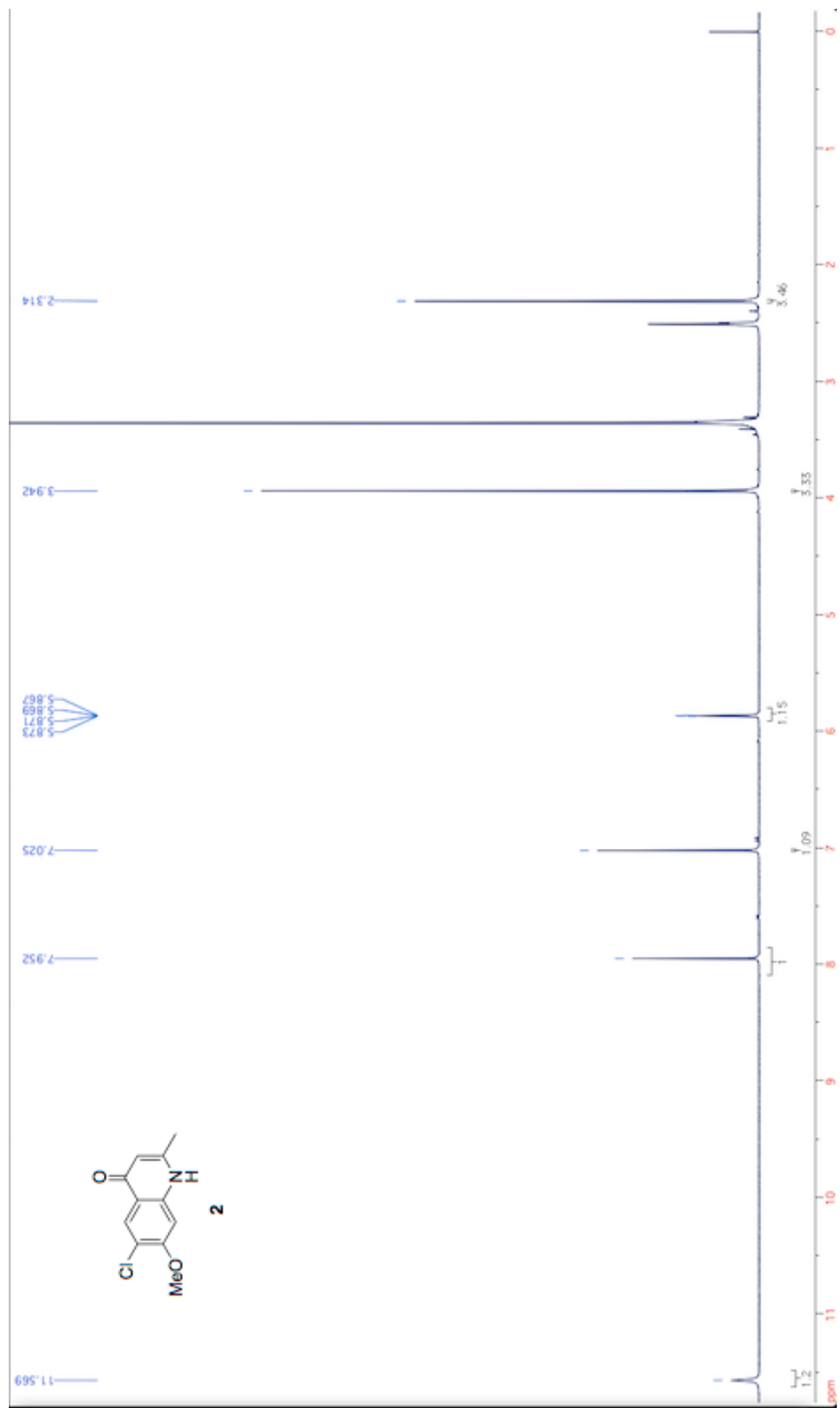


Figure A.1: ^1H NMR spectrum of compound (2) in $\text{DMSO-}d_6$.

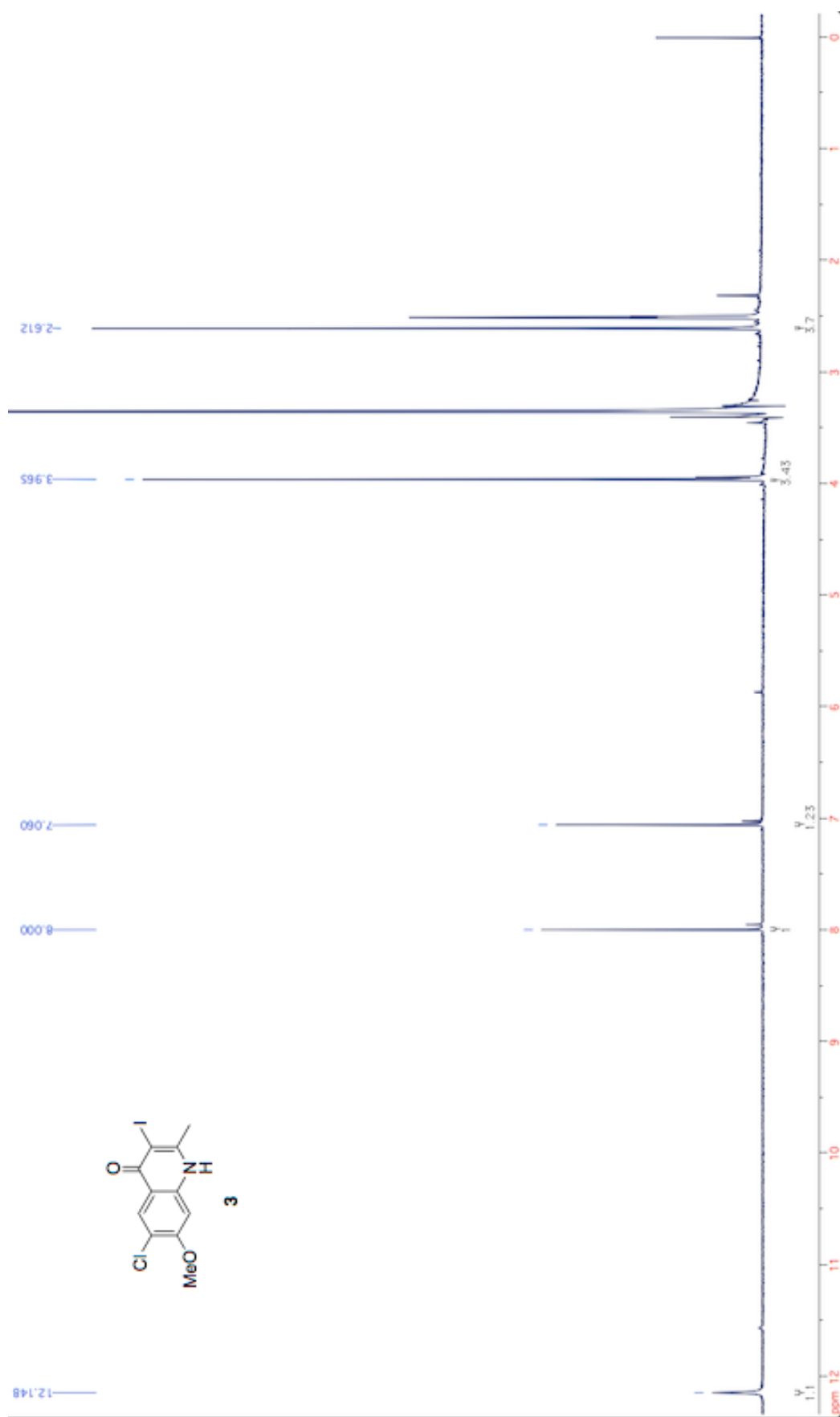


Figure A.2: ^1H NMR spectrum of compound (3) in $\text{DMSO-}d_6$.

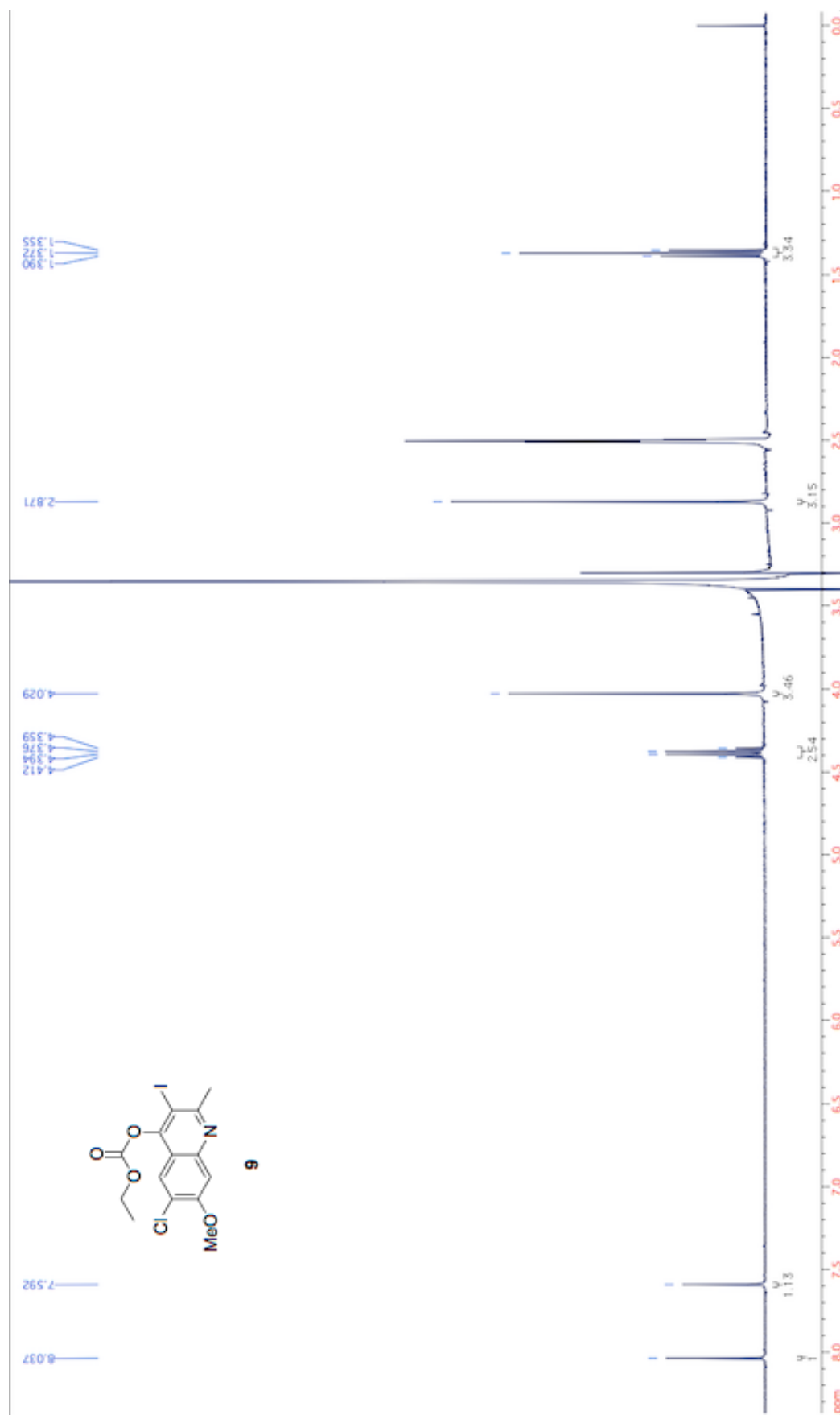


Figure A.3: ^1H NMR spectrum of compound (9) in $\text{DMSO-}d_6$.

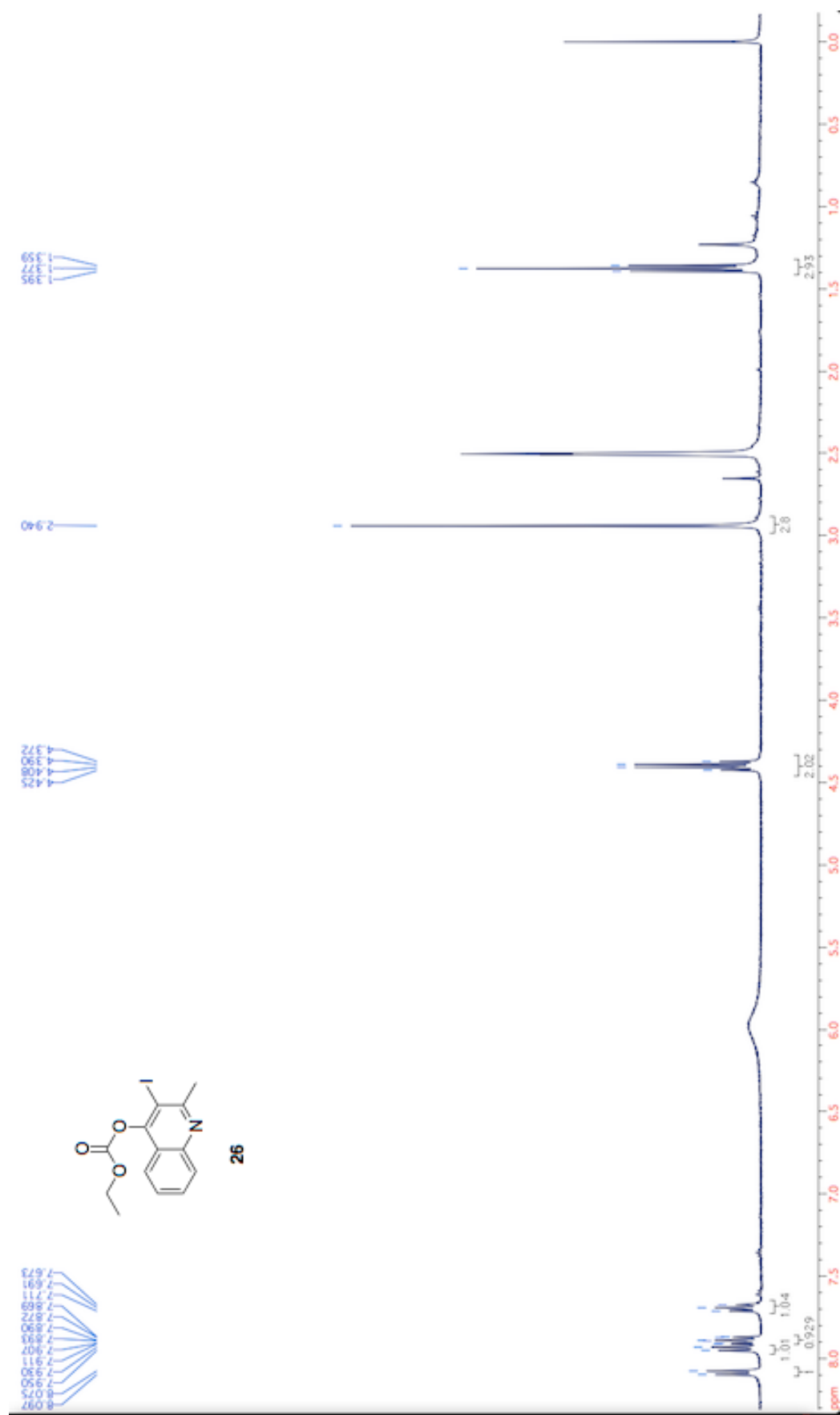


Figure A.5: ^1H NMR spectrum of compound (26) in $\text{DMSO-}d_6$.

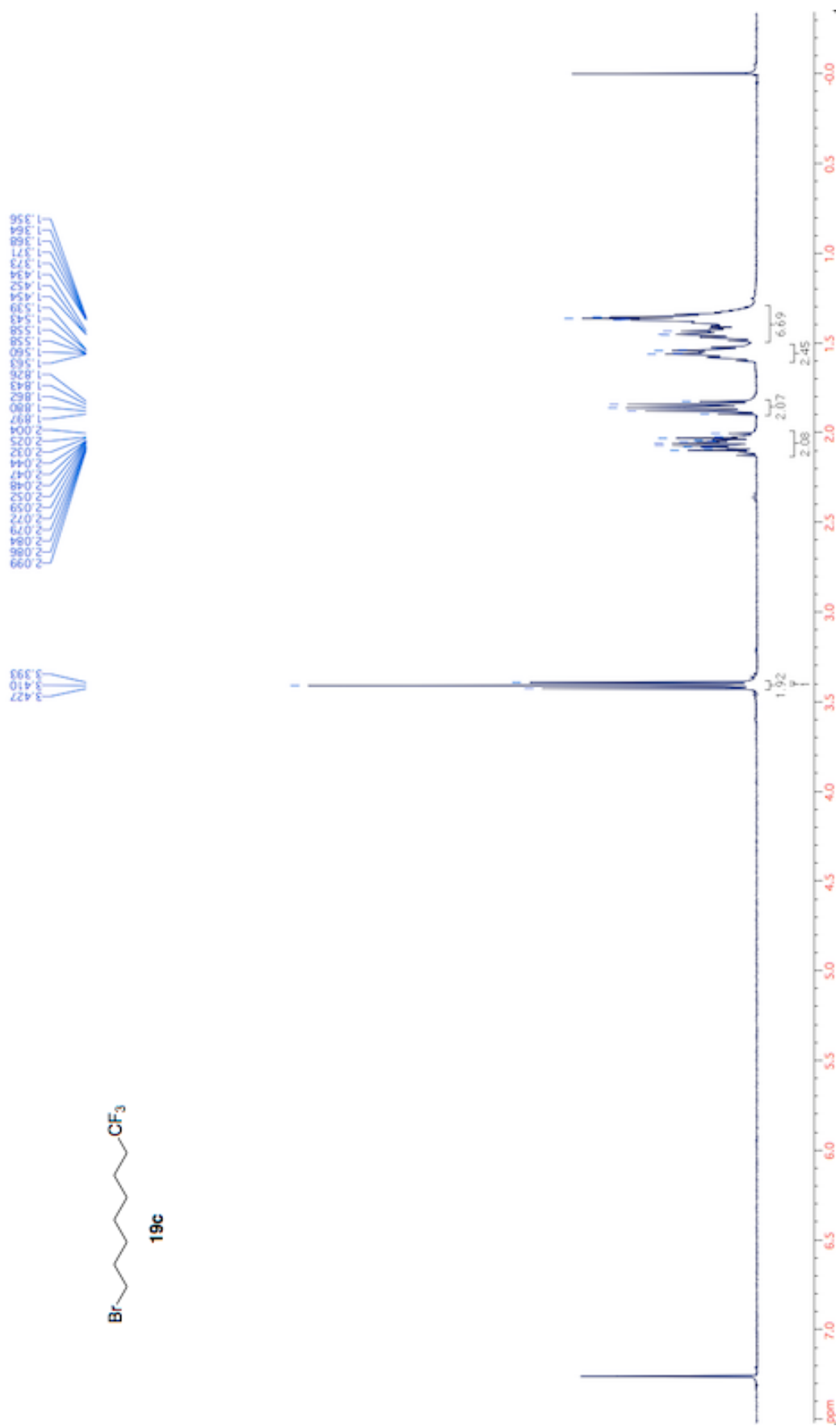


Figure A.6: ^1H NMR spectrum of compound (**19c**) in CDCl_3 .

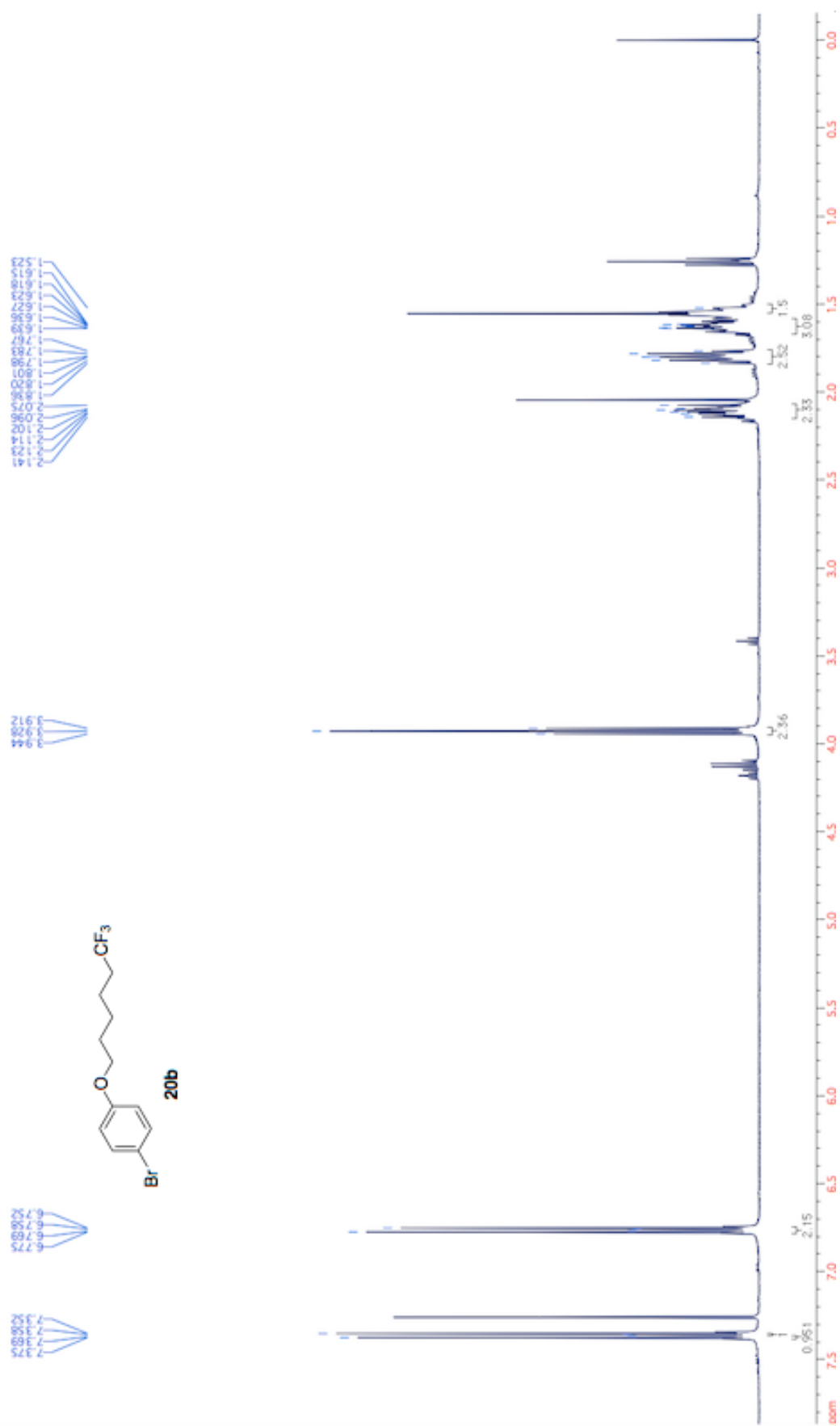


Figure A.8: ^1H NMR spectrum of compound (**20b**) in CDCl_3 .

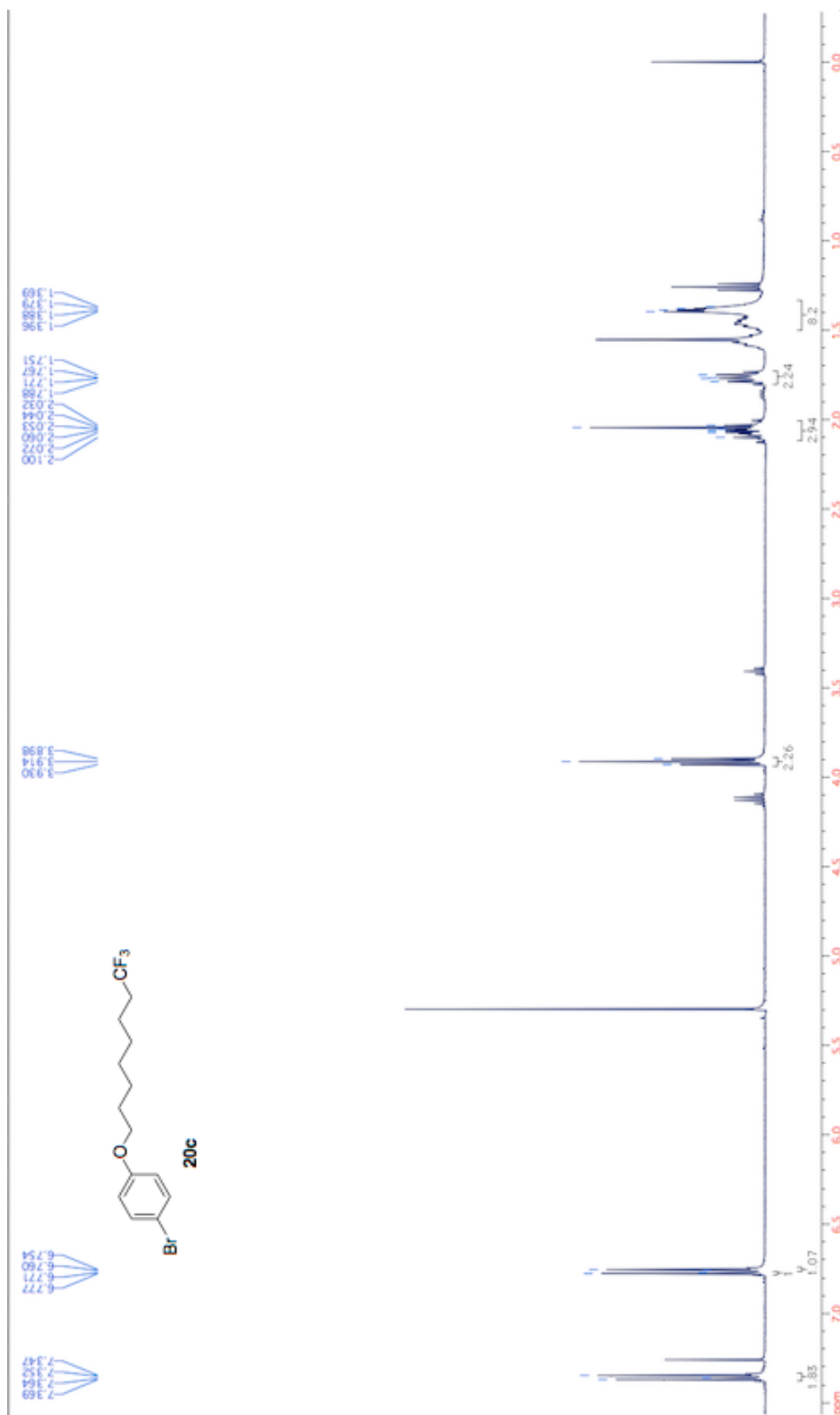


Figure A.9: ^1H NMR spectrum of compound (**20c**) in CDCl_3 .

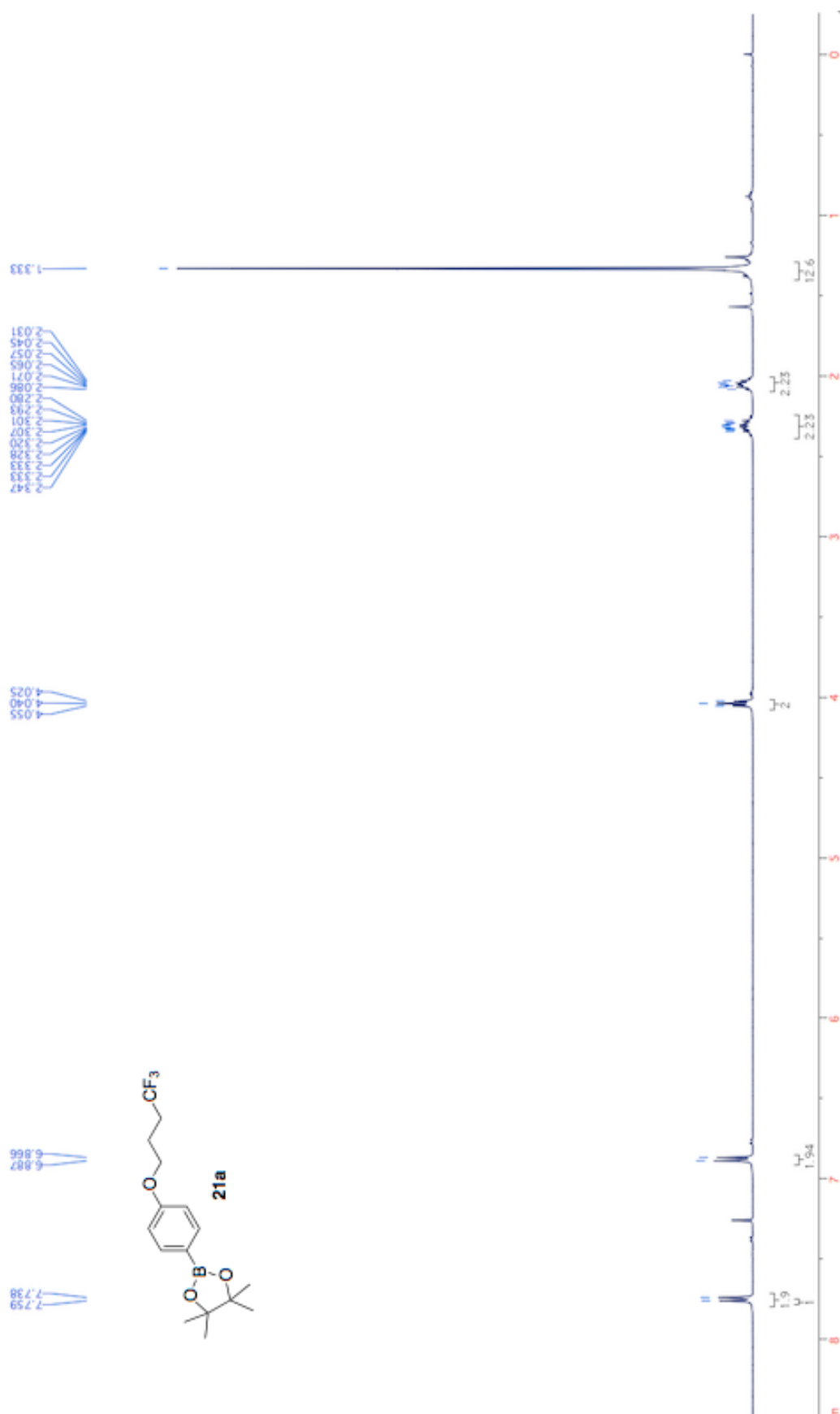


Figure A.10: ^1H NMR spectrum of compound (**21a**) in CDCl_3 .

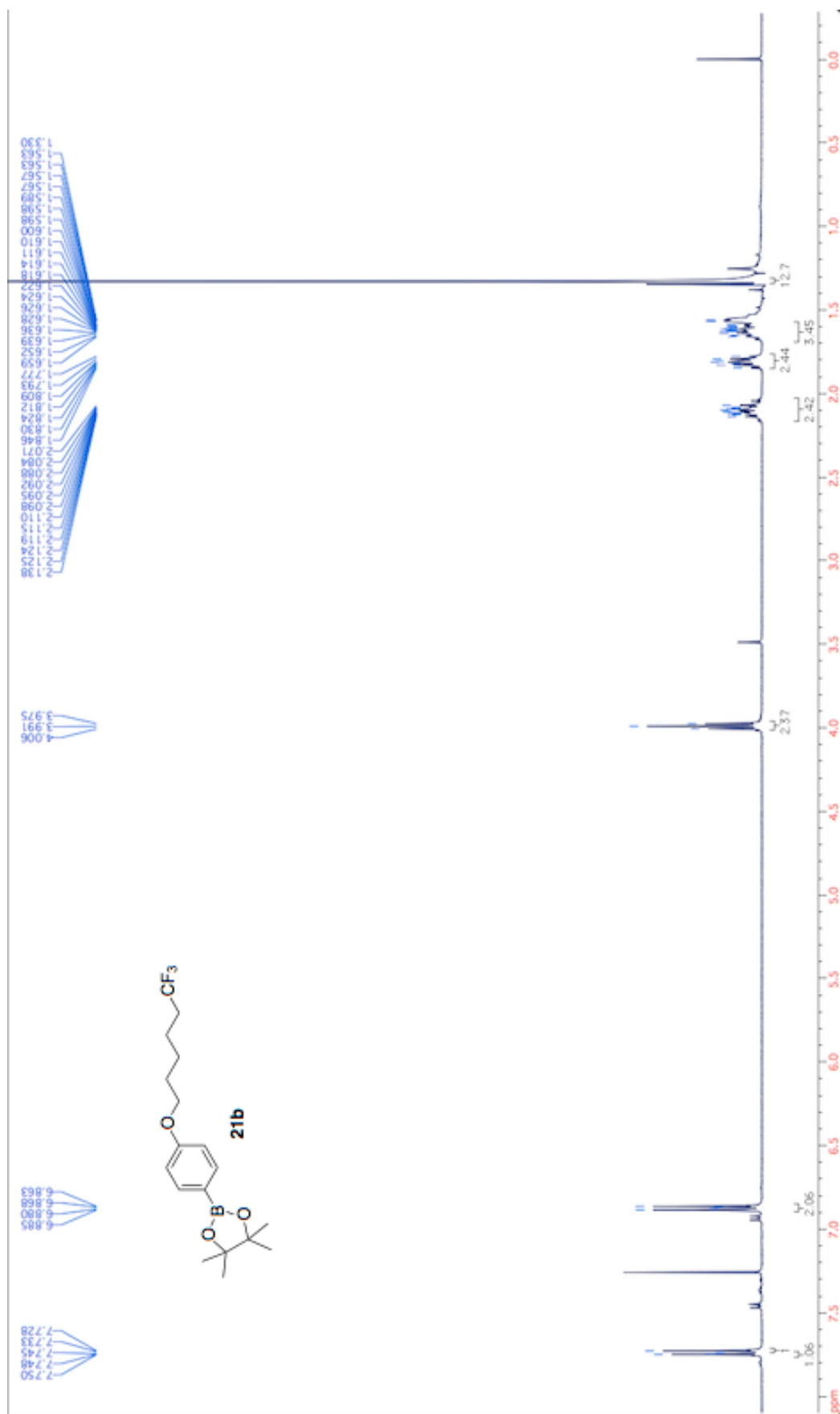


Figure A.11: ^1H NMR spectrum of compound (**21b**) in CDCl_3 .

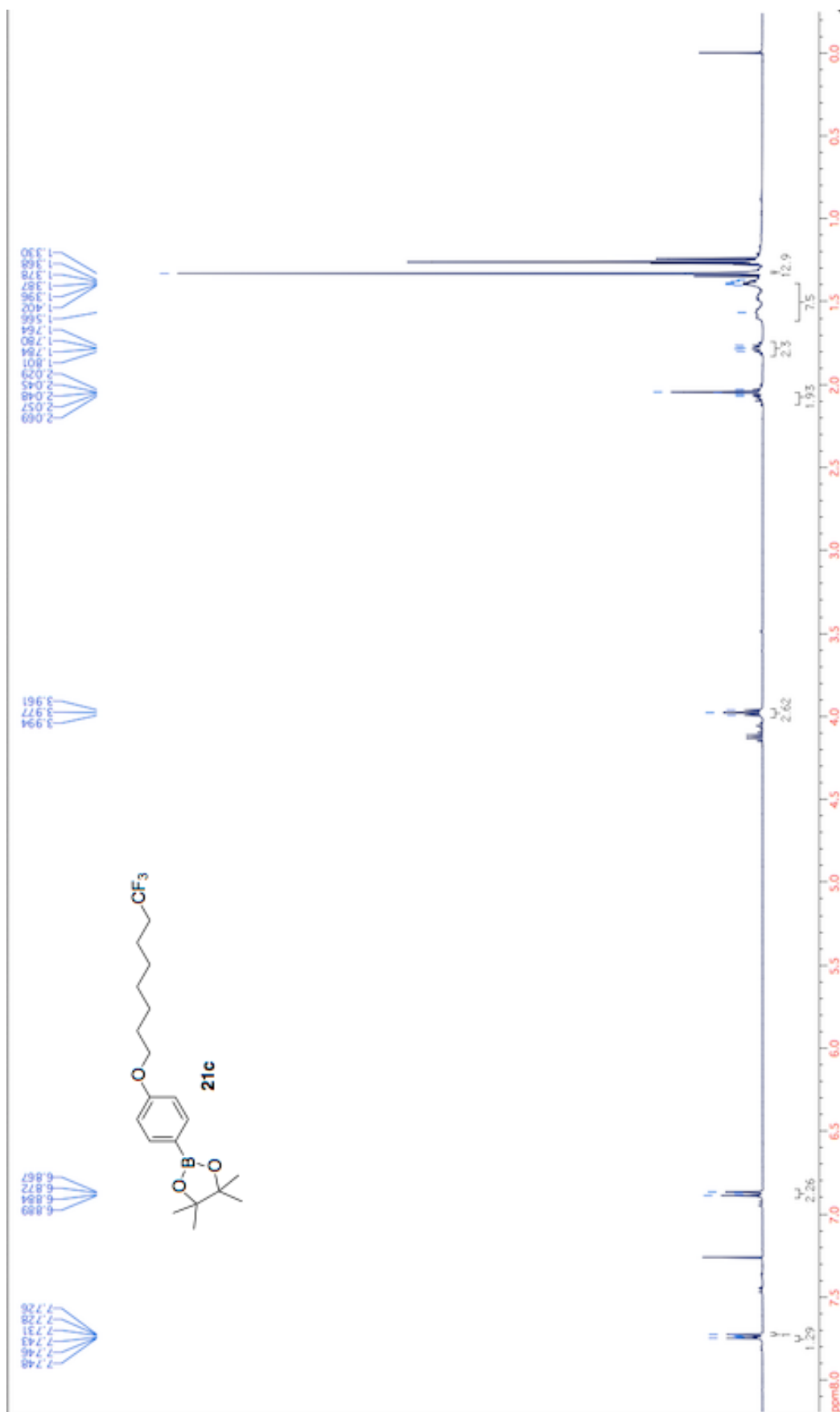


Figure A.12: ^1H NMR spectrum of compound (**21c**) in CDCl_3 .

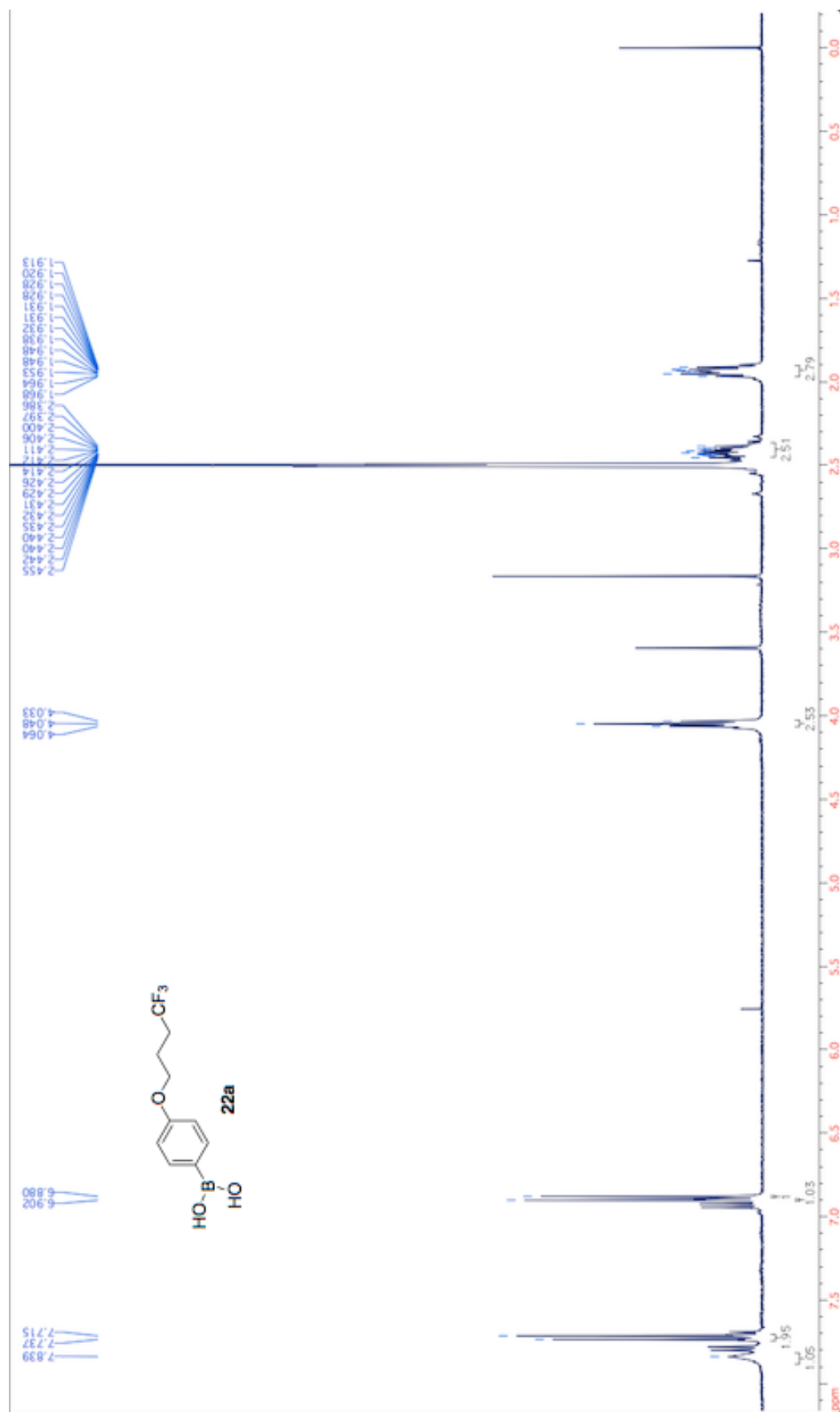


Figure A.13: ^1H NMR spectrum of compound (**22a**) in $\text{DMSO-}d_6$.

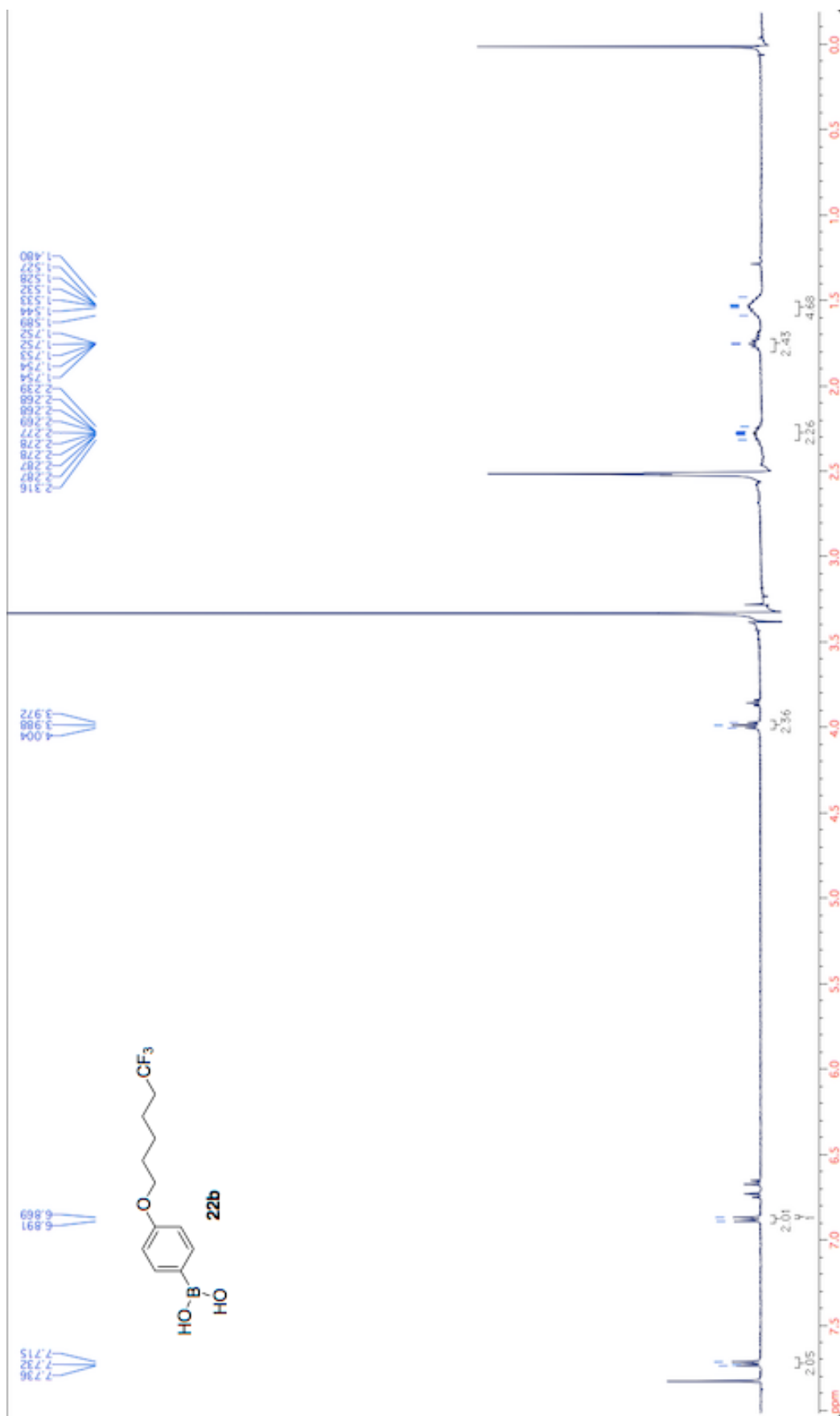


Figure A.14: ^1H NMR spectrum of compound **(22b)** in $\text{DMSO-}d_6$.

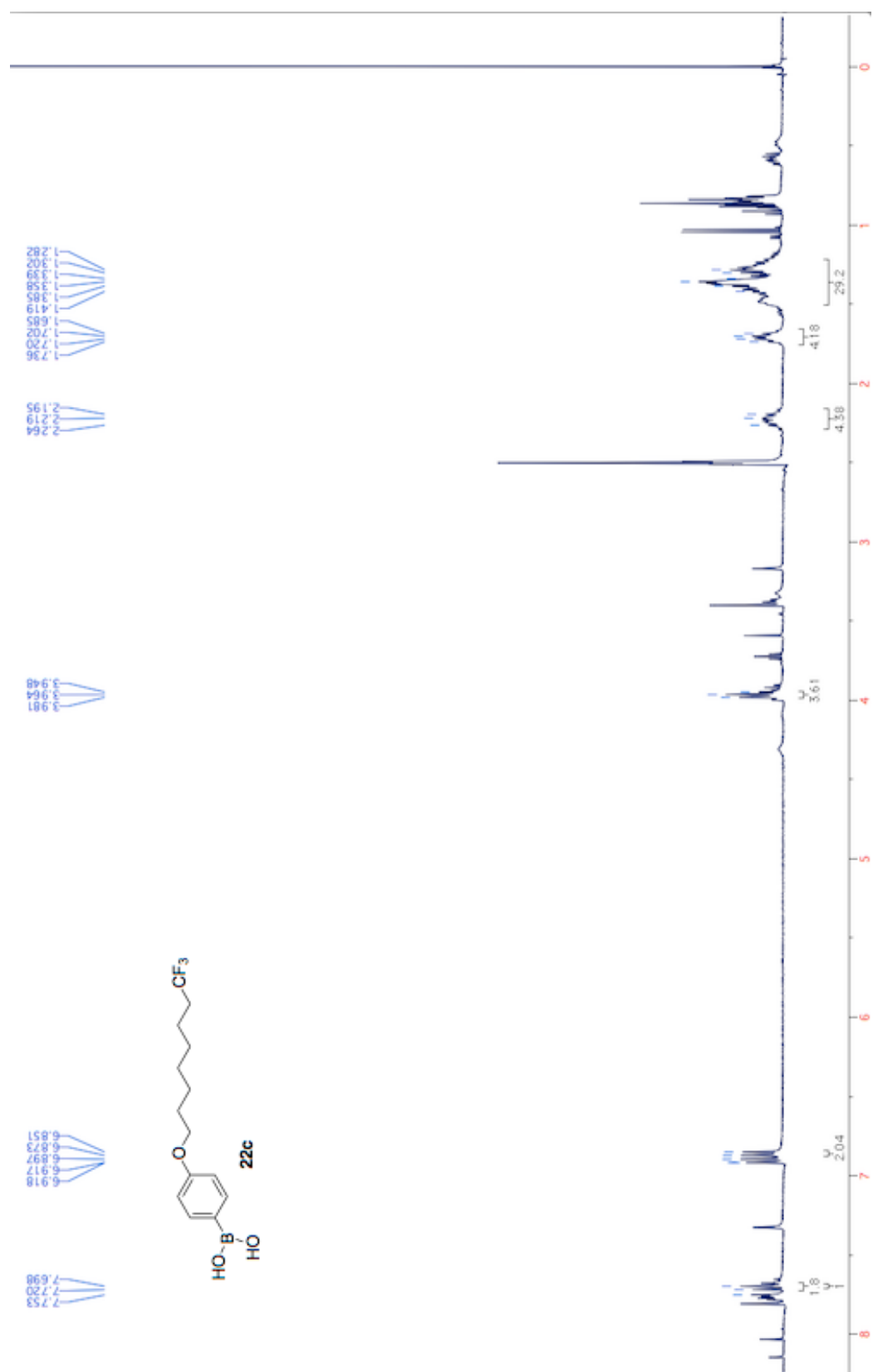


Figure A.15: ^1H NMR spectrum of compound (**22c**) in $\text{DMSO-}d_6$.

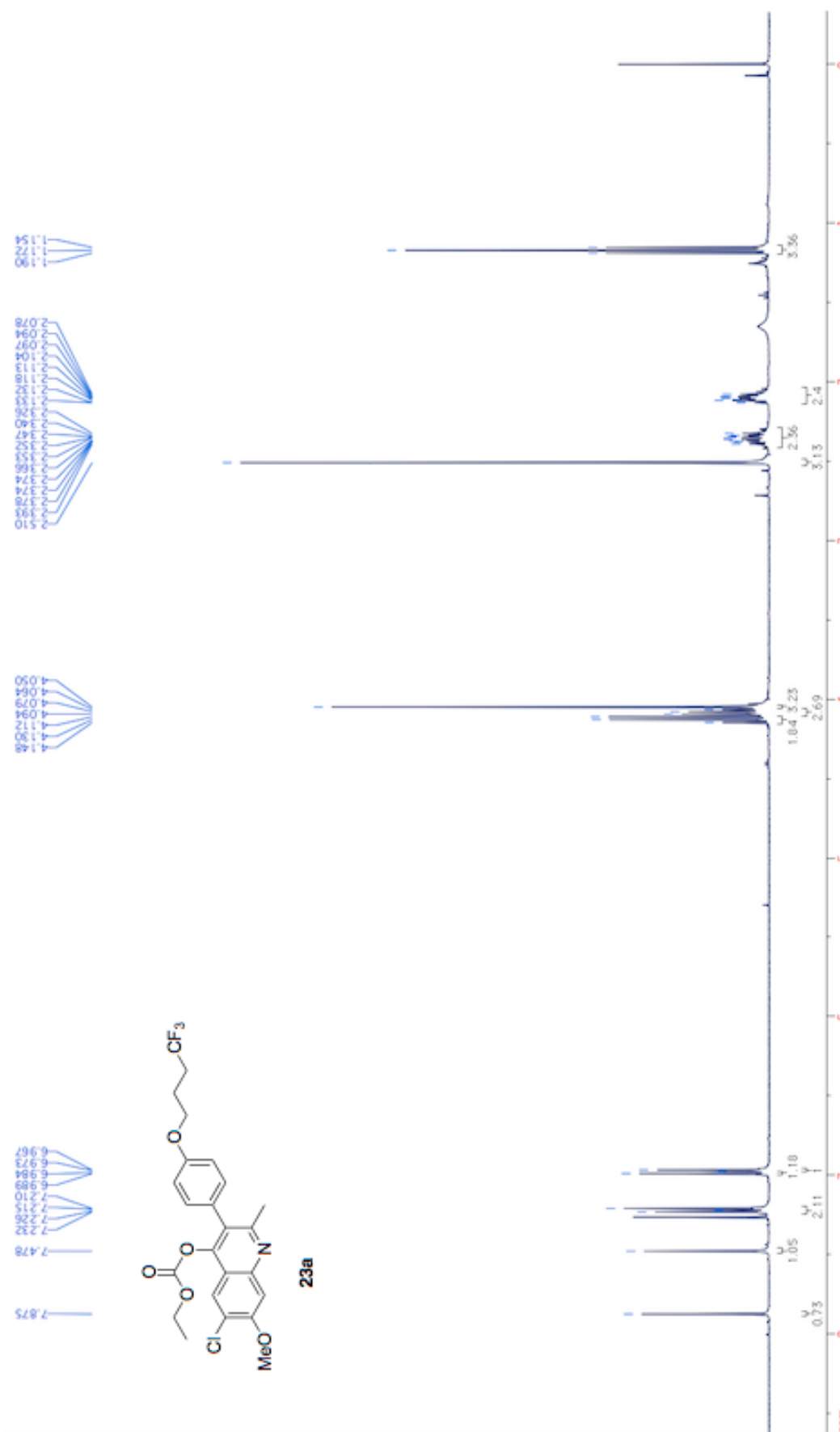


Figure A.16: ¹H NMR spectrum of compound (**23a**) in CDCl₃.

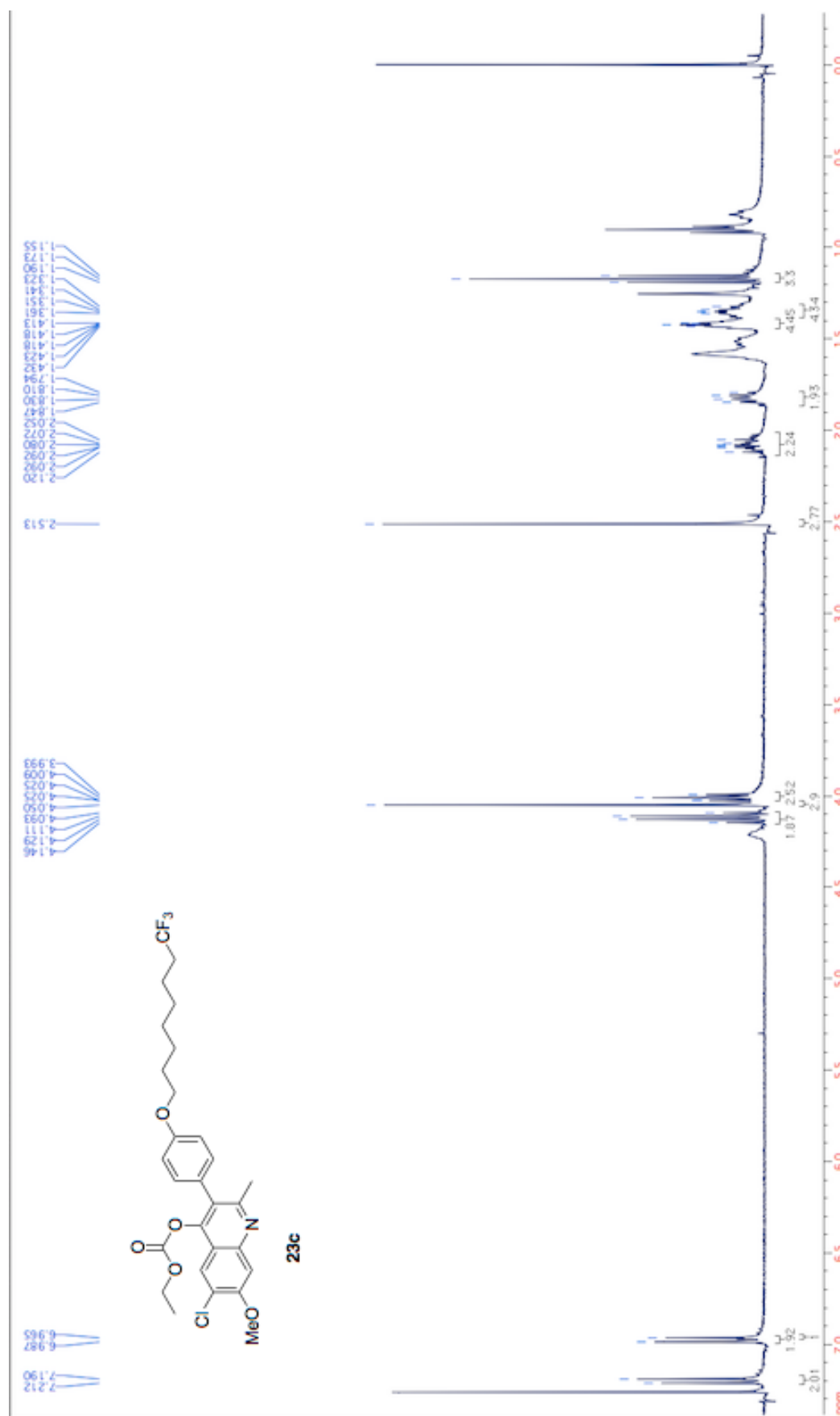


Figure A.17: ^1H NMR spectrum of compound (**23c**) in CDCl_3 .

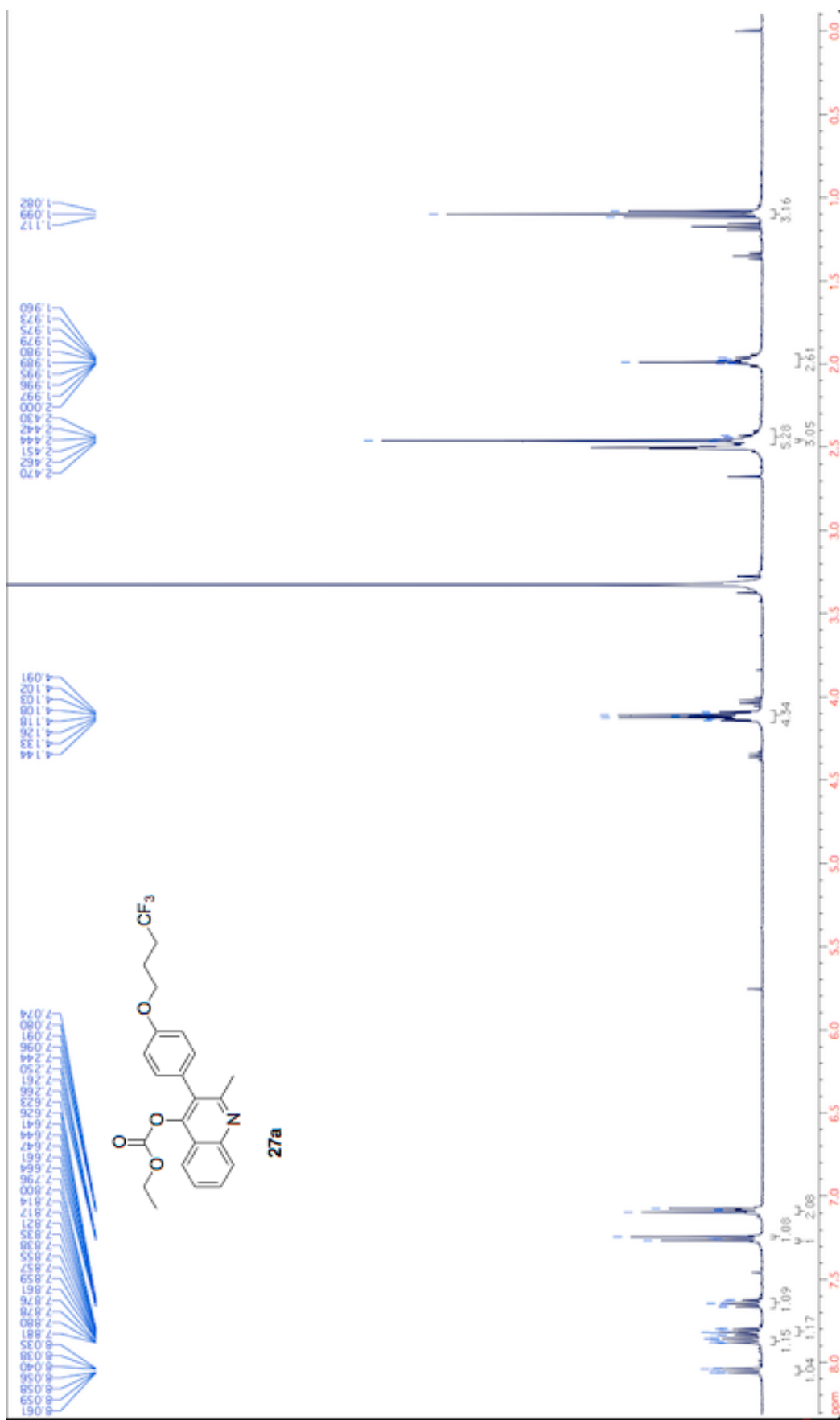
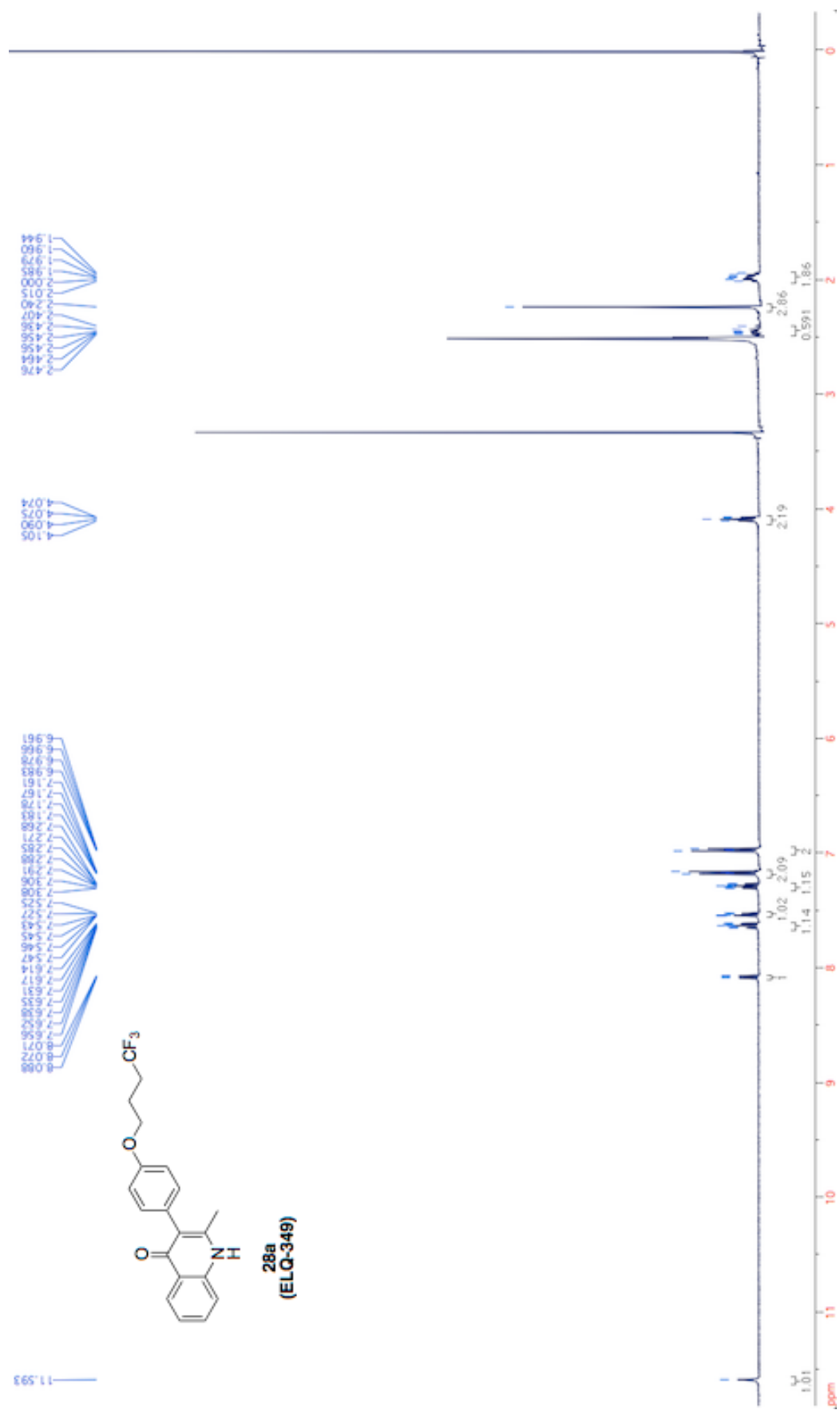


Figure A.18: ^1H NMR spectrum of compound (**27a**) in $\text{DMSO-}d_6$.



References

- [1] WHO — World Malaria Report 2013. http://www.who.int/malaria/publications/world_malaria_report_2013/en/.
- [2] Global Malaria Mapper web application. <http://worldmaliareport.org/home>.
- [3] Malaria. 2012; www.cdc.gov/malaria/.
- [4] Wernsdorfer, W. H., McGregor, S. I., Eds. *Malaria: Principles and Practice of Malariology*; Churchill Livingstone Inc.: New York, NY, 1988; Vol. 1.
- [5] Gilles, H.; Warrell, D. *Bruce-Chwatt's Essential Malariology*, 3rd ed.; Oxford University Press: New York, NY, 1993.
- [6] Institute of Medicine Staff, *Malaria: Obstacles and Opportunities*; National Academies Press: Washington, DC, USA, 1991.
- [7] Meshnick, S. R.; Dobson, M. J. In *Antimalarial Chemotherapy: Mechanisms of Action, Resistance, and New Directions in Drug Discovery*; Rosenthal, P., Ed.; Humana Press Inc.: Totwa, NJ, 2001.
- [8] Dünschede, H.-B. *Tropenmedizinische Forschung bei Bayer*; Michael Triltsch Verlag Düsseldorf: Düsseldorf, Germany, 1971.
- [9] Krafts, K.; Hempelmann, E.; Skórska-Stania, A. *Parasitol. Res.* **2012**, *111*, 1–6.
- [10] Winter, R.; Kelly, J. X.; Smilkstein, M. J.; Hinrichs, D.; Koop, D. R.; Riscoe, M. K. *Exp. Parasitol.* **2011**, *127*, 545–551.
- [11] *Science and the Pacific War: Science and Survival in the Pacific, 1939-1945*; Kluwer Academic Publishers: Dordrecht, The Netherlands, 2000.

- [12] Primaquine Information Paper. 2005; <https://midrp.amedd.army.mil/info/prima.jsp>.
- [13] Beteck, R. M.; Smit, F. J.; Haynes, R. K.; N'Da, D. D. *Malar. J.* **2014**, *13*, 339.
- [14] Fernando, D.; Rodrigo, C.; Rajapakse, S. *Malar. J.* **2011**, *10*, 351.
- [15] History of Vector Control. <http://www.ivcc.com/saving-lives/how-we-save-lives/history-of-vector-control>.
- [16] CDC How Can Malaria Cases and Deaths Be Reduced? Indoor Residual Spraying. http://www.cdc.gov/malaria/malaria_worldwide/reduction/irs.html.
- [17] Raghavendra, T. R. B. S. P. D. A., K.I.; Barik *Parasitol Res.* **2011**, *108*, 757–759.
- [18] WHO — Malaria. <http://www.who.int/mediacentre/factsheets/fs094/en/>.
- [19] Dondorp, A. M. et al. *N. Engl. J. Med.* **2009**, *361*, 455–467.
- [20] Webb Jr., J. L. A. *The Long Struggle against Malaria in Tropical Africa*; Cambridge University Press, 2014.
- [21] Wichmann, O. et al. *J Infect Dis.* **2004**, *190*, 1541–1546.
- [22] Nilsen, A. et al. *Sci Transl Med* **2013**, *5*, 177ra37–177ra37.
- [23] Casey, A. C. *J. Med. Chem.* **1974**, *17*, 255–256.
- [24] Winter, R. W.; Kelly, J.; Smilkstein, M. J.; Dodean, R.; Hinrichs, D.; Riscoe, M. K. *Exp. Parasitol.* **2008**, *118*, 487–497.
- [25] Cross, R. M.; Monastyrskyi, A.; Mukta, T. S.; Burrows, J. N.; Kyle, D. E.; Manetsch, R. *J. Med. Chem.* **2010**, *53*, 7076–7094.
- [26] Nilsen, A. et al. *J Med Chem* **2014**, *57*, 3818–3834.
- [27] Yeates, C. L. et al. *J. Med. Chem.* **2008**, *51*, 2845–2852.
- [28] Painter, H. J.; Morrissey, J. M.; Mather, M. W.; Vaidya, A. B. *Nature* **2007**, *446*, 88–91.

- [29] Barton, V.; Fisher, N.; Biagini, G. A.; Ward, S. A.; O'Neill, P. M. *Curr Opin Chem Biol* **2010**, *14*, 440–446.
- [30] Crofts, A. R. *Annu. Rev. Physiol.* **2004**, *66*, 689–733.
- [31] Mitchell, P. *FEBS Lett.* **1975**, *52*, 137–139.
- [32] Fry, M.; Pudney, M. *Biochem. Pharmacol.* **1992**, *43*, 1545–1553.
- [33] Birth, D.; Kao, W.-C.; Hunte, C. *Nat Commun* **2014**, *5*, 4029.
- [34] Arav-Boger, R.; Shapiro, T. A. *Annu. Rev. Pharmacol. Toxicol.* **2005**, *45*, 565–585.
- [35] Fisher, N.; Abd Majid, R.; Antoine, T.; Al-Helal, M.; Warman, A. J.; Johnson, D. J.; Lawrenson, A. S.; Ranson, H.; O'Neill, P. M.; Ward, S. A.; Biagini, G. A. *J. Biol. Chem.* **2012**, *287*, 9731–9741.
- [36] Doggett, J. S. Division of infectious Diseases, OHSU/VAMC, Portland, OR. Unpublished results presented at group lab meeting, 2015.
- [37] Fujii, S.; Chang, S. Y.; Burke, M. D. *Angew. Chem. Int. Ed. Engl.* **2011**, *50*, 7862–7864.
- [38] Santos, W. L.; Lynch, K. R.; Macdonald, T. L.; Kennedy, A.; Kharel, Y.; Raje, M. R.; Houck, J. Preparation of alkylphenyloxadiazolyimidamide derivatives and analogs for use as sphingosine kinase inhibitors. 2013.
- [39] Miyaura, N. *Journal of Organometallic Chemistry* **2002**, *653*, 54–57.
- [40] Lennox, A. J. J.; Lloyd-Jones, G. C. *Chem. Soc. Rev.* **2014**, *43*, 412.
- [41] Sun, J.; Perfetti, M. T.; Santos, W. L. *J. Org. Chem.* **2011**, *76*, 3571–3575.
- [42] Tzschucke, C. C.; Murphy, J. M.; Hartwig, J. F. *Org. Lett.* **2007**, *9*, 761–764.
- [43] Smilkstein, M.; Sriwilaijaroen, N.; Kelly, J. X.; Wilairat, P.; Riscoe, M. *Antimicrob. Agents Chemother.* **2004**, *48*, 1803–1806.
- [44] Capper, M. J.; O'Neill, P. M.; Fisher, N.; Strange, R. W.; Moss, D.; Ward, S. A.; Berry, N. G.; Lawrenson, A. S.; Hasnain, S. S.; Biagini, G. A.; Antonyuk, S. V. *Proc. Natl. Acad. Sci. U.S.A.* **2015**, *112*, 755–760.

-
- [45] Kelley, L. A.; Sternberg, M. J. E. *Nat. Protocols* **2009**, *4*, 363–371.
- [46] Glide, version 6.6. 2015.
- [47] Consortium, T. U. *Nucl. Acids Res.* **2015**, *43*, D204–D212.
- [48] Maestro, version 10.1. 2015.
- [49] Schuster, F. L. *Clin. Microbiol. Rev.* **2002**, *15*, 355–364.
- [50] Trager, W.; Jensen, J. B. *Science* **1976**, *193*, 673–675.
- [51] Ritz, C.; Streibig, J. C. *Journal of Statistical Software* **2005**, *12*.